RECOVERY OF RARE EARTH ELEMENTS (REEs) FROM LEACH SOLUTIONS BY SOLVENT EXTRACTION WITH PREDISPERSION

A THESIS SUBMITTED TO
THE GRADUATE SCHOOL OF NATURAL AND APPLIED SCIENCES
OF
MIDDLE EAST TECHNICAL UNIVERSITY

BY

MUHAMMAD ZUBAIR RAHIM

IN PARTIAL FULFILLMENT OF THE REQUIREMENTS
FOR
THE DEGREE OF DOCTOR OF PHILOSOPHY
IN
MINING ENGINEERING

JUNE 2024

Approval of the thesis:

RECOVERY OF RARE EARTH ELEMENTS (REEs) FROM LEACH SOLUTIONS BY SOLVENT EXTRACTION WITH PREDISPERSION

submitted by **MUHAMMAD ZUBAIR RAHIM** in partial fulfillment of the requirements for the degree of **Doctor of Philosophy** i**n Mining Engineering, Middle East Technical University** by,

Prof. Dr. Naci Emre Altun
Dean, **Graduate School of Natural and Applied Sciences** _____

Prof. Dr. Naci Emre Altun
Head of the Department, **Mining Engineering** _____

Prof. Dr. Ali Ihsan Arol
Supervisor, **Mining Engineering** _____

Examining Committee Members:

Prof. Dr. Naci Emre Altun
Mining Engineering, METU _____

Prof. Dr. Ali Ihsan Arol
Mining Engineering, METU _____

Assoc. Prof. Dr. Özlem Biçak
Mining Engineering, Hacettepe University _____

Assoc. Prof. Dr. Metehan Erdoğan
Metallurgy and Materials Engineering, Ankara Yıldırım Beyazıt University _____

Assist. Prof. Dr. Şeniz Uçar
Metallurgy and Materials Engineering, METU _____

Date: 25.06.2024

I hereby declare that all information in this document has been obtained and presented in accordance with academic rules and ethical conduct. I also declare that, as required by these rules and conduct, I have fully cited and referenced all material and results that are not original to this work.

Name, Surname: Muhammad Zubair Rahim

Signature:

ABSTRACT

RECOVERY OF RARE EARTH ELEMENTS (REEs) FROM LEACH SOLUTIONS BY SOLVENT EXTRACTION WITH PREDISPERSION

Rahim, Muhammad Zubair
Doctor of Philosophy, Mining Engineering
Supervisor: Prof. Dr. Ali Ihsan Arol

June 2024, 123 pages

Rare Earth Elements (REEs) are crucial in various modern industrial products, renewable energy systems, and catalysis. Due to their increasing demand and limited natural abundance, efficient extraction methods are imperative for ensuring a stable supply chain. Solvent extraction (SX) is typically considered the best commercial approach for extracting REEs because it can handle massive volumes of diluted pregnant liquors. Conventional SX equipment have some operational limitations, causing a decrease in the recovery of the product and process kinetics. These issues include insufficient mass transfer because of the poly-dispersed droplets and phase separation of product streams, thus requiring a huge settling chamber for mixer-settler, and back-mixing of feed solutions in spray columns, reducing the efficiency of mass transfer between the two immiscible streams. These problems have been addressed and overcome by the newly designed "solutions spray system." In this new technique, the feed solutions were sprayed counter-currently in the form of mono-dispersed micro-sized droplets in the mixing column, where the mass transfer took place, and the emulsion produced was continuously sent to the settling column, where the two product phases were separated. The geometry of this settling column enhanced the quick separation in the aqueous raffinate solution and the loaded

organic stream. The primary aim of this experimental study was to study the performance of this solutions spray system with the intent to enhance the recovery of the REEs and kinetics of SX operation.

Variables like feed solution pH, DEHPA concentration, ionic strength, concentrations of REEs in the aqueous feed, type of feed solutions, and aqueous/organic (A/O) phase ratio were studied and evaluated the performance of this setup while extracting lanthanum (La), neodymium (Nd), and europium (Eu) from their synthesized chloride solutions. For feed solution having 1.0 g/L of each REO, the %E of La, Nd, and Eu was 95.03%, 99.36%, and 99.98%, respectively, at 2.0 pH, and 1.54 mol/L ionic strength of the solution while using 0.303 M DEHPA. Under these conditions, the distribution ratio for La, Nd, and Eu was 19.14, 155.25, and 4165, respectively, representing complete extraction in a single-stage operation. Moreover, the values of separation factors, $SF_{Eu/La}$ = 6.69, $SF_{Eu/Nd}$ = 5.33, and $SF_{Nd/La}$ = 1.26 at 0.50 pH, showed the selective separation of these elements. Stripping of loaded DEHPA was performed with 2.0 – 6.0 M HCl, and 2.0 M HCl strip solution gave good results of REEs recovery. Furthermore, for aqueous feed representative of Beylikova leach solution having 6.0 g/L La_2O_3, 2.5 g/L Nd_2O_3, and 100 mg/L Eu_2O_3, the %E of La, Nd, and Eu was 70.32%, 85.31%, and 99.26%, respectively, under the same variable conditions, and 4.0 M HCl stripping solution showed better recoveries in this case. McCabe Thiele diagrams were plotted to see the number of theoretical stages in recovering REEs as a group and their selective separation from each other for extraction and stripping sections. Additionally, the extraction of these REEs was also observed from sulfate solutions, and it was found that %E was superior from the HCl solution compared to the H_2SO_4 solution, especially at lower pH values of feed solutions. Finally, the two immiscible phases were mixed with the mechanical mixer, and the ultrasound mixing, and the extraction results were compared to that of the solutions spray system. The percent extraction of REEs was superior in the case of the solutions spray system, followed by ultrasound mixing and mechanical mixing. In light of these findings, the solutions spray system seemed

better in terms of recovery of REEs and time of mixing and separation, thus enhancing the performance of the SX operation.

Keywords: Solvent extraction, Rare earth elements, DEHPA, Solutions spray system

ÖZ

LİÇ ÇÖZELTİLERİNDEN NADİR TOPRAK ELEMENTLERİNİN (NTE) ÖN DAĞITIMLI ÇÖZÜCÜ EKSTRAKSİYON YÖNTEMIYLE KAZANILMASI

Rahim, Muhammad Zubair
Doktora, Maden Mühendisliği
Tez Yöneticisi: Prof. Dr. Ali Ihsan Arol

Haziran 2024, 123 sayfa

Nadir Toprak Elementleri (NTE), elektronik, yenilenebilir enerji sistemleri ve katalizörler dahil olmak üzere çeşitli modern teknolojilerde önemli bir rol oynamaktadır. Artan talep ve sınırlı doğal kaynak nedeniyle, istikrarlı bir tedarik zinciri sağlamak için verimli ekstraksiyon yöntemleri zorunludur. Çözücü ekstraksiyonu, büyük hacimlerde seyreltilmiş yüklü çözeltileri işleyebildiğinden, NTE ekstraksiyonu için genellikle en iyi ticari yaklaşım olarak kabul edilir. Geleneksel çözücü ekstraksiyonu ekipmanının, genel prosesin termodinamiğini ve kinetiğini olumsuz etkileyen bazı operasyonel sınırlamaları vardır. Bu sorunlar arasında, çok-dağılmış damlacıklar ve ürün akışlarının faz ayrımı nedeniyle yetersiz kütle transferi, dolayısıyla karıştırıcı-çöktürücü için büyük bir çökeltme hacminin gerekli olması ve besleme çözeltilerinin püskürtme kolonlarında geri karışması, böylece ürünler arasındaki kütle aktarımının verimliliğinin azaltılması yer alır. Bu sorunlar, yeni tasarlanan "çözelti püskürtme sistemi" ile etkili bir şekilde ele alınmakta ve sözü edilen sorunların üstesinden gelinmektedir. Bu yeni teknikte, besleme çözeltileri kütle aktarımının gerçekleştiği karıştırma kolonunda mono dağılmış mikro boyutlu damlacıklar halinde ters akımla püskürtülmekte ve üretilen

emülsiyon sürekli olarak, iki ürün fazının birbirinden ayrıldığı, çökeltme kolonuna gönderilmektedir. Deneylerde kullanılan çökeltme kolonunun geometrisi, sulu rafinat ile yüklü organik faz arasındaki ayırımın hızlı bir şekilde gerçekleşebilmesi amacıyla tasarlanmıştır. Bu çalışmada, çözücü ekstraksiyonu işleminin kinetiğini geliştirmek amacıyla bu çözelti püskürtme sisteminin performansı araştırılmıştır.

Besleme çözeltisinin türü, pH'ı, DEHPA konsantrasyonu, iyonik gücü, NTE konsantrasyonları, sulu/organik faz oranı gibi değişkenler,bu kurulumun sentetik çözeltilerinden lantan (La), neodimyum (Nd) ve öropiyumun (Eu) ekstraksiyonu performansını değerlendirmek için incelenmiştir. Her bir nadir toprak oksitin 1.0 g/L içeren besleme çözeltisi için, 0.303 M DEHPA kullanıldığında, pH 2.0 ve 1.54 mol/L iyonik güçte, La, Nd ve Eu'nun ekstraksiyon yüzdeleri, sırasıyla 95.03%, 99.36%, and 99.98% olmuştur. Bu koşullar altında La, Nd ve Eu için dağılım oranı sırasıyla 19.14, 155.25 ve 4165 olup, tek aşamalı bir işlemde tam ekstraksiyon olduğunu göstermektedir.. Ayrıca, 0.50 pH'da ayırma faktörlerinin değerleri, $SF_{Eu/La}$ = 6.69, $SF_{Eu/Nd}$ = 5.33 ve $SF_{Nd/La}$ = 1.26 olup, bu elementlerin seçici olarak ayrıldığını göstermektedir. Yüklenen DEHPA'nın sıyrılması, 2.0 – 6.0 M HCl ile gerçekleştirilmş ve 2.0 M HCl sıyırma çözeltisi, NTE'lerin geri kazanımında iyi sonuçlar vermiştir. Ayrıca, 6.0 g/L La_2O_3, 2.5 g/L Nd_2O_3 ve 100 mg/L Eu_2O_3 içeren, Beylikova liç çözeltisini temsil eden sulu beslemeden La, Nd ve Eu ekstraksiyon yüzdesi sırasıyla 70.32%, 85.31% ve 99.26% olmuştur. Aynı değişken koşullar altında ve 4.0 M HCl sıyırma çözeltisi ile iyi geri kazanımlar elde edilmiştir. NTE'leri grup olarak geri kazanmak için teorik aşamaların sayısını ve birbirlerinden seçici olarak ayrılmalarını görmek amacıyla bu iki farklı besleme çözeltisinden ekstraksiyon ve sıyırma işlemleri için McCabe Thiele diyagramları da oluşturulmuştur. Ayrıca bu NTE'lerin sülfat çözeltilerinden de ekstraksiyonu gözlenmiş ve özellikle besleme çözeltilerinin düşük pH değerlerinde, klorür çözeltisinden ekstraksiyonun sülfat çözeltisine göre daha üstün olduğu bulunmuştur. Son olarak, karışmayan sulu ve organik fazların, mekanik karıştırıcı ve ultrasonik karıştırma ile karıştırılarak, ekstraksiyon sonuçları, çözelti püskürtme sistemiyle

karşılaştırılmıştır. Çözelti püskürtme sistemi ile NTE'lerin daha yüksek verimle kazanıldığı, bunu ultrasonla karıştırma ve mekanik karıştırmanın izlediği görülmüştür. Bu bulguların ışığında, NTE'lerin yüklü liç çözeltilerinden çözücü ekstraksiyon yöntemi ile kazanımında, çözelti püskürtme sisteminin işleminin kinetiğini iyileştirdiği belirlenmiştir.

Anahtar Kelimeler: Çözücü ekstraksiyonu, Nadir toprak elementlerinin, DEHPA, Sçözeclti püskürtme sistemi

This work is dedicated to my family

ACKNOWLEDGMENTS

My sincere gratitude goes out to the following people and organizations that have been instrumental in helping me finish this Ph.D. thesis:

First and foremost, I am immensely grateful to my advisor, Prof. Dr. Ali Ihsan Arol, for his unwavering support, guidance, and scholarly insights throughout this research process. His mentorship has been invaluable, shaping not only the direction of this thesis but also my growth as a researcher.

I sincerely appreciate the members of my doctoral committee, Prof. Dr. Naci Emre Altun and Assoc. Prof. Dr. Özlem Biçak, for their constructive feedback and thoughtful suggestions that have significantly enriched the quality of this work.

I am thankful to the administration of Nadir Toprak Elementleri Araştırma Enstitüsü (NATEN), Turkey, for providing REOs and DEHPA, and AR-GE laboratory, Eti Bakir a.ş, Turkey, for providing kerosene and conducting ICP-OES analysis which enabled me to pursue this Ph.D. successfully.

I want to acknowledge the administration of the Department of Mining Engineering, Middle East Technical University, Ankara, for providing the necessary resources and a conducive research environment that helped me to complete this Ph.D.

Lastly, I am grateful to my wife, Aisha Sadiqa, for her unwavering support, love, and understanding throughout this academic endeavor. To my children, Mahad Ibrahim and Muhammad Haider, your smiles, love, and presence gave me strength and motivation to cope with the challenges of this journey. I am deeply grateful for their sacrifices to help me pursue my research goals.

Thank you all for being an integral part of my academic journey.

TABLE OF CONTENTS

ABSTRACT v

ÖZ viii

ACKNOWLEDGMENTS xii

TABLE OF CONTENTS xiii

LIST OF TABLES xvi

LIST OF FIGURES xvii

LIST OF ABBREVIATIONS xxi

CHAPTERS

1 INTRODUCTION 1

1.1 Background of REEs 2

1.2 Minerals and deposits of REEs 3

1.3 Physical and chemical properties of REEs 6

1.4 Uses of REEs 8

1.5 Sustainability of REEs supply 11

1.6 Ore processing 14

1.7 Dissertation outline 15

2 PROPOSED RESEARCH 17

2.1 Problem statement 17

2.2 Research approach 18

2.3 Research significance 19

3 LITERATURE REVIEW 21

3.1 REEs extraction processes 21

3.1.1 Physical treatment/beneficiation operations 21
3.1.2 Hydrometallurgical operations / chemical treatment 24
3.2 Efficiency and kinetics of solvent extraction 28
3.3 Solvent extraction equipment 31
3.3.1 Mixer settler 31
3.3.2 Continuous column contactors 33
3.4 Solvent extraction reagents 40
3.4.1 Classification of organic solvents 41
3.5 Di-(2-ethylhexyl) phosphoric acid (DEHPA / D2EHPA / P204) 43
3.6 REEs extraction with DEHPA 45
4 MATERIALS AND METHODS 51
4.1 Materials 51
4.2 Equipment and method 51
4.3 Evaluation of experimental data 55
4.4 Experiments 56
4.4.1 Study of the solutions spray system for the chloride feed having 1.0 g/L of each REO 56
4.4.2 Study of the solutions spray system for the sulfate feed solution having 1.0 g/L of each REO 58
4.4.3 Study of different mixing systems 58
4.4.4 Study of the solutions spray system for the chloride feed solution having REEs concentration representative of Beylikova leach 59
5 RESULTS AND DISCUSSION 61
5.1 Study of the solutions spray system for the chloride feed solution having 1.0 g/L of each REO 61

5.1.1 Effect of pH 61
5.1.2 Effect of ionic strength of feed solution 64
5.1.3 Effect of DEHPA concentration 68
5.1.4 Stoichiometry of the extracted REEs complexes 72
5.1.5 McCabe Thiele diagrams for the extraction operation 76
5.1.6 Stripping of REEs 79
5.1.7 McCabe Thiele diagrams for stripping of REEs 80
5.2 Study of the solutions spray system for the sulfate feed solution having 1.0 g/L of each REO 83
5.3 Study of different mixing systems 86
5.4 Study of the solutions spray system for the chloride feed solution having REEs concentration representative of Beylikova leach 90
5.4.1 Effect of pH 90
5.4.2 Effect of DEHPA concentration 93
5.4.3 Stoichiometry of the extracted REEs 94
5.4.4 McCabe Thiele diagrams for the extraction operation 96
5.4.5 Stripping of REEs 98
5.4.6 McCabe Thiele diagrams for stripping of REEs 100
6 CONCLUSION AND RECOMMENDATIONS 103
REFERENCES 107
CURRICULUM VITAE 123

LIST OF TABLES

TABLES

Table 1.1: Some of the worldwide RE deposits (Dushyantha et al., 2020b)..... 5
Table 1.2: Some properties of REEs (Wall, 2021)..... 7
Table 1.3: Some commercial applications of REEs (Xie et al., 2014)..... 10
Table 3.1: Comparison of conventional systems for mixing and separation of phases in SX operation (Naganawa, 2017)..... 39
Table 3.2: SF with DEHPA and IONQUEST 801 (Abreu & Morais, 2014)..... 47
Table 3.3: Percent extraction and separation factor values for Gd, Tb, and Eu (Budiman et al., 2021)..... 48
Table 5.1: Comparison of the present study with some of the work from literature with respect to %E, D, and mixing time..... 75
Table 5.2: Comparison of the extraction of REEs from chloride solutions having different concentrations with 0.303 M DEHPA..... 92
Table 5.3: Amount of La, Nd, and Eu recovered by stripping through HCl form loaded DEHPA having 3000 mg/L La, 2200 mg/L Nd, and 99.69 mg/L Eu..... 99
Table 6.1: Effect of different parameters on complete recovery of REEs as a group and their selective separation in extraction and stripping stages..... 105

LIST OF FIGURES

FIGURES

Figure 1.1: Concentration of REEs in the earth crust (Wall, 2021)..... 3
Figure 1.2: World REEs reserves (Bartolomeo et al., 2021) 4
Figure 1.3: Lanthanides contraction (Wall, 2021) 8
Figure 1.4: Percent uses of REEs in different products (Patel et al., 2023)..... 9
Figure 1.5: Commercial uses of REEs (Krishnamurthy, 2020) 9
Figure 1.6: REEs production history (King, 2019)..... 12
Figure 1.7: Worldwide production of REEs (Bartolomeo et al., 2021)..... 13
Figure 1.8: Proportion of different REE resources and active mines around the world (Liu et al., 2023) 13
Figure 1.9: Schematic diagram for rare earth ore processing (Cen et al., 2021) 15
Figure 3.1: Process flow diagram of SX operation (Kislik, 2012b) 27
Figure 3.2: McCabe Thiele diagram for counter-current SX operation (Xie et al., 2014) 30
Figure 3.3: Mixer settler with baffled settling chamber (Weatherley, 2020) 32
Figure 3.4: Spray column: (a) organic solution dispersed in continuous aqueous phase; (b) aqueous phase dispersed in continuous organic solution..... 33
Figure 3.5: Back-mixing in a spray column (Weatherley, 2020)..... 34
Figure 3.6: Visualization of drop behavior in a packed column (Weatherley, 2020) 35
Figure 3.7: Outline of the emulsion flow continuous solvent extractor (Nagano et al., 2014) 36
Figure 3.8: Mechanism of droplet mixing and separation in emulsion flow apparatus (Naganawa, 2017)..... 38
Figure 3.9: Liquid spraying system vs Mechanical stirring system (Shimogouchi et al., 2019) 38
Figure 3.10: Difference in the phase separation between droplets generated by spraying and mechanical mixing (Shimogouchi et al., 2019)..... 38

Figure 3.11: Structure of DEHPA 43
Figure 3.12: DEHPA monomer to dimer 44
Figure 3.13: Reaction of DEHPA dimer with metal cation..... 44
Figure 4.1: Schematic diagram of solutions spray system for SX process 52
Figure 4.2: Dimensions of solutions spray system..... 53
Figure 4.3: Real-time picture of the solutions spray system 54
Figure 4.4: Ultrasound mixing system 55
Figure 5.1: pH effect on %E of La, Nd, and Eu (1.0 M HCl aqueous phase having 1.0 g/L of each REO and 0.303 M DEHPA as organic phase) 62
Figure 5.2: Effect of pH on D of La, Nd, and Eu (1.0 M HCl aqueous phase having 1.0 g/L of each REO and 0.303 M DEHPA as organic phase) 63
Figure 5.3: Effect of ionic strength (I) on the extraction of La, Nd, and Eu from aqueous solutions with different pH values a) 1.0 pH, b) 1.5 pH, c) 2.0 pH 66
Figure 5.4: Effect of ionic strength (I) on the distribution ratio (D) of La, Nd, and Eu from aqueous solutions at different pH values a) 1.0 pH, b) 1.5 pH, c) 2.0 pH 68
Figure 5.5: Effect of DEHPA concentration on the %E of La, Nd, and Eu from a solution having 1.0 g/L each REO at: a) 1.0 pH , b) 2.0 pH 70
Figure 5.6: Effect of DEHPA concentration on the distribution ratio of REEs a) La, b) Nd, c) Eu 70
Figure 5.7: Effect of pH value at equilibrium on the stoichiometry of REEs extraction 72
Figure 5.8: Effect of DEHPA concentration on the stoichiometry of REEs extraction 74
Figure 5.9: Effect of A:O phase ratio on % extraction of La, Nd, and Eu 77
Figure 5.10: McCabe Thiele diagram for extraction of REEs using DEHPA..... 78
Figure 5.11: Effect of HCl molarity on the stripping of La, Nd, and Eu 80
Figure 5.12: McCabe Thiele diagram for stripping of REEs using 2.0 M HCl 81
Figure 5.13: pH effect on %E of La, Nd, and Eu from H_2SO_4 solution..... 83
Figure 5.14: Comparison of extraction of La, Nd, and Eu from HCl (dashed lines) and H_2SO_4 (solid lines) feed solutions 84

Figure 5.15: Pourbaix diagrams of La, Nd, and Eu in HCl solution (https://next-gen.materialsproject.org/pourbaix) 85
Figure 5.16: Pourbaix diagrams of La, Nd, and Eu in H_2SO_4 solution (https://next-gen.materialsproject.org/pourbaix) 86
Figure 5.17: pH effect on %E of La, Nd, and Eu from HCl solution using ultrasonic probe system 87
Figure 5.18: Comparison of extraction of La, Nd, and Eu from HCl feed solutions using ultrasound mixing (USM) and spray mixing (SM) 87
Figure 5.19: pH effect on %E of La, Nd, and Eu from HCl solution using a mechanical mixer 88
Figure 5.20: Comparison of extraction of La, Nd, and Eu from HCl feed solutions using mechanical mixing (MM) and spray mixing (SM) 89
Figure 5.21: Comparison of mechanical mixing (MM), ultrasound mixing (USM), and solutions spray mixing (SM) for the extraction of a) La, b) Nd, and c) Eu 89
Figure 5.22: pH effect on %E of La, Nd, and Eu (aqueous feed representative of Beylikova leach, and 0.303 M DEHPA)..... 91
Figure 5.23: Comparison of %E of La, Nd, and Eu from the two aqueous feeds (aqueous feed having 1.0 gm/L of each REO vs aqueous feed representative of Beylikova leach and 0.303 M DEHPA)..... 91
Figure 5.24: Effect of pH on D of La, Nd, and Eu (aqueous feed representative of Beylikova leach, and 0.303 M DEHPA)..... 92
Figure 5.25: DEHPA concentration effect on %E of La, Nd, and Eu (aqueous feed representative of Beylikova leach)..... 93
Figure 5.26: Effect of DEHPA concentration on the distribution ratio of La, Nd, and Eu (aqueous feed representative of Beylikova leach) 94
Figure 5.27: Effect of pH at the equilibrium on the extraction stoichiometry of REEs (aqueous feed representative of Beylikova leach and 0.303 M DEHPA) 95
Figure 5.28: Effect of DEHPA concentration on the extraction stoichiometry of REEs (aqueous feed representative of Beylikova leach) 95

Figure 5.29: Effect of A:O phase ratio on % extraction of REEs (aqueous feed representative of Beylikova leach, and 0.303 M DEHPA) 96
Figure 5.30: McCabe Thiele diagrams for La, Nd, and Eu extraction (aqueous feed representative of Beylikova leach and 0.303 M DEHPA) 98
Figure 5.31: Effect of HCl molarity on stripping of La, Nd, and Eu from loaded DEHPA 99
Figure 5.32: McCabe Thiele diagrams for stripping of La, Nd, and Eu using 2.0 M HCl 100
Figure 5.33: McCabe Thiele diagrams for stripping of La, Nd, and Eu using 4.0 M HCl 101

LIST OF ABBREVIATIONS

ABBREVIATIONS

REEs: Rare earth elements

LREEs: Light rare earth elements

HREEs: Heavy rare earth elements

MREEs: Middle rare earth elements

REO: Rare earth oxide

SX: Solvent extraction

DEHPA: Di-(2-ethylhexyl) phosphoric acid

PC88A or HEH(EHP) or IONQUEST 801: 2-ethylhexyl phosphonic acid mono-2-ethylhexyl ester

Cyanex 272: bis(2,4,4-trimethylpentyl) phosphinic acid

TOPO: Trioctylphosphine oxide

%E: Percent extraction

D: Distribution ratio

SF: Separation factor

%S: Percent stripping

CHAPTER 1

INTRODUCTION

Rare earth metals (REMs) are critical in our society, aiding shifting to a more sustainable civilization. These metals in pure form are utilized in modern applications like smartphones, electric car batteries, and wind turbines; therefore, the manufacturing sector needs access to these metals in high purity. As a result, the metal streams must be separated and purified from primary and secondary resources (Lommelen, 2021).

Yttrium and scandium, along with 15 lanthanides, are classified as rare earth elements (REEs). These elements are scandium (Sc), yttrium (Y), lanthanum (La), cerium (Ce), prasiodymium (Pr), neodymium (Nd), promethium (Pm), samarium (Sm), europium (Eu), gadolinium (Gd), terbium (Tb), dysprosium (Dy), holmium (Ho), erbium (Er), thulium (Tm), ytterbium (Yb) and lutetium (Lu). These seventeen chemically similar elements are frequently found in trace concentrations in various rocks and ores. Pm is the only rare earth element (REE) created by fission and does not occur naturally. Because of their distinct characteristics, REEs are essential for many high-tech products, such as cell phones, wind turbines, hybrid vehicles, and defense technology. The elements from lanthanum to europium are classified as light rare earth elements (LREEs), and from gadolinium to lutetium, including yttrium, they are classified as heavy rare earth elements (HREEs). However, some scholars and researchers have included middle rare earth elements (MREEs) as a third group consisting of Sm, Eu, and Gd. One of the primary research concerns in this area is the efficient and inexpensive extraction of REEs and their separation from each other because of their demand as individual elements for different green technologies (Dashti et al., 2021; Dushyantha et al., 2020a; Wall, 2021).

This chapter discusses the background of REEs, global distribution, physical and chemical characteristics, their uses as vital components in many sectors, supply and demand in different countries, and an introduction to ores processing to recover REEs.

1.1 Background of REEs

The phrase "rare earths" predates the term "lanthanides" and was used to emphasize how difficult it was to separate the elements from one another. The total abundance of REEs in the earth's crust is about 169 ppm, with 137.8 ppm of LREEs and 31.2 ppm of HREEs. Therefore, these elements are not as rare as is misled by their name. Most REEs are as prevalent in the Earth's crust as most industrial metals, such as lead, tungsten, tin, nickel, copper, zinc, and chromium. For example, the Earth's crust's copper content (60–70 ppm) and that of cerium almost precisely match. Hence, the word "rare" in this context expresses the scarcity of profitable deposits of REEs worldwide. There are up to 200 times as many LREE minerals as HREE. Most LREE minerals contain Ce as the most abundant element, accompanied by La, Pr, and Nd. Similarly, Y is the most dominant element in HREE minerals and is more abundant than other HREEs. Some rare earth (RE) compounds have names based on the scientists who first discovered their chemical properties, while others have names based on the locations of their discovery (Dushyantha et al., 2020b; A. R. Jha, 2014).

Swedish, Norwegian, and other European scientists significantly impacted the early development of REEs and their oxides. They found their important features like chemical, metallurgical, magnetic, electro-optical, and nuclear properties. They also had a significant impact on mining techniques. Around 1787, a miner discovered a mysterious mineral in a feldspar pit close to the Swedish village of Ytterby, which was first known as Ytterbite. This discovery marked the beginning of the REEs' fascinating history. It is interesting to note that this particular Swedish hamlet is the source of several REEs' names. The others came after during the next 153 years, and in 1947, scientists in the USA chemically extracted the radioactive element

promethium. Processing and refining rare earth ores remains difficult since it is challenging to separate REEs from one another (Ariana, 2016; Evans, 1996; A. R. Jha, 2014; Wall, 2021).

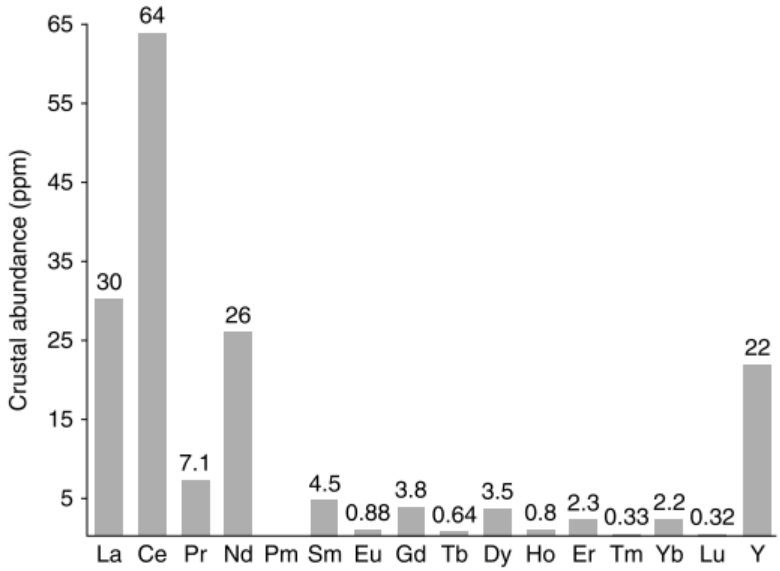

Figure 1.1: Concentration of REEs in the earth crust (Wall, 2021)

1.2 Minerals and deposits of REEs

The International Mineralogical Association has recognized over 250 RE minerals. Although many REE minerals are uncommon, fewer minerals on the list are more likely to be found as significant components of an ore deposit. Regarding mined minerals, bastnasite (La, Ce)FCO_3, monazite (Ce, La, Y, Th)PO_4, and xenotime YPO_4 stand out, and a single mineral grain may include several different mineral species. Most minerals are enriched in either light or heavy REEs instead of having equal enrichment of all REEs because of the variation in cation sizes (Dushyantha et al., 2020a; Wall, 2021).

The major deposits of REEs are frequently linked with carbonatites and alkaline-peralkaline igneous rocks, and their weathering creates secondary deposits like placer and ion adsorption. Carbonatite ore bodies, where LREEs are typically abundant, contain the majority of REEs (Dushyantha et al., 2020b).

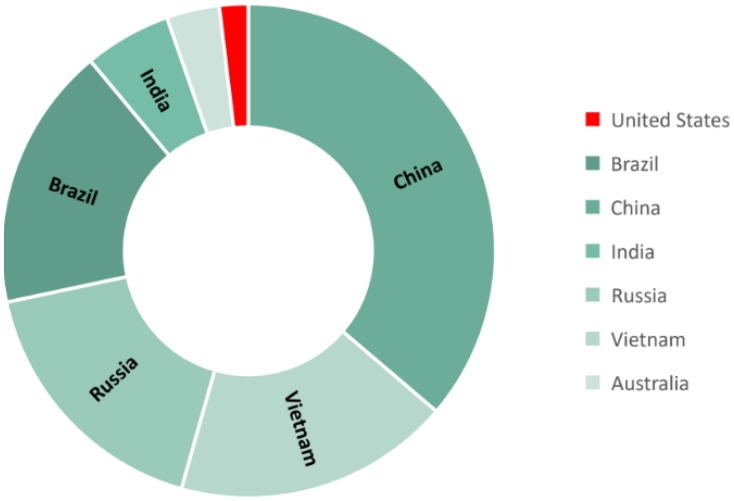

Figure 1.2: World REEs reserves (Bartolomeo et al., 2021)

Bastnasite deposits, primarily located in China and the USA, contain most of the world's reserves of REEs. Noteworthy existences include several bastnasite deposits in the Chinese province of Sichuan, the sizable deposit at Bayan Obo, and the bastnasite deposit at Mountain Pass in California. The second most significant contributor of REEs is monazite mineral, and its deposits have been found in many countries, including Australia, Brazil, India, Malaysia, and South Africa, in addition to China and the USA. Due to monazite's excellent weathering resistance and durability during transport, it is absorbed into sedimentary rocks and found in placer deposits (Bartolomeo et al., 2021).

Monazite can develop during weathering and is found in hydrothermal deposits as well. It almost always has a significant enrichment in light REE. Compared to carbonatite, monazite made from granite often has higher concentrations of thorium and uranium. Calcium or silicon must be paired with thorium substitution in monazite to maintain charge balance. The remaining resources are apatite, cheralite, phosphorites, secondary monazite, spent uranium solutions, and xenotime. The prevailing HREE mineral is xenotime-(Y), which is found in granite, gneiss, and other igneous and metamorphic rocks. It is also found in placer deposits and is resilient enough to be integrated into sedimentary rocks. The calcium phosphate mineral apatite, found in many types of rocks, is the dominant non-rare earth mineral

with a considerable concentration of REEs. Apatite is typically only found in trace amounts but can be a major rock-forming material in carbonatites and alkaline igneous rocks. Additionally, significant hosts for REE are zircon and fluorite. Zircon prefers the heavier REE but only has a trace or small amounts of it. REE is often only present in trace amounts in fluorite (Ariana, 2016; Wall, 2021; Wang et al., 2013; Xie et al., 2014).

Table 1.1: Some of the worldwide RE deposits (Dushyantha et al., 2020b)

Deposit	Location	Type	Main REEs	REE mineral (s)
Bayan Obo	China	Carbonatite	La, Ce, Nd	Bastnasite, parasite, monazite
Mountain Pass	USA	Carbonatite	LREEs	Bastnasite
Kızılcaören (Beylikova)	Turkey	Carbonatite	LREEs	Bastnasite
Mount Weld	Australia	Carbonatite / laterite	LREEs	Apatite, monazite, churchite
Illimaussaq	Denmark	Peralkaline igneous	La, Ce, Nd, HREEs	Eudialyte, steenstrupine
Steenkampskraal	South Africa	Vein	La, Ce, Nd	Monazite, apatite
Hoidas Lake	Canada	Vein	La, Ce, Pr, Nd	Apatite, allanite
Ion adsorption deposits	China	Soils	La, Nd, HREEs	Clay minerals
Maoniuoing	China	Carbonatite	LREEs	Bastnasite

The formations and deposits of REE resources are also found in Turkey, including carbonatite, sedimentary phosphate, and ion adsorption clay-type deposits. Out of these deposits, the carbonatite deposits in Kızılcaören (Eskişehir) and Kuluncak-Başören (Malatya) are the most attractive and valuable. The Kızılcaören carbonatite

deposit is the largest in Turkey, with a good grade of REEs, having thorium along with REEs. This reserve is estimated to have 0.95 MT of REOs, 11.37 MT of fluorite, 9.42 MT of barite, and 0.38 MT of thorium. The main RE mineral is bastnasite, and the major composition of this deposit is 37.44% CaF_2, 31.04% $BaSO_4$, 2.01% Ce, 0.39% Nd, 0.20% Th, and traces of other REEs (Turker et al., 2023; Zeki Çizmecioğlu et al., 2018). Kuluncak is another RE-bearing Fluorite deposit with bastnasite minerals and apatite, calcite, and quartz. Furthermore, Keban and Divriği deposits also contain LREEs (Öztürk, Altuncu, et al., 2019). Some of the bauxite deposits in the Taurus area have a substantial amount of REEs. Bauxites from the Mortaş deposit contain about 282-986 ppm of total REEs. Whereas the red mud waste from the Seydişehir alumina smelter has total REEs of about 1777 ppm and 80 ppm of Y. Other notable bauxite deposits are Yalvaç-Şarkikaraağaç and Bolkardağı, which are enriched with HREEs. In terms of placer deposits, the Burdur region in Çanaklı is the most attractive, having total REEs in the range of 627-808 ppm (Öztürk, Altuncu, et al., 2019; Öztürk, Hanilçi, et al., 2019).

1.3 Physical and chemical properties of REEs

REEs are silver-tinted, soft, ductile metals with a high melting point that tarnishes easily in the air. They have unique and sharp absorption and emission spectra due to their electrical properties and unique colors in solution. One of their most important properties is the magnetism. Most REEs are strong paramagnetic elements and are connected with transition metals like Fe and Co (Klinger, 2015; Wall, 2021).

Despite the similarity of the REEs' physical and chemical characteristics, the lanthanide series causes several of these characteristics to shift gradually and smoothly. Contrary to popular belief, lanthanide cation size decreases gradually with increasing atomic number, which is one of the most crucial characteristics in influencing chemical behavior. This phenomenon is called the lanthanide contraction (Figure 1.3). Generally speaking, REEs are found in the +3 valence state in nature, which forms the oxide (RE_2O_3). However, Ce^{3+} is oxidized to a smaller Ce^{4+} (CeO_2)

cation in oxidizing environments, while Eu produces the larger Eu^{2+} cation in reducing environments. Furthermore, Sm, Tm, and Yb are also found in the laboratory in the +2 valence state (Dushyantha et al., 2020a; Wall, 2021).

Table 1.2: Some properties of REEs (Wall, 2021)

Element	Atomic number	Atomic weight	Density at 25 °C (kg/m^3)	Melting point	Cation radium (pm)	Color of +3 cation in solution
Sc	21	44.96	2992	1541	87	Colorless
Y	39	88.91	4475	1522	107.5	Colorless
La	57	138.91	6174	918	121.6	Colorless
Ce	58	140.12	6711	798	119.6	Colorless
Pr	59	140.91	6779	931	117.9	Yellow-green
Nd	60	144.24	7000	1021	116.3	Rose
Pm	61	144.91	7220	1042	-	Pink
Sm	62	150.36	7536	1074	113.2	Yellow
Eu	63	151.96	5248	822	112	Colorless
Gd	64	157.25	7870	1313	110.7	Colorless
Tb	65	158.93	8267	1356	109.5	Pale pink
Dy	66	162.50	8531	1412	108.3	Pale yellow-green
Ho	67	164.93	8797	1474	107.2	Yellow
Er	68	167.26	9044	1529	106.2	Pink
Tm	69	168.93	9325	1545	105.2	Greenish tint
Yb	70	173.04	6966	819	104.2	Colorless
Lu	71	174.97	9842	1663	103.2	Colorless

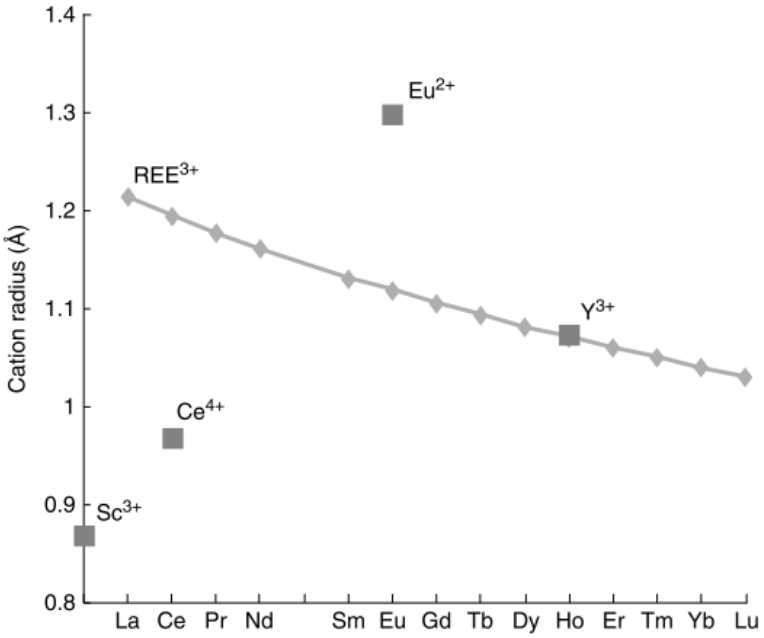

Figure 1.3: Lanthanides contraction (Wall, 2021)

1.4 Uses of REEs

An extensive amount of research has examined REMs' place in the modern economic era and evaluated how much they have contributed to scientific and technological advancements. They are considered essential for green technologies in addition to their strategic values, and on occasion, they are referred to as the "vitamins of modern society." The competition for exploiting these elements is forecasted to be compared with that of the oil business. Their diverse applications stem from their exceptional properties, including magnetic, luminescent, and catalytic properties. These characteristics make REEs crucial in producing state-of-the-art products, green energy technologies, and numerous other industrial processes. The current hurdles in supplying the industry with the necessary REEs significantly hamper the nation's progress in science and technology, particularly in areas like green energy and low-carbon development (Cherepovitsyn & Solovyova, 2022; Dushyantha et al., 2020a).

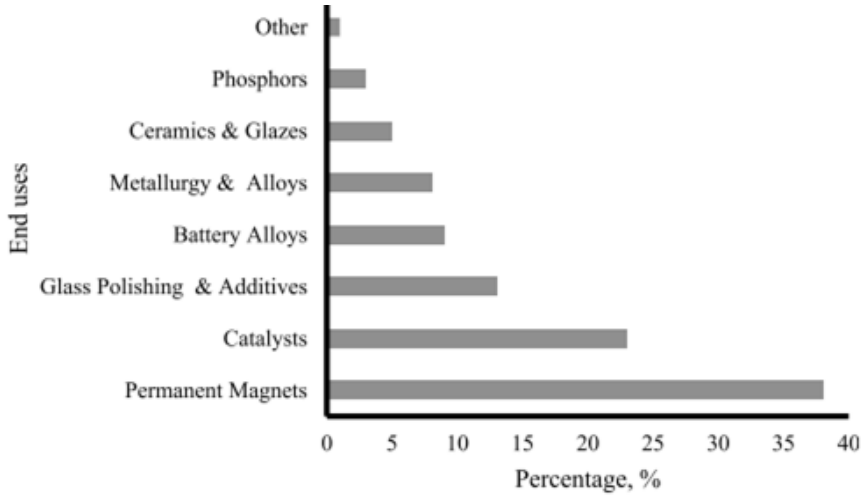

Figure 1.4: Percent uses of REEs in different products (Patel et al., 2023)

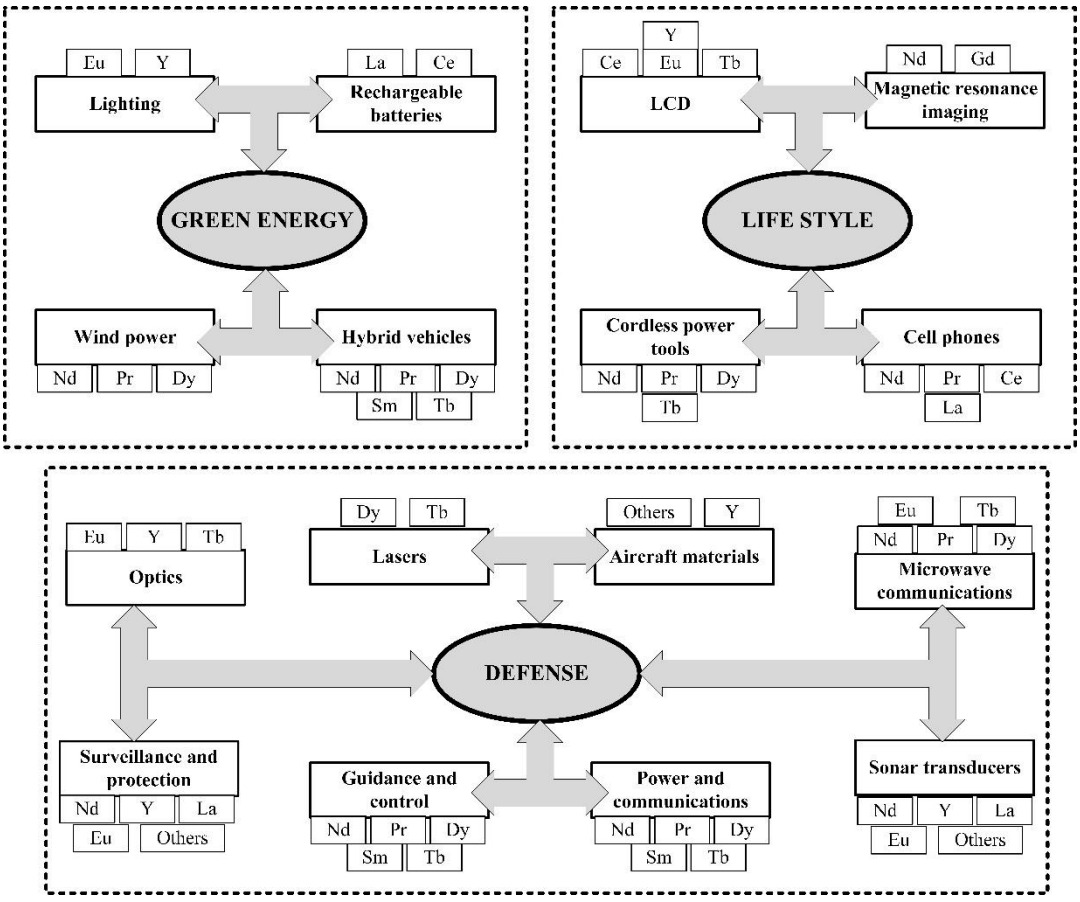

Figure 1.5: Commercial uses of REEs (Krishnamurthy, 2020)

Table 1.3: Some commercial applications of REEs (Xie et al., 2014)

Application	Technology	REEs
Hybrids, plug-ins, and electric vehicles	RE permanent magnet	Nd, Pr, Dy, Tb
Wind and hydropower generation	RE permanent magnet	Nd, Pr
Computer disc drivers	RE permanent magnet	Nd, Pr, Dy, Tb
Medical imaging - MRI	RE permanent magnet	Nd, Pr, Dy, Tb, Y, Eu
Flat screen display	RE phosphors	Y, Eu, Tb, Gd, Ce
Catalytic converters and other emission-reduction technologies	Ability to oxidize CO and ozone to CO_2 and O_2	Ce, La
Fiber optics	RE doped optical fibers	Y, Eu, Tb, Er
Ni metal hydride batteries	Energy storage	La
Capacitors with high energy density	RE doped ceramic, tantalum, and other types of capacitors	Various REEs

Nowadays, REEs are being used in different chemical forms for several products. The primary usage of REEs is in producing permanent magnets in which Pr, Nd, Dy, and Tb are used. Catalytic compounds employ La and Ce as stabilizers, which accounts for the second-highest consumption of REEs. Light-emitting diodes (LEDs) and compact fluorescent lights (CFLs) use REEs in their high-efficiency lighting phosphors because of the fluorescence properties of some of the REEs. The famous example, Eu, became a highly sought-after REE along with Tb and Y due to their use as a color-producing phosphor on television screens. REEs are referred to as "The Vitamins of Modern Industry" because of the way they have accelerated efficiency improvements and reduced the demand for additional materials in modern technology (Dushyantha et al., 2020b; Patel et al., 2023; Xie et al., 2014).

1.5 Sustainability of REEs supply

Growing global economic growth rates and advances in material applications have enormously raised the demand for REEs during the past several decades. By launching color televisions in the 1960s, RE demand saw its initial rapid surge. Due to REEs' widespread use in clean technologies, their demand is escalating continuously. Similarly, the cost of REOs is rising in line with demand (Amato et al., 2019; Dushyantha et al., 2020b; K. Zhang et al., 2017).

According to the Department of Energy (DOE) USA, elements including Dy, Nd, Tb, Eu, and Y are in a critical position, and Ce and La are on the verge of becoming critical (Jyothi et al., 2020). In contemporary applications, various rare earths are required to meet the demand. Some applications only require a single REE, like La in nickel-metal hydride batteries, while others claim a combination of REEs, such as RE magnets, need both Nd and Pr (Dushyantha et al., 2020a; Xie et al., 2014). Wind turbines, and hybrid and electric cars will be the primary sources of NdFeB magnet consumption until 2026. However, additional demand growth will be supported by the magnets' use in other applications. Rare earth permanent magnets are expected to be used more often in the motors and sensors of robotic production machinery as manufacturing processes in most developed countries become more automated and will need more supply of these REEs (Goodenough et al., 2018).

REE supply and production have changed significantly worldwide over the past few decades. The key producers of REEs up to 1948 were India and Brazil, but during the 1950s, South Africa took over this position. The Mountain Pass Mine Corporation in the USA served as the world's leading supplier of REOs from the 1960s to the 1980s, and the USA assumed a dominating position in the international market. However, by the 1990s, China had surpassed all other countries regarding reserves and managed the supply chain of the world by producing more than 90% of global REE demand (Bartolomeo et al., 2021; Klinger, 2015).

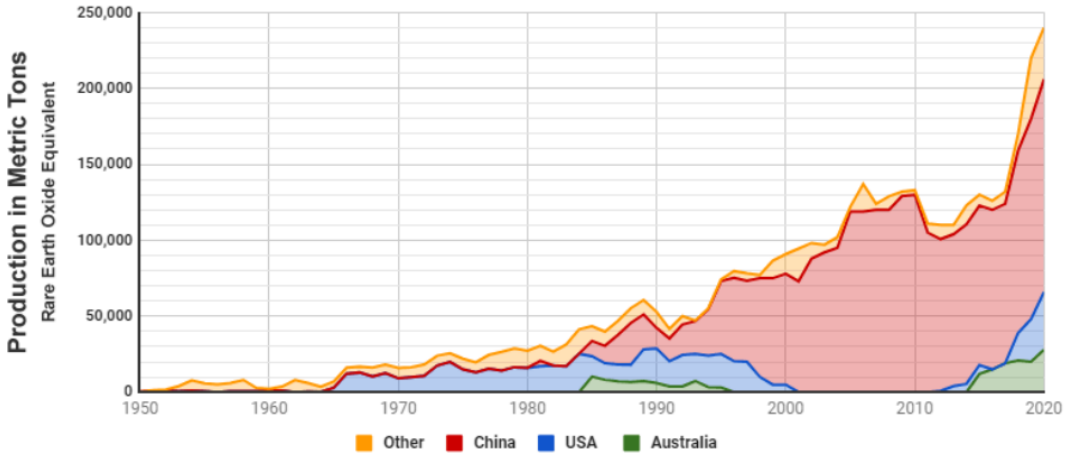

Figure 1.6: REEs production history (King, 2019)

Due to several factors, including the abundance of REE reserves in the country, lower labor and regulatory costs, and rising production and export of manufactured goods, including electronic goods, China has gradually become a dominant player in the world market for REEs. In addition, the Mountain Pass mine closure in 2002 because of environmental concerns further aided China's hegemony. At the time, China, the key producer of REEs, produces about 95% of the world's demand for REEs. Furthermore, China manufactures rare earth permanent magnets exceeding 90% of the world's production, giving the country a solid competitive edge. The production of Tb, Dy, Lu, and other HREEs, as well as other REO exports, from China since 2009, has dropped, which has caused a decline in overall worldwide REO production. This is because of the need to control illegal mining and smuggling as well as the fast-growing demand for REEs in the local Chinese market. These restrictions stimulated other countries to start REE production, and several projects were started around the world (Bartolomeo et al., 2021; King, 2019; D. Li et al., 2004; Wang et al., 2013; Xie et al., 2014).

A study revealed that there are about 146 ongoing projects in the world for the production of REEs, including the active mines and the advanced projects on 126 deposits, and these projects are run by 84 companies. These deposits have about 303.4 million tons of REOs, and most of the production from these deposits is met by carbonatite deposits (Liu et al., 2023).

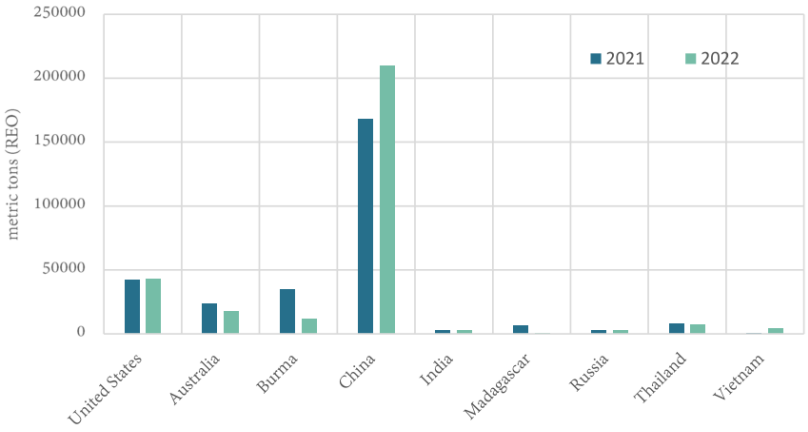

Figure 1.7: Worldwide production of REEs (Bartolomeo et al., 2021)

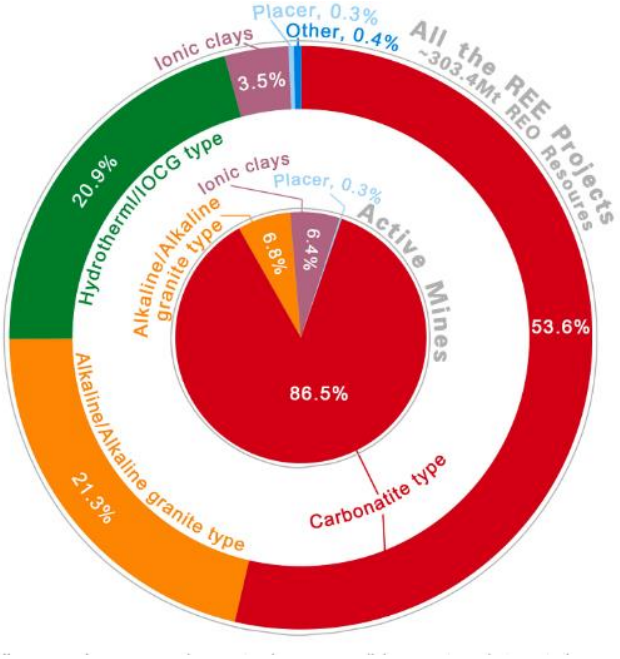

Figure 1.8: Proportion of different REE resources and active mines around the world (Liu et al., 2023)

A study found that the deposits of REEs in China, USA, Russia, Australia, and other countries make up roughly 36%, 13%, 19%, 3.5%, and 5.5%, respectively, of the total global reserves (A. R. Jha, 2014). Whereas Turkey has a share of about 0.09% in the global RE reserves (Chen, 2011).

Sustainable methods (such as urban mining and e-waste recycling) can be among the leading suppliers to fulfill the forthcoming demand of markets because of the high

usage of REEs in consumer electronics (Z. Li et al., 2019; Tansel, 2017). The recovery of these elements from secondary sources and end-of-life supplies also includes extraction from coal and coal ash. Compared to REE-bearing ores, coal fly ashes, generated during coal burning, contain a more significant fraction of crucial REEs. They may become the ideal future source of REEs if suitable, cost-effective recovery techniques are created (Dushyantha et al., 2020b; Rybak & Rybak, 2021).

1.6 Ore processing

Several processing methods have been developed to extract REEs from commercially important ores of RE minerals. After mining and comminution, physical separation methods such as gravity/magnetic/electric separation and flotation beneficiation are used to process these ores. The chosen approach is determined by the mineral's characteristics, the quality of the products, financial gain, and the overall environmental effects. The concentrate of these physical techniques is subjected to leaching with acid or alkaline solutions. In the case of acidic leaching of bastnasite, the carbonate minerals are decomposed by roasting the concentrate before the leaching operation, which reduces the consumption of acid. In this roasting process, Ce^{3+} is also oxidized to $Ce^{4+,}$ which is not dissolved in the acid lixiviant and is selectively recovered from other REEs at this initial stage. A leach solution having almost all of the REEs in the ore is usually obtained by the leaching operation because of the similar characteristics of REEs that are to be dissolved in the lixiviants. This leach solution is further processed through ion exchange (IX) and solvent extraction (SX) processes to recover individual REEs. Because SX can handle large volumes of diluted pregnant liquors, it is now regarded as the most commercially feasible approach for separating rare earth elements. Furthermore, precipitation is mostly done to decontaminate the solution before solvent extraction because the leachate typically contains contaminants, including iron, aluminum, and thorium (Cen et al., 2021; Hidayah & Abidin, 2018; Kumari et al., 2015; Pereao et al., 2018; Wu, Wang, Zhao, et al., 2018; Xie et al., 2014).

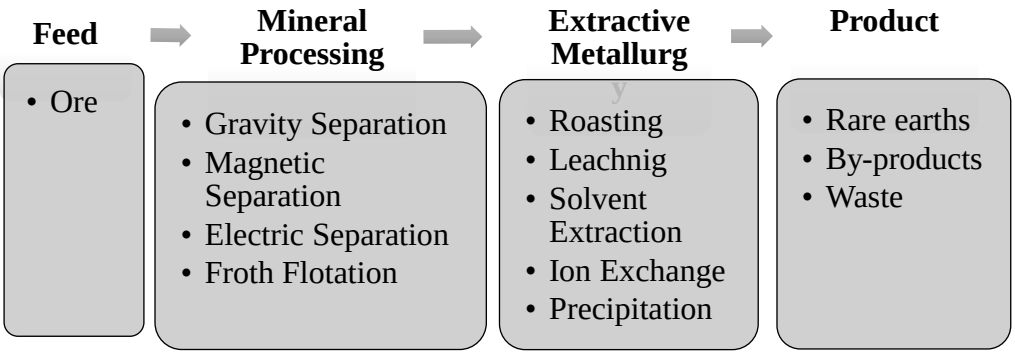

Figure 1.9: Schematic diagram for rare earth ore processing (Cen et al., 2021)

1.7 Dissertation outline

This dissertation consists of six chapters. Following Chapter 1, which gives an introduction to rare earth elements along with their supply and demands, the outline of each chapter is as follows:

- Chapter 2 elaborates on the research problem, research approach, and, finally, the scope and significance of this work.
- Chapter 3 discusses the literature review on conventional solvent extraction methods, types of organic solvents, and the previous work done to separate REEs using DEHPA.
- Chapter 4 contains the details of the materials and reagents used in this work, along with the details of the experimental setup, experimental procedure, and analysis conducted to determine REEs.
- Chapter 5 shows the experimental results and the discussion on the effect of different operational parameters.
- Chapter 6 represents the overall summary of this work as well as the major conclusions and finally provides recommendations for future studies.

CHAPTER 2

PROPOSED RESEARCH

2.1 Problem statement

REEs are critical raw materials for advanced technologies, and their demand has escalated sky-high with the increase in green technologies. This demand makes every country struggle for the supply of these elements to fulfill the needs of their local industry. Up to 2009, there was no issue importing REOs since China, the biggest producer of these elements, used to export these elements to the world. However, after 2010, China reduced the export of these REOs and increased the price. This was due to the rapidly growing demand for the local Chinese market, as reported by China. As can be seen from the usage of REMs, these are economic and strategic assets, making their supplies crucial for every country. This restriction from China motivated other countries to produce REEs from their indigenous resources. Still, there are a few producers worldwide, China being the largest by far and controlling the market. Like other countries, Turkey is also exploring its RE resources and planning to get their production. Turkey has some valued RE resources; out of them, the bastnasite deposit in Beylikova, Eskişehir, is the most promising in REEs. A new administrative body, namely Nadir Toprak Elementleri Araştırma Enstitüsü (NATEN), was founded in 2018 to do research on REEs in Turkey and produce REOs to fulfill the demand of the local market.

In general, REEs are leached with acid and recovered with solvent extraction. Conventional solvent extraction is usually accomplished through mixer-settler processes, which involve many extraction stages for good selectivity and recovery. The problem with these mixer settlers is the inefficient mass transfer in the mixing section and the slow kinetics of separation operation in the separation section.

Therefore, many extraction and stripping stages are required for the final product, making it costly in terms of money and time.

2.2 Research approach

This work aims to increase the recovery through efficient mass transfer and improve the kinetics of solvent extraction operations. Mass transfer in the mixer-settler is low, and phase separation is inefficient because of the poly-dispersed droplet production inside the mixing section and the geometry of the settling section, respectively. Mass transfer efficiency can be increased with the production of mono-dispersed droplets with the help of a spray nozzle. (Shimogouchi et al., 2019) conducted an experiment to analyze the size distribution of droplets produced close to the mixing equipment (a spray nozzle for aqueous spraying or an impeller head for mechanical mixing). The shape and volumes of the vessels for the two devices were the same to have an equal volume of aqueous phases. When a liquid was sprayed, the mono-dispersed droplets produced were densified and agglomerated to one another at random, and as a result, they were emulsified. A clear phase separation was observed in this case. Whereas mechanical mixing produced the emulsion by generating poly-dispersed droplets, and in this case, the emulsion was difficult to separate into two distinct phases.

A setup was developed to enhance the efficiency of SX operation, considering the pros and cons of all the conventional SX techniques. The designed setup consists of separate mixing and separation/settling columns. The mass transfer between the immiscible phases is achieved in the mixing column, and the mass transfer process is boosted by the production of mono-dispersed micro-droplets of both phases using the spray nozzles. The separation column, by its unique design, not only generates clear phases but also separates these phases swiftly and produces a high-quality product, thus increasing the kinetics of separation along with the quality of the product.

2.3 Research significance

Every industry strives to find efficient and economical methods of producing their end products without compromising their qualities. The supply of REEs is a dire need for the growth of modern industries, and competition for their production has been generated among the countries. The widely used mixer-settler system in the solvent extraction operation of REEs is not very attractive in terms of mass transfer, product quality, and kinetics of the overall system. This study will provide the foundation for a potential, completely new system for the solvent extraction of REEs. The designed setup is more attractive in terms of cost, time, and final product quality compared to the mixer-settler.

CHAPTER 3

LITERATURE REVIEW

3.1 REEs extraction processes

In the geological environment, REEs are primarily found as carbonate and phosphate minerals, which substitute for other elements in the mineral matrix. These days, bastnasite [(Ce,La)(CO_3)F] and monazite [(Ce,La,Nd, Th)PO_4] are the most valuable commercial REEs minerals. Because of the substitution-dominated character of REEs, these materials' extraction, concentration, and processing may differ depending on the characteristics of the ore. These intricacies are extra risk factors that should be considered when planning mining and processing procedures for REEs, and building expensive processing facilities may prevent the mining of ore bodies with lower grades of REEs. This indicates that low-grade deposits could only be economically viable to develop if they are sizable because doing so would require costly infrastructure with lengthy payback periods, which would make it impossible to sell to shareholders during challenging economic situations (Weng et al., 2014).

3.1.1 Physical treatment/beneficiation operations

When attempting to extract the valuable elements from the ore mineral, it is typically more cost-effective to concentrate the ore minerals and eliminate as many gangue minerals as feasible. Following the same technique, bastnasite and monazite are liberated from their surrounding minerals and subsequently concentrated by physical methods followed by flotation (Wall, 2021). The primary means of pre-concentrating RE minerals are to take advantage of variations in the specific gravity, surface chemistry, magnetic, and electrical characteristics of the RE and gangue minerals. Flotation collectors specific to REMs are commonly used in the flotation of these

elements. However, other gangue minerals, such as iron oxide minerals, might also be recovered using these reagents. Under such circumstances, physical separation techniques can eliminate these gangue minerals before or after froth flotation (Jordens et al., 2013, 2016). The mostly used methods for physical separation are:

- Gravity separation
- Magnetic separation
- Electrostatic separation
- Froth Flotation

3.1.1.1 Gravity separation

The specific gravities of REE minerals are high, ranging from 4 to 7, allowing the use of the multi-gravity separation (MGS) technique to concentrate them by removing gangue minerals with lower specific gravities, including quartz. The most popular use of gravity separation is in the beneficiation process of monazite. To obtain a concentration of up to 90% of heavy minerals from beach sand, cone concentrators are first used to concentrate it up to 30%, followed by concentration with spiral concentrators. Gravity separators are used in different sequences with magnetic and electrostatic separators, subject to the mineralogy of each ore body (Abaka-Wood et al., 2016; Jordens et al., 2013, 2016).

3.1.1.2 Magnetic separation

The bulk magnetic properties of REEs indicate that the LREEs are less paramagnetic than the HREEs. Magnetic separation is often utilized at the initial stage of RE mineral beneficiation to reject ferromagnetic materials. The magnetic susceptibilities of REEs from Gd to Er are the highest compared to other lanthanides, which are responsible for the three-times increase in magnetic susceptibility of xenotime in comparison to monazite. Magnetic separators are essential, in addition to gravity

separation, to beneficiate monazite from beach sands. At the initial stage, low-intensity magnetic separators are employed to reject ferromagnetic gangues. Whereas, at the later stage, high-intensity magnetic separators are used to separate paramagnetic monazite from rutile and zircon. Similarly, xenotime, which is stronger paramagnetic compared to monazite, is also separated from gangues (Abaka-Wood et al., 2016; Jordens et al., 2013, 2016; X. Yang et al., 2015).

3.1.1.3 Electrostatic separation

Electrostatic separation uses the variations in conductivity of various minerals to separate them. The electrostatic separation technique has separated Xenotime and monazite from gangue minerals. Due to their reversible negative charge, the majority of the monazite grains were drawn to the static electrode that was positively charged (Abaka-Wood et al., 2016; Jordens et al., 2013, 2016).

3.1.1.4 Froth flotation

By taking advantage of variations in the wettability of their surfaces, minerals can be separated using froth flotation. It has proven extremely important for the beneficiation of complex and low-grade ores, which are costly to process (Abaka-Wood et al., 2016). Compared to other beneficiation methods, froth flotation of RE minerals has been the subject of comparatively extensive investigation. The studies have mostly concentrated on the surface characteristics of monazite and bastnasite in relation to flotation response and flotation tests conducted in facilities like Mountain Pass and Bayan Obo (Jordens et al., 2013).

The flotation process may differ for various RE minerals; however, fatty acids and hydroxamates are usually used as collectors for these minerals. An increase in surface hydrophilicity of gangue minerals is achieved by coating them with depressants. In contrast, hydrophobicity of REE mineral surfaces is achieved by treating them with fatty acids or alkyl hydroxamate for selective flotation. The

findings of all the studies indicated that the recovery of selected RE minerals using flotation requires mineral liberation, which is the key to selective recovery (Abaka-Wood et al., 2016; X. Yang et al., 2015).

3.1.2 Hydrometallurgical operations / chemical treatment

Hydrometallurgy and pyrometallurgy are the techniques utilized in the industry to recover the REEs and their selective separation. The disadvantage of pyrometallurgy is that it requires a high reaction temperature and energy expenditure for the calcination of the feed using a combination of fluxing and reducing chemicals. In addition to these negative aspects, it produces significant amounts of greenhouse gases (SO_x, NO_x, CO_2, and CO) (GHGs) (J. Zhang et al., 2018).

Hydrometallurgy is one of the most effective chemical techniques for extracting REEs and other valuable metals. Leaching, solvent extraction (liquid-liquid extraction), solid-liquid extraction, and precipitation are the hydrometallurgical processing steps used to recover REEs. The main advantages of hydrometallurgy are its cheap production costs, little solid waste formation, and low levels of harmful gases, which make it a clean and environmentally safe method. The ore is initially chemically leached in hydrometallurgical processing, and then it is purified using one of the following techniques: liquid-liquid/solid-liquid extraction or precipitation. Due to its broad range of applications and dependable features, solvent extraction (SX) technology is used for the bulk of RE extractions throughout downstream separation operations (M. K. Jha et al., 2016; Yoon et al., 2016).

3.1.2.1 Leaching

Ore leaching is the initial stage of hydrometallurgical processing, and RE minerals are usually leached with acids like H_2SO_4, HCl, and HNO_3. Under normal circumstances, the RE minerals are not readily soluble because they are either fluorocarbonates (bastnasite) or phosphates (monazite and xenotime). Because of

this, leaching is mostly done in plants and laboratories after these ores are roasted and combined with sodium hydroxide or sulfuric acid. The literature indicates that the following sequence represents the greatest dissociation constant (K_e) values for the decomposition of REE oxides in acid: Oxides > carbonates > phosphates > sulfates > fluorides > oxalate. This shows that REEs readily precipitate with oxalate, followed by fluoride, and so on. Moreover, REEs are easily precipitated when leaching is employed using H_2SO_4 (Demol et al., 2019a; Han et al., 2014).

Numerous researchers have worked on bastnasite leaching and found the possibility of leaching finely milled bastnasite ores in acidic solutions without applying heat beforehand. Nevertheless, roasting with sulfuric acid or alkali before leaching has been employed in most REEs extraction studies from bastnasite ores. It is a common procedure to bake it with H_2SO_4 at 200–300 ^oC, followed by leaching it with water or a weak acid. In the case of alkaline roasting, the ores are often combined with caustic soda or soda ash, roasted at 400–500 ^oC, and then acid-leached (Han et al., 2014; Zou et al., 2020). Molycorp developed the oxidative roast and acid leach process to produce REEs at Mountain Pass, which was later replaced by a caustic conversion procedure. China also treats bastnasite concentrates using an oxidative roast/acid leach procedure, and it has been reported that caustic conversion is used to convert about 10% of the Bayan Obo concentrate (Demol et al., 2019b; Friedrich, 2012; Guo et al., 2018).

Monazite and xenotime are often heated to 400–600 ^oC using sulfuric acid or alkali compounds and then leached. The only industrial process technique for monazite is baking with strong sulfuric acid or digesting in caustic soda. The industrial preferred technique for treating high-grade monazite sands is caustic conversion, whereas lower-grade ores and concentrates are usually treated with sulfuric acid bake. Monazite having Th and U along with REEs is one of the main distinctions between REE-phosphates like monazite and xenotime and REE-fluorocarbonate like bastnasite. Therefore, after digestion, there ought to be more procedures involving the elimination of Th. It is worth noting that most REEs leach with RE^{3+} in solution because of their stability in the aqueous phase in this valence state. On the other

hand, some elements, like Ce, Pr, and Tb, can be oxidized to the +4 valance and separated from the solution due to the extremely low solubility of these MeO_2. Conversely, +2 valence is a characteristic of REEs like Sm, Eu, Tm, and Yb that distinguishes them from other elements. Specifically, Eu and Sm can be reduced to the +2 valance, precipitate as sulfates, and separate from other REEs (Demol et al., 2019a; Han et al., 2014).

3.1.2.2 Solvent extraction

Many studies on the leaching of REEs have been published; however, because of their similar chemical behavior, the primary unfinished and challenging task is their separation from the solution, either individually or collectively. Ion exchange (IX) technology was the sole practical means of extracting REEs before large-scale SX was developed on an industrial scale in the 1960s. Nowadays, SX is typically considered the best commercial approach for extracting REs because it can handle massive volumes of diluted pregnant liquors. Many plants currently use this technique to extract mixed REEs into separate LREEs, MREEs, and HREEs (Battsengel, Batnasan, Haga, et al., 2018; Dashti et al., 2021; Xie et al., 2014).

SX involves transferring ions between immiscible liquids to separate or purify particular elements. The valued component is occasionally removed from the original solution, leaving the impurities in the feed solution and vice versa (Poole, 2020). SX involves the diffusion of ions between the immiscible phases, and sometimes, many stages of phase mixing and interaction are required for the complete transfer and extraction of ions. The general reaction between the aqueous and organic phases is represented by Equation 3.1 (Izzaty et al., 2004);

$$M_{aq}^{n+} + nHA_{org} \leftrightharpoons MA_{n_{org}} + nH_{aq}^{+} \qquad 3.1$$

On mixing the two immiscible solutions, the mass transfer takes place depending on the distribution ratio of the target ions in the solutions (Izzaty et al., 2004).

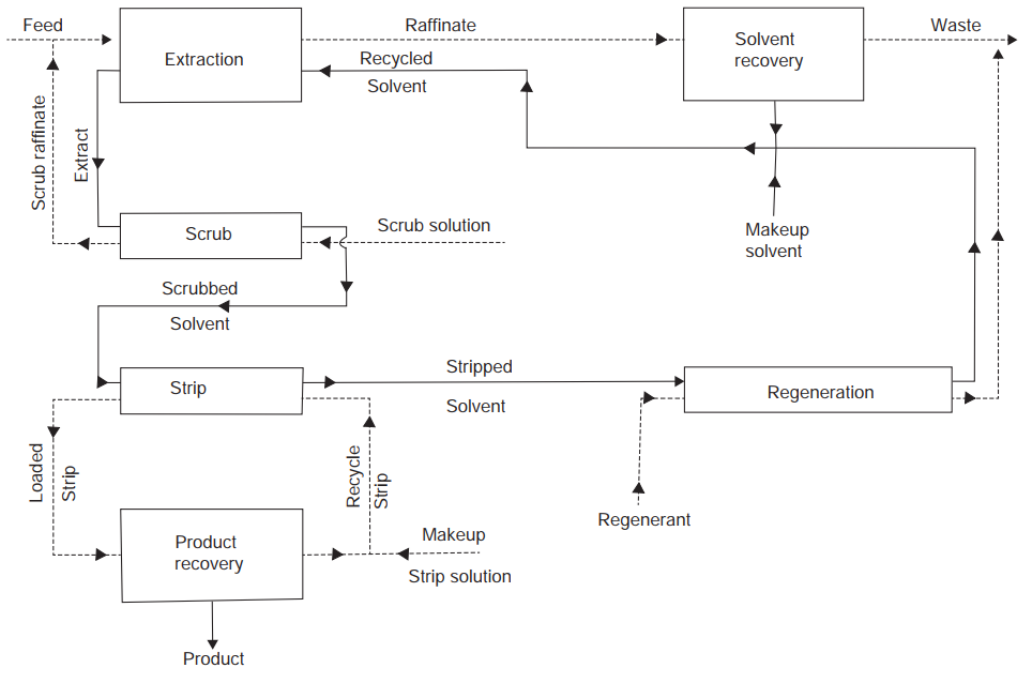

Figure 3.1: Process flow diagram of SX operation (Kislik, 2012b)

Following are the fundamental processes in SX operation, which are shown in Figure 3.1:

- Extraction
- Scrubbing
- Stripping
- Regeneration of organic solvent

Both the desired and unwanted components are present in the feed solution. During the extraction stage, the two phases come into contact, and mass transfer occurs, transferring values from the aqueous to the organic solvent. After passing through the extraction stage, the unloaded aqueous phase, the raffinate, is further processed to recover the byproducts and unseparated solvent, which is recycled to the extraction stage. Following the extraction step, a scrub stage may be added to remove some unwanted impurities from the extract using a scrubbing solution. The extracted or scrubbed extract moves to the next stripping stage, where the required component is recovered using a stripping aqueous solution. The desired component is eventually

collected from the loaded strip solution during the product recovery phase. After being stripped, the solvent can either be recycled straight to the extraction stage or go through a regeneration stage to change its chemical composition back to what is needed for effective extraction (Kislik, 2012b).

Every step in the simplest procedure consists of a single stage; however, in the industry, each stage consists of multiple steps that improve the product's recovery. Furthermore, the stage-wise extraction step can be:

- Cross-flow
- Counter-current

If the fresh solvent is used to re-extract the raffinate at the same phase ratio as the first extraction, the inadequate degree of extraction can be enhanced with a similar purity in the second extract. Combining the first and second extracts results in a superior overall recovery than extracting in a single stage (Kislik, 2012a, 2012b).

3.2 Efficiency and kinetics of solvent extraction

A solute disperses between two immiscible feed streams in SX operation until the equilibrium condition is reached. The right choice of solvents and the concurrent modification of several factors, including solvent amount, pH, additives, ionic strength, extraction technique, etc., might result in the desired separation (Izzaty et al., 2004; Poole, 2020). The following are some parameters that determine the efficiency of the solvent extraction process.

Extraction efficiency (E)
$$\%E = \frac{[\mathrm{RE}]_{in} - [RE]_{eq}}{[RE]_{in}} X\ 100 \qquad 3.2$$

Distribution ratio (D)
$$D = \frac{[RE]_{in} - [RE]_{eq}}{[RE]_{eq}} \times \frac{V_a}{V_o} \qquad 3.3$$

Separation factor (SF)
$$SF = \frac{D_1}{D_2} \qquad 3.4$$

Stripping efficiency (S) $$\%S = \frac{[RE]_{eq} \times V_a}{[RE]_{o,in} \times V_o} \times 100 \quad (3.5)$$

Where $[RE]_{in}$ and $[RE]_{eq}$ are, respectively, the metal concentrations at the initial and equilibrium states of the aqueous phase, while V_a and V_o are the volumes of aqueous and organic phases. Moreover, D_1 and D_2 denote metal 1 and metal 2 distribution ratios, and $[RE]_{o,in}$ is the initial concentration of the solute loaded in the organic stream (Su et al., 2021).

The distribution ratio represents the proportion of ions in the loaded solvent at equilibrium with reference to its total concentration in aqueous feed. This term defines how easily and completely ions' transfer takes place towards the organic solvent. The greater value of this term shows an easy and complete extraction, which is actually a requirement for the SX process to be effective and efficient. The D value of 1.0 represents the equal distribution of metal between the two solutions. Furthermore, the separation factor, which is a ratio between the distribution ratios of two elements (D_1/D_2), represents the separation of two metals. A separation factor equal to 1 shows that the metals under study are not separable from each other, and the selectivity increases as the value goes above 1. For processes with small values of separation factors, complete separation of individual elements will be achieved with many extraction stages (Izzaty et al., 2004; Kislik, 2012b; Moyer, 2019).

Furthermore, McCabe Thiele diagrams are built, which define the theoretical number of extraction, scrubbing, and stripping stages for maximal recovery at a specific phase ratio (Ouchi et al., 2022; Xie et al., 2014). Connecting extraction or stripping points at the aqueous:organic (A:O) ratio first creates the equilibrium curve. After that, the x-axis is used to draw a feed line vertically. Thirdly, an operating line is drawn between the equilibrium curve and aqueous feed concentration. Afterward, draw a vertical line from the equilibrium curve to the operating line and a horizontal line from the feed solution line to the equilibrium curve. Repeating this process until no more horizontal line can be drawn gives the number of theoretical stages for complete recovery (Joo et al., 2017).

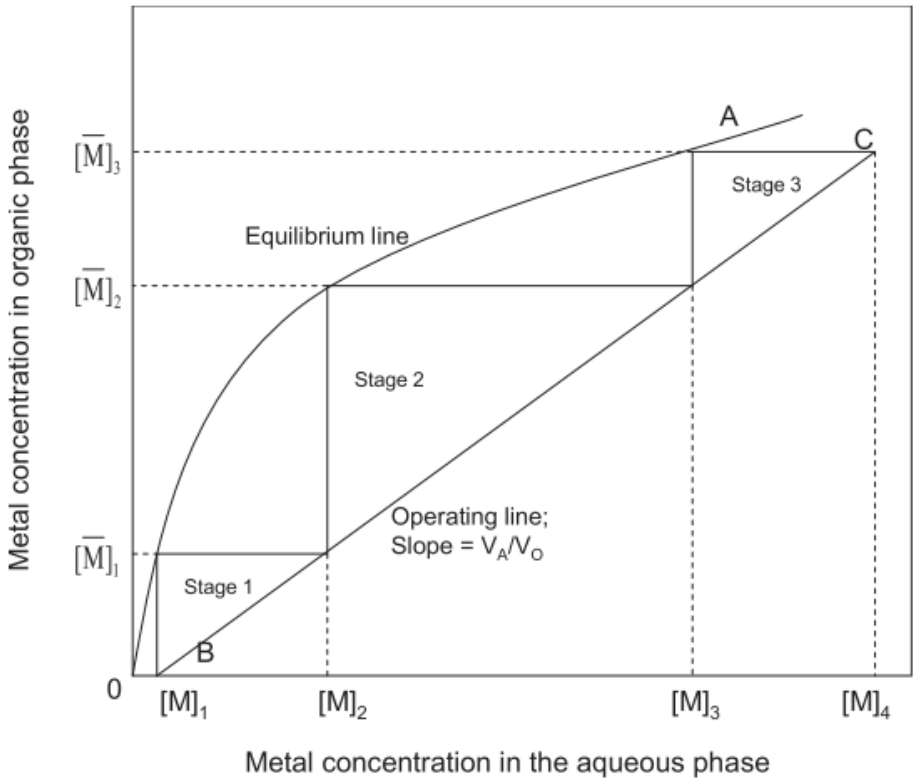

Figure 3.2: McCabe Thiele diagram for counter-current SX operation (Xie et al., 2014)

In Figure 3.2, $[M]_1$, $[M]_2$, and $[M]_3$ are respective molar concentrations of target ion in the raffinate leaving stages 1, 2, and 3, and aqueous feed concentration is $[M]_4$. Whereas, $[\bar{M}]_1$, $[\bar{M}]_2$ and $[\bar{M}]_3$ are the molar concentrations of the target ion in the organic phase, leaving stages 1, 2, and 3. V_A and V_O represent the flow rates of aqueous and organic streams, respectively (Xie et al., 2014).

The kinetics of SX extremely relies on the movement of the ions to and from the interphase, and it is proportional to the concentration gradient of the solute in the system along with the distribution ratio of that ion in the system. This kinetics is enhanced by phases' agitation in most SX equipment. The kinetics of chemical reactions can significantly influence the total kinetics of the extraction process. Therefore, there is a need to opt for such methods and solvents that not only increase the reaction kinetics but also the diffusion of solute (Izzaty et al., 2004; Kislik, 2012b).

3.3 Solvent extraction equipment

Improving the fluid dynamics and interfacial phenomena that control mass transport, as well as phase separations, are the primary goals of improvements in SX equipment design. Effective mass transfer depends on enhancing the interfacial shear between the two phases (droplets and the continuous phase) and droplet instability. After mass transfer, effective separation of the product streams is the second important component of the operations. This is crucial to maintain the product quality by minimizing the amount of trace elements from the other phase (Weatherley, 2020).

Following are the major equipment being used in the SX industry;

i. Mixer settlers

ii. Continuous columns

iii. Centrifugal extractors

Most contemporary high-performance contact equipment uses turbulence for liquid mixing to ensure high mass transfer rates by applying mechanical energy (Weatherley, 2020).

3.3.1 Mixer settler

Mixer settlers, consisting of stirred tanks and settlers, have proved to be the backbone of major commercial SX industries. A classical mixer settler is shown in Figure 3.3.

With reference to Figure 3.3, the unit's left-hand side displays the mixing chamber, which has an impeller mounted on a vertical drive shaft. Getting a constant flow while maintaining thoroughly mixed conditions inside the mixing tank is an essential mixer design criterion. Several factors are crucial to achieving uniform mixing in this situation, including the mixing impeller's design, rotation speed, placement in relation to the mixing chamber base, baffle design and placement, and operating circumstances. One of the challenges in solution mixing is the necessity to prevent

the creation of a stable emulsion while simultaneously creating an interfacial area for significant mass transfer by dispersion (Kislik, 2012b; Weatherley, 2020).

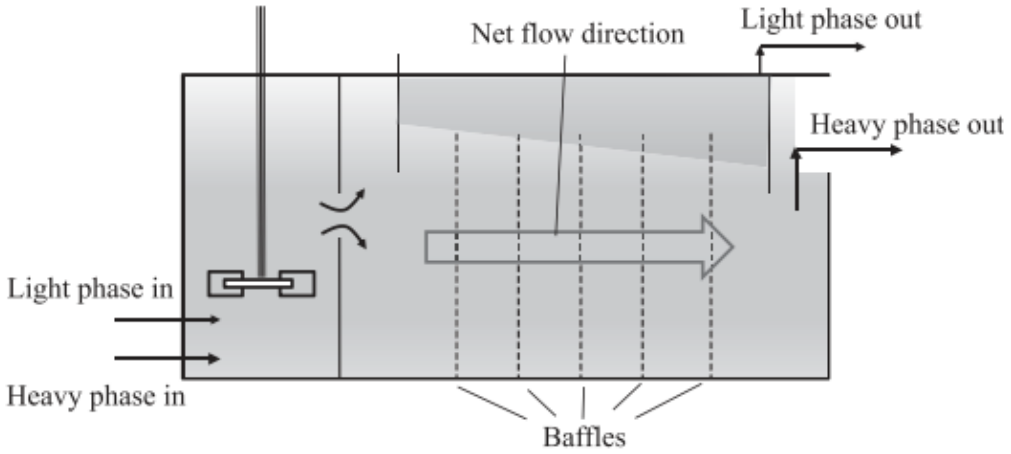

Figure 3.3: Mixer settler with baffled settling chamber (Weatherley, 2020)

The emulsion generated then enters the settling chamber, where both immiscible phases should ideally separate completely by optimizing the settling time and the hydrodynamic environment therein. Product loss, solvent loss, and under-quality products will be the outcomes in case of contamination in any of the outlet streams, in addition to environmental problems. In general, the separation is achieved by settling under gravity, whereas it can be boosted by centrifugal force and coalescence by adding some flocculant. Gravity settling is, however, opted for mainly because of its cost-effectiveness. In gravity settling, separation is based on the difference in phase densities addressed by Stokes' law and coalescence between the droplets of phases. Because of the droplet's low vertical velocities, huge equipment with a large cross-section is required for efficient separation. This separation can further be enhanced by adding baffles in this chamber, which will increase the path length for efficient settling and reduce the compartment's dimension (Weatherley, 2020).

Practically in all impeller mixing systems, a considerable percentage of the droplets are not separated easily and remain trapped in the other phase product stream (Izzaty et al., 2004).

3.3.2 Continuous column contactors

Continuous column contactors are a common type of SX equipment used in chemical industries and other areas, including the nuclear sector. Column contactor design has advanced to a mature state, and improvements are limited to small enhancements of current systems (Weatherley, 2020).

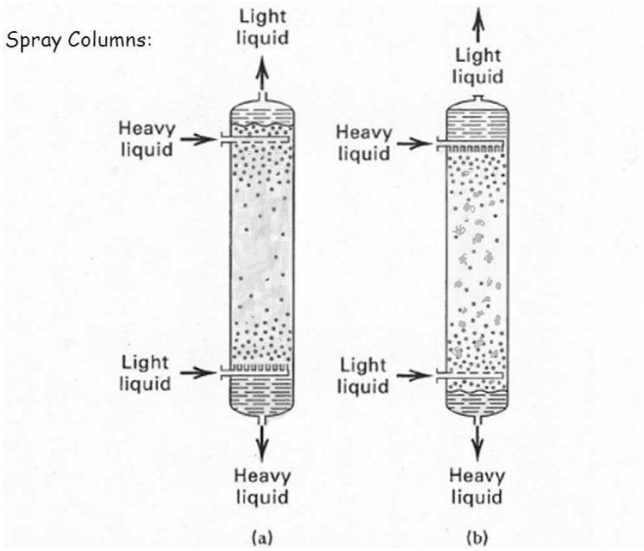

Figure 3.4: Spray column: (a) organic solution dispersed in continuous aqueous phase; (b) aqueous phase dispersed in continuous organic solution

Spray column (Figure 3.4) is among the earliest designs of continuous column contactors. In the case of a mixer-settler system, mixing and separation of the phases take place in two separate compartments, whereas these two operations are achieved in a single column in the case of a spray column (Izzaty et al., 2004; Weatherley, 2020). Being the simplest continuous column contactor, it has a few internals and is simple to operate and handle. Here, droplets of either phase are introduced against the continuous flow of the other, and the mass transfer occurs during the counter flow of droplets through the continuous phase. Meanwhile, the separation is achieved by gravity because of the density difference between the two solutions. Generally, heavy aqueous feed flows continuously from top to bottom, while a sparger in the spray column introduces the light organic phase as droplets. When these droplets pass through the continuous aqueous phase, they progressively coalesce and create a

continuous organic phase collected from the column's upper outlet. Meanwhile, raffinate is received at the bottom of the column (Izzaty et al., 2004).

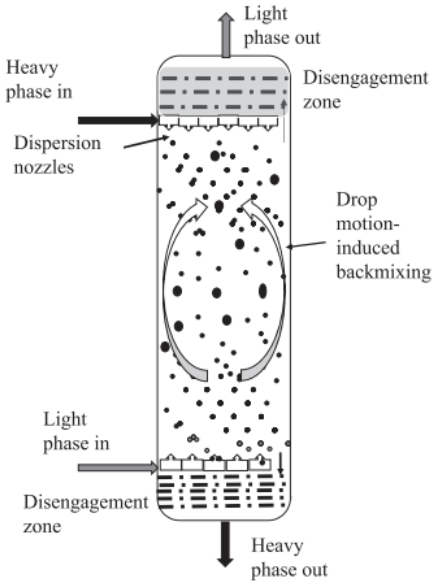

Figure 3.5: Back-mixing in a spray column (Weatherley, 2020)

The primary flaw in the spray column design is the back-mixing of the continuous and dispersed phases (Figure 3.5), which significantly reduces loading capacity and mass transfer efficiency. Furthermore, the low efficiency of a spray column is caused by a low interfacial area and a limited number of dispersion-coalescence cycles. Taller columns with large diameters are needed to lessen entrainment and other effects (Pasteur & Koch, 2020; Sovilj et al., 2019; Weatherley, 2020). The invention of packed columns was the first step in accelerating SX processes in continuous columns to improve the operation. According to Batey and Thornton, a stable droplet size distribution and a decrease in back-mixing are common reasons of better operation by packed columns with reference to spray columns. Additionally, they highlighted the significance of effects like droplet collision, drop-splitting, and coalescence in conjunction with re-dispersion in boosting mass transfer rates (Batey & Thornton, 1992).

Structured packing in packed column design has recently focused on improving the process and equipment handling. Structured packing is significantly easier to install

and replace than random packing. The Schiebel, Karr, rotating disc contactor, pulsed, sieve tray, Kuhni, and pulsed columns are examples of further developments in these continuous columns. Various designs aim to increase separation performance and mass transfer efficiency (Figure 3.6). Furthermore, these columns provide low maintenance with quite a basic design and flexibility regarding drive units (Weatherley, 2020).

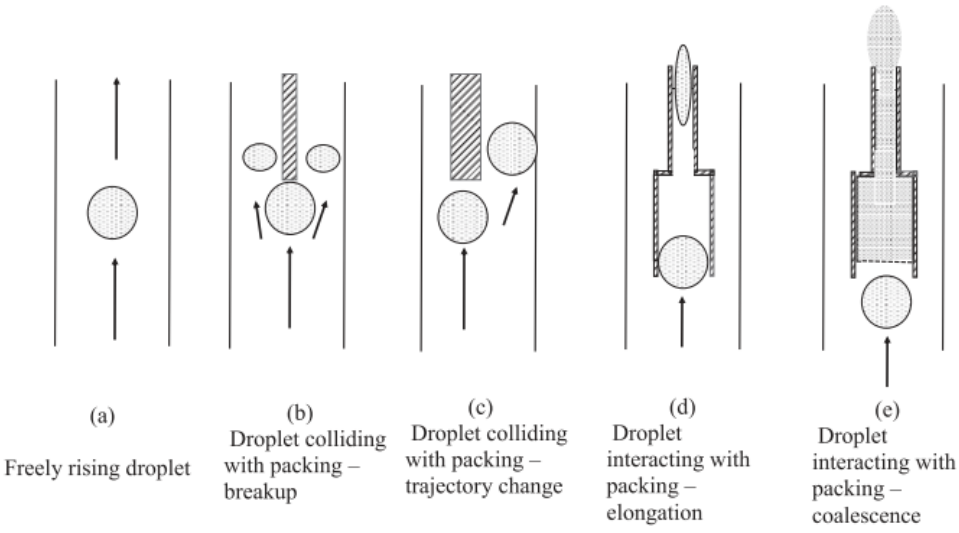

Figure 3.6: Visualization of drop behavior in a packed column (Weatherley, 2020)

3.3.2.1 Rotary contactor

Rotary contactors are the most intensified devices for SX operations, which use a high-gravity centrifugal field to facilitate the contact and separation of the two liquids. This contactor has a cylindrical shape and uses the density difference to control the net flow of all the phases. The capacity to process liquids incorporating solid components without requiring extensive pretreatment, a small plant footprint, and an extremely short residence time for effective phase separation are the characteristics that set rotary extractors apart from mixer-settler or other column extractors. Despite all of these benefits, the largest disadvantage is the costly capital and operating costs, making it less practical for most industries (Weatherley, 2020).

3.3.2.2 Emulsion-flow system

The main objectives of improvements in solvent extraction equipment design are enhancing fluid dynamics and interfacial phenomena, which govern mass transport and phase separations. For efficient mass transfer, it is essential to have droplet instability along with the interfacial shear between the droplets and the surrounding phase, followed by separating the product streams. This is vital to maximize efficiency and reduce contamination of each liquid stream, leaving the process (Weatherley, 2020).

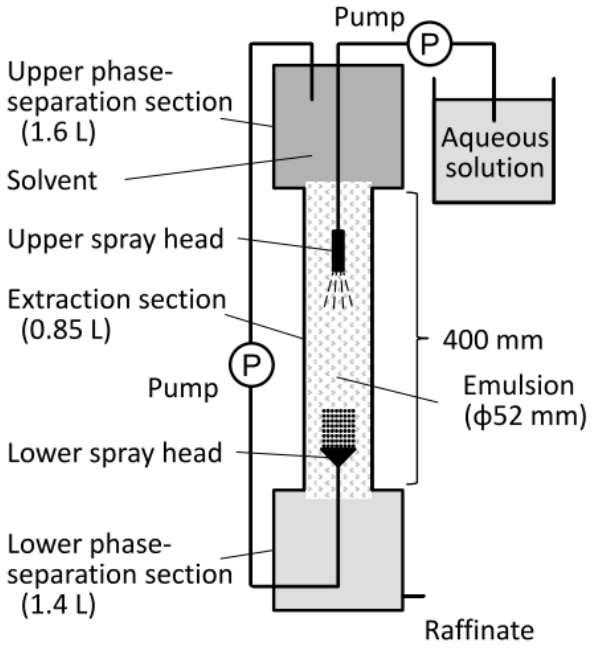

Figure 3.7: Outline of the emulsion flow continuous solvent extractor (Nagano et al., 2014)

The "emulsion flow" approach is another SX technique developed by the Japan Atomic Energy Agency (JAEA) with the expectation of producing high-quality products from precise mixing and separation of immiscible phases. The emulsion of inlet streams is created by ejecting micro-sized organic droplets against the droplet flow of an aqueous stream (Yanase et al., 2011). The main components of this apparatus are two sections for phase separation at the top and bottom of the extraction

section and an extraction section in the middle (Figure 3.7). Before the ejection of phases through spray heads, aqueous and organic solutions were introduced into the apparatus with their interphase between the two spray heads. During continuous operation, mass transfer of target material from aqueous feed takes place, and the loaded organic stream is collected in the upper section of the equipment (Nagano et al., 2014).

The emulsion flow technique aims to produce an almost monodisperse emulsion, and separation is controlled by utilizing the internal shape change within the device. Droplets of aqueous and organic phases move in opposite directions because of the difference in their densities. These droplets slow down as the emulsion moves from the mixing region to the phase separation section due to the sudden increase in cross-sectional area, which promotes droplet aggregation (Figure 3.8). In other words, droplets that do not slow down collide with the already-reached droplets in the separation sections, which leads to the droplets' coalescence and resulting a continuous phase in both separation sections (Naganawa, 2017). Compared to conventional industrial SX methods, emulsion flow extractors are superior in efficiency and speed at the lowest cost (Naganawa, 2017).

In an experiment, Shimogouchi and colleagues sought to ascertain the size distribution of droplets in two different apparatuses (a mechanical mixer and mixing by spray nozzles), having identical volumes and shapes for their main body vessels. The two configurations in Figure 3.9 illustrate the droplets created by mechanical stirring and spraying (Shimogouchi et al., 2019).

Upon spraying a liquid, the monodispersed droplets generated near the bottom nozzle undergo densification, randomly agglomerate together, and form emulsion. The aqueous product in the settling section is constantly transparent and free of organic droplets, making it possible to rapidly separate and clean product streams (Figure 3.10). While it is challenging to differentiate between the many phases of the mixture created by the mechanical stirrer, and this is because of the generation of poly-dispersed droplets of both phases (Shimogouchi et al., 2019).

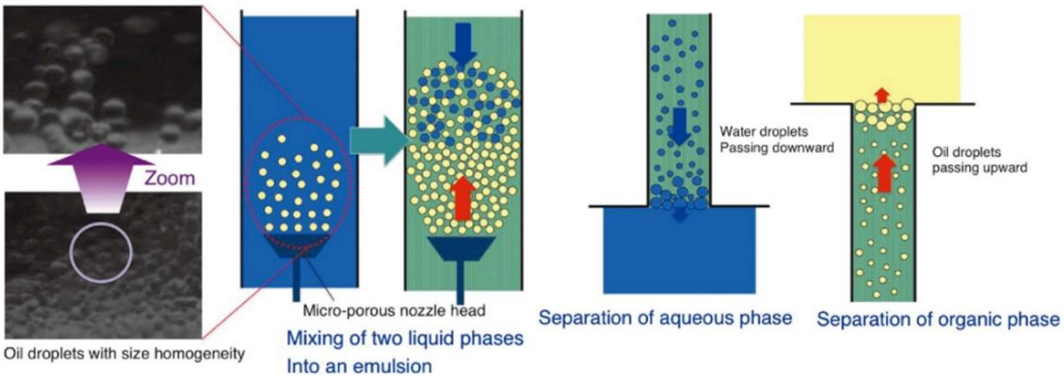

Figure 3.8: Mechanism of droplet mixing and separation in emulsion flow apparatus (Naganawa, 2017)

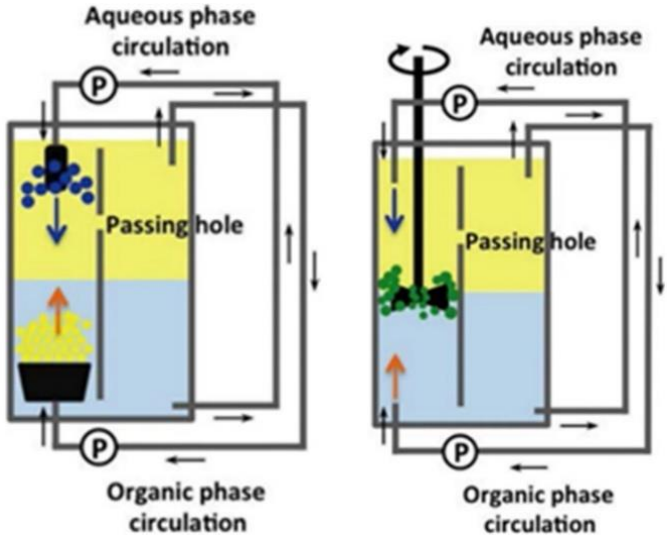

Figure 3.9: Liquid spraying system vs Mechanical stirring system (Shimogouchi et al., 2019)

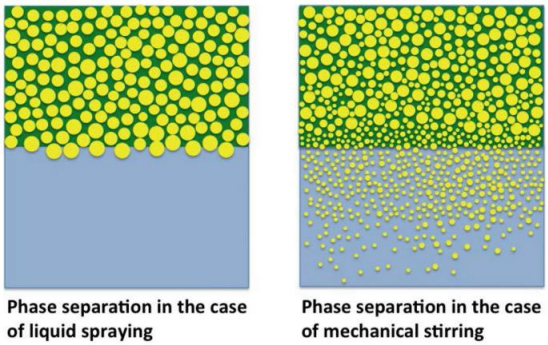

Figure 3.10: Difference in the phase separation between droplets generated by spraying and mechanical mixing (Shimogouchi et al., 2019)

Table 3.1: Comparison of conventional systems for mixing and separation of phases in SX operation (Naganawa, 2017)

Equipment	Mixing Manner	Separating Manner	Cost (Simplicity, etc.)	Efficiency (Mixing ability)	Speed (Separating ability)
Mixer-settler	Impeller rotation	Gravity separation	Medium	High	Low
Pulse column	Pulsation	Gravity separation	Medium	Low	Medium
Spray column	Droplets spray	Gravity separation	Low	Very low	Medium
Centrifugal extractor	Impeller rotation	Centrifugal force	Very high	Very high	Very high
Emulsion flow extractor	Droplet spray	Flow change	Very low	High	High

Table 3.1 shows a comparison between different conventional systems being used in the SX industry. Devices that require external mechanical forces, such as impeller rotation, pulse vibration, and centrifugal force, in addition to liquid transfer, are costly. The spray column is superior in terms of low cost and simplicity but is disadvantageous in mixing the two phases. On the other hand, centrifugal extractors, which require external mechanical force for mixing and phase separation, are the most disadvantageous in terms of cost (Naganawa, 2017).

Good extraction efficiency can also be attributed to good mixing ability. Mixer-settler and centrifugal extractors are better in terms of higher extraction efficiency than spray columns, which do not produce an emulsified condition. Additionally, the equipment can be made smaller if the processing speed is swift. With the centrifugal extractor, compactness is improved since centrifugal force is used to speed up phase separation. However, because the phases cannot be quickly separated, the mixer-

settler system has a drawback in terms of compactness. Even though spray columns use gravity to separate phases, mixing does not produce an emulsified state (because of low mixing capacity). Hence, phase separation can be accomplished faster than a mixer-settler. Comparing the emulsion flow device to traditional devices, it achieves low cost, simplicity, great performance, and compactness. In terms of performance and compactness, it is equivalent to the centrifugal extractor, which is the most superior conventional device. In contrast, in terms of low cost and simplicity, it is superior to the spray columns (Naganawa, 2017).

3.4 Solvent extraction reagents

Solvent extraction processes use organic solvents to selectively extract valuable materials from the aqueous streams and separate them from the gangues. There is a variety of extractants available for application in hydrometallurgy. The most common reagents utilized in commercial operations are extractant-based formulations that are combined with modifiers to improve solubility, phase disengagement characteristics, and metal transfer (Batnasan et al., 2021; Flett, 2005; Wilson et al., 2014; Xie et al., 2014).

A solvent's typical boiling and melting point, expressed as a temperature range, defines its use for an SX operation. Additional advantages are low corrosivity, good thermal stability, high vapor pressure, low toxicity, and a high flash point for safety. Moreover, chemical stability is advantageous regarding shelf life and reactivity with target compound functional groups. Furthermore, a high capacity for the species to be removed and excellent selectivity are attractive qualities (Gmehling & Schedemann, 2014; Kislik, 2012b; Poole, 2020).

Due to the necessity of accepting tradeoffs among the desired features, real solvents typically differ from ideal solvents. To recycle the solvent through distillation, for instance, a high vapor pressure is not ideal even though it lessens safety and environmental concerns. A density differential is necessary for effective demixing

following agitation in two-phase systems. Mass transfer properties are better for low-viscosity solvents. Mass transmission across the phase boundary is aided by low interfacial tension, which is linked to the production of emulsions in two-phase liquid systems and makes it easier to break down solvent droplets with slight agitation. This can be mitigated by choosing low-viscosity solvents with a significant density differential (Okamura & Hirayama, 2020; Poole, 2020).

3.4.1 Classification of organic solvents

Organic solvents are categorized on their mode of metal transport from the aqueous phase, involving the transfer of metal cations (M^{n+}), metalate anions (MX_x^{n-}), or metal salts (MX_x). Depending on the chemistry, the solvent extractants are classified into the following four categories (Flett, 2005; Wilson et al., 2014; Xie et al., 2014; Yoon et al., 2016):

1. Cation Exchangers (Acidic / Cationic extractant)
2. Anion Exchangers (Basic / Anion extractant)
3. Solvation Extractants (Neutral extractant)
4. Chelating Extractants

3.4.1.1 Cation exchangers

With cation exchange extractants, the total process of removing REEs from the aqueous phase can be broadly summarized as shown in Equation 3.6 (Han et al., 2014; Xie et al., 2014);

$$RE_{aq}^{3+} + HA_{org} \leftrightharpoons REA_{3_{org}} + 3H_{aq}^{+} \quad 3.6$$

Where RE represents REE, and A is an organic anion. In non-polar organic solutions, the cation exchangers are typically accumulated to form dimmers, lowering their polarity; hence, the process is typically more complex than Equation 3.6. Therefore,

the RE complexes produced during SX can also include undissociated exchangers; consequently, a realistic representation of this cation exchange process is (Meshram & Abhilash, 2020);

$$RE_{aq}^{3+} + 3H_2A_{2_{org}} \leftrightharpoons RE(HA_2)_{3_{org}} + 3H_{aq}^{+} \quad 3.7$$

The term "H_2A_2" in Equation 3.7 refers to the organic acid in its dimeric form. Raising feed solution pH facilitates the extraction of REEs using cation exchangers, whereas increasing the acidity facilitates the stripping process. Two distinct kinds of cation exchangers commonly utilized for separating REEs are organic derivatives of phosphorous acids and carboxylic acids (Flett, 2005; Hu et al., 2020; Wilson et al., 2014; Xie et al., 2014).

3.4.1.2 Anion exchangers

Anion exchangers are effective for solutions in which metal ions are present as anion complexes. Previous research revealed that in chloride media, the separation factors were low for neighboring REEs containing primary or tertiary amines, but in sulfate solutions, they gave promising results (Xie et al., 2014). Metal anion complexes from the aqueous feed form the neutral assemblies in the organic product and are separated. Moreover, extraction and stripping processes can also be controlled by changing counter anion Y^- concentration, as shown in Equation 3.8 (Han et al., 2014; Wilson et al., 2014).

$$n(LY)_{org} + MCl_x^{n-} \leftrightharpoons [(L)_n MCl_x]_{(org)} + nY^- \quad 3.8$$

3.4.1.3 Chelating extractants

In chelating extractants, H^+ is replaced by metal ions through a cation exchange process identical to that of a cation exchanger. However, the organic anion stabilizes the resultant organic complexes by coordinating the core cation in at least two places. Eu extraction from HNO_3 solution and Ce along with La from HCl solution have

been investigated using chelating extractants; nevertheless, extraction was poor compared to that of acidic extractants (Han et al., 2014; Xie et al., 2014).

3.4.1.4 Solvating extractants

Solvating extractants get their name from the fact that these chemicals tend to form salts with metal cations and anions in the solution (Wilson et al., 2014). The nitrate complex of REs was coordinated by TBP, thus forming a complex and is expressed as (Han et al., 2014; Meshram & Abhilash, 2020; Xie et al., 2014):

$$RE^{3+} + 3NO_3^- + 3TBP_{org} \leftrightharpoons RE(NO_3)_3(TBP)_{3_{org}} \quad 3.9$$

Using a combination of solvent extractants is a common strategy in extractive hydrometallurgy for attaining effective metal separation and concentration. To improve extraction, most such synergistic systems rely on the compatibility of the extractants with distinct modes of action (Wilson et al., 2014).

3.5 Di-(2-ethylhexyl) phosphoric acid (DEHPA / D2EHPA / P204)

Organophosphorus acids are one of the most popular cation exchangers for extracting REEs. The fact that the phosphorous acid extractants create stable dimeric complexes in non-polar solvents is one of their characteristics. One hydrogen bond in the dimer is retained during the production of metal complexes when the extractant is abundant, while the second H^+ is substituted with a metal cation (Xie et al., 2014).

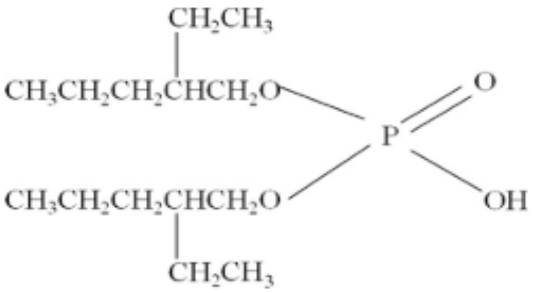

Figure 3.11: Structure of DEHPA

Among these organophosphorus acids, DEHPA [$(C_8H_{17}O)_2PO_2H$] is broadly used to extract uranium and REEs. Peppard and associates investigated the application of DEHPA for RE fractional extraction from HCl solution in the 1950s. Moreover, the majority of the DEHPA is present in dimeric structure in the organic phase (Figure 3.12), and each trivalent RE ion is connected to three of these dimers (Figure 3.13) (Meshram & Abhilash, 2020). The kinetics of lanthanides (Ln^{3+}) extraction with DEHPA from Cl^- and NO_3^- is superior compared to SO_4^{2-} solution with relatively higher separation from Cl^- complexes (Kislik, 2012a). According to the early discoveries, DEHPA provides a usual separation factor of about 2 among neighboring REEs, which is the foundation for its application. According to the reports, the order in which organophosphorus extractants decrease their ability to extract REEs is DEHPA > PC88A (EHEPA) > Cyanex 272. In contrast, the value of the separation factor is maximum for Cyanex 272, followed by PC88A and DEHPA (Y. Yang et al., 2017). However, a highly acidic stripping solution is needed to recover HREEs from DEHPA (Ferdowsi & Yoozbashizadeh, 2017; Jia et al., 2009; Zhao, 2016). The cation exchange process by DEHPA is represented by Equation 3.7.

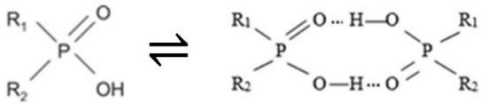

Figure 3.12: DEHPA monomer to dimer

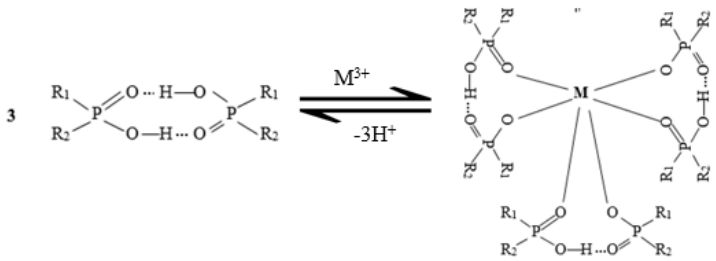

Figure 3.13: Reaction of DEHPA dimer with metal cation

Because of its high distribution coefficients, DEHPA is appropriate for separating REEs from impurities and concentrating them from diluted acidic solutions. Before

precipitation, REEs are often divided into two, three, or occasionally four groups (Batnasan et al., 2021; Belova, 2017). With its many applications, DEHPA has become increasingly useful in effectively and efficiently extracting REEs from different complex aqueous solutions. All elements above Eu are entirely extracted from chloride solution by DEHPA solution at pH = 2. Furthermore, the separation factor values drop as the pH of this solution decreases. However, a less pronounced dependence on pH is seen for selective separation in the case of sulfate systems (Kislik, 2012b). DEHPA is also observed to be economical compared to other extractants of its class and is, therefore, widely used in the SX industries to recover valuable metals (Parhi et al., 2015).

3.6 REEs extraction with DEHPA

As discussed previously, DEHPA is extensively used to extract REEs because of its selectivity towards these elements and lower cost. Its efficiency rises as we move from La to Lu (rise in atomic number) and decreases with the increase in atomic radii (Abreu & Morais, 2014; Gergoric et al., 2017). Following are some examples from the literature regarding the extraction of REEs at the laboratory scale using a mechanical mixer.

It was observed in a study that the separation factor for Nd/La (8.40) and Eu/Nd (12.50) was very high when using DEHPA instead of Cyanex 301 or a mixture of Cyanex 301 + Cyanex 923 (Reddy et al., 1999).

To extract REEs from HCl aqueous feed having 0.094 g/L of REMs and impurities like Mn, Cu, Fe, and Co, three organophosphorus reagents (DEHPA, PC88A, and CYNEX 272) were tested, and DEHPA was determined to be most effective. Their extraction efficiency was as follows: DEHPA > PC88A > CYANEX 272. Moreover, an enrichment of REEs up to 60 times was achieved in this study (Parhi et al., 2015).

DEHPA diluted in kerosene was used to extract REEs from the chloride complex. It was found that extraction decreased with the rise in HCl concentration, and the SF

for the neighboring REEs was around 2.5. Moreover, the extraction was inferior from nitrate media compared to chloride (M. K. Jha et al., 2016).

From a Ce and La chloride mixture, extractions were up to 98% using 10% DEHPA (0.303 M) with an O:A ratio of 2. The striping was done with 1.0 M HCl solution (Meshram & Abhilash, 2020).

In a study, the extraction efficiencies of DEHPA in hexane were studied to extract La and Eu along with other REEs, and it found that La (95%) and Eu (100%) were extracted with 1.0 M DEHPA at a pH of 1.5 (Ochsenkühn-Petropulu et al., 1995).

A chloride solution with 1.5 g/L of Nd, Tb, and Dy was treated with DEHPA, Cyanex 272, and PC 88A to separate Nd from other REEs selectively. Under the optimum variables conditions, DEHPA showed maximum extraction, followed by PC 88A and Cyanex 272. Almost 100% extraction was achieved for all REEs using 0.60 M DEHPA at 1.30 pH, and enrichment was observed about 11.7 times for Nd (Arellano Ruiz et al., 2020).

In a leaching process with HCl, almost 90% of lanthanum, neodymium, and about 60% of cerium were recovered from monazite. SX with DEHPA showed positive results with almost 100% recoveries of these REEs at a pH value of 1.5. Furthermore, increased contact time increased the efficiency of the process (Echeverry-Vargas & Ocampo-Carmona, 2022).

SX using 5% DEHPA was observed for La, Nd, and Pr, while 1% isodecanol was used as a modifier to enhance organometallic complexes during operation. At the optimum values of variables, maximum values of separation factors were achieved at pH values of 2.0 and 1.7 for Nd/La and Pr/La, respectively, and the values were 17.73 and 12.69, respectively. Moreover, the extraction of REEs reached almost 100% with the rise in pH from 0.5 to 2.5 (Kumari et al., 2019a).

In a study to extract HREEs, seven solvents were tried, including acidic extractants, anion extractants, and a mixture of DEHPA/TOPO. The acidic solvents were studied against HCl and H_2SO_4, while the anions were evaluated from H_2SO_4 solutions. It

was observed that the separation factors were superior and comparable with DEHPA and IONQUEST 801. The comparison of these extractants from a solution having 0.3 mol/L H+ is given in Table 3.2. Furthermore, the behavior of these solvents was superior in HCl solutions compared to H_2SO_4 (Abreu & Morais, 2014).

Table 3.2: SF with DEHPA and IONQUEST 801 (Abreu & Morais, 2014)

SF	1.0 M DEHPA	1.0 M IONQUEST 801
Tb/Dy	2.5	2.7
Dy/Ho	2.1	2.4
Ho/Er	1.9	2.1
Ho/Y	2.0	2.1
Y/Er	1.1	1.5

SX with DEHPA and HEH/EHP was studied by varying HCl feed concentrations, CH_3COOH concentrations, and the concentrations of REEs. The results showed that the D and SF escalated on increasing pH, CH_3COOH, and REEs concentration. Moreover, the loading capacity increased with the rise in CH_3COOH concentration. The maximum separation factor values were $SF_{Ce/La}$=4.09, $SF_{Pr/Ce}$=1.96 and $SF_{Nd/Pr}$=1.53 for feed at 2.0 pH and 0.35 mol/L REEs with DEHPA (Chang et al., 2010).

La was extracted from nitrate media with DEHPA and PC88A. DEHPA showed superior results compared to PC88A, with maximum recoveries of 99.8% and 85% for 0.50 M DEHPA and 0.60 M PC88A, respectively. Furthermore, 100% stripping of La was achieved with 5.0 mol/L HCl, H_2SO_4, and HNO_3 in a single-stage operation (Acharya et al., 2015).

Nd and Dy were extracted from chloride feed with the help of DEHPA while observing the effect of different aliphatic and aromatic diluents. Results showed an excellent separation between Dy and Nd for all diluents while using 0.50 M DEHPA (Batchu & Binnemans, 2018).

Experiments were conducted to separate HREEs and U from wet-process phosphoric acid (WPA). 1.0 M DEHPA gave promising results and recovered 89.4% HREEs and 94.2 % U by mixing the two immiscible phases for 15 minutes, having a 1:1 phase ratio. Finally, 6.0 M HCl was used to selectively strip the HREEs and showed 98.1% recovery in a 3-stage operation, while 97.8 % U precipitation was achieved using 15% HF or 20% Na_2CO_3 (Wu, Wang, Zhang, et al., 2018).

Another study used DEHPA to extract La, Pr, and Er from a 1.0 M citric acid solution. The extraction of these REEs increased with the rise in pH from 1.0 to 4.0 and by increasing DEHPA concentration (Mustafa et al., 2019).

La, Nd, and Ce were recovered from HNO_3 and H_2SO_4 solution using DEHPA diluted in kerosene. The results showed that the extraction of Nd and La was slightly higher from the HNO3 solution, compared to the H2SO4 solution, and Ce was recovered 100 % in all the cases. The maximum recoveries from 0.10 M HNO_3 were 99.4%, 99.7%, and 100% for La, Nd, and Ce, respectively, while using 1.0 M DEHPA (Khaironie et al., 2014).

Experiments were performed to see the %E of Gd, Tb, and Eu with DEHPA while changing the pH of the feed solution. The values obtained at 4.0 pH are presented in Table 3.3. The results show that Gd can be separated from Tb and Eu using pH 4.0 (Budiman et al., 2021).

Table 3.3: Percent extraction and separation factor values for Gd, Tb, and Eu (Budiman et al., 2021)

Parameter	Value
$\%E_{Gd}$	98.90%
$\%E_{Tb}$	94.10%
$\%E_{Eu}$	98.29%
$SF_{Gd/Tb}$	5.63
$SF_{Gd/Eu}$	1.83
$SF_{Tb/Eu}$	0.32

Recovery of light and heavy REEs from leach solution of Mongolian apatite ore was studied using DEHPA. In the extraction process using 1.2 M DEHPA, up to 87% of HREEs were transferred to DEHPA, leaving 91% of the LREEs in the raffinate. In the stripping stage, 3.0 M H_2SO_4 was used, which recovered about 100% of the HREEs from DEHPA. Finally, the LREEs and HREEs were precipitated using oxalic acid, and the recoveries were 76% and 77%, respectively, compared to the concentration in the apatite sample (Battsengel, Batnasan, Narankhuu, et al., 2018).

REEs were extracted from the H_2SO_4 leach of apatite using DEHPA, PC88A, TBP, TOA, and TOPO. The results showed that DEHPA was superior among these solvents in extracting and selectively separating HREEs. Furthermore, 4.0 M HCl was used to strip these REEs and gave up to 75% recovery (Batnasan et al., 2021).

Using DEHPA (0.3 to 1.2 M), the extraction of REEs from the waste NdFeB magnet leach solution was investigated. Leach fluid consisted of 9.10 mM of Nd, 2.70 mM of Dy, 3.20 mM of Pr, 0.69 mM of Gd, 0.17 mM of Co, and 0.55 mM of B. 0.3 M DEHPA diluted in hexane gave the best extractions. Moreover, 2.0 M or higher concentration of HCl stripped 100% REEs from DEHPA (Sethurajan et al., 2019).

In a study, coal ash was processed to extract LREEs. Leaching was done using HNO_3, and SX was performed with TBP, Cyanex572, and DEHPA. According to the results, DEHPA was superior in extracting REEs from this solution, and almost all REEs were extracted at pH 1.5 (Peiravi et al., 2017).

NdFeB magnet was roasted, followed by leaching it with H_2SO_4. The leach solution containing Nd, Dy, Pr, Gd, Co, and B was processed further with DEHPA diluted in Solvent 70, octane, hexane, chloroform, cyclohexanone, toluene, and 1-octanol to explore the effect of these diluents. The maximum separation factors between HREEs and LREEs were observed using 0.303 M DEHPA in hexane, while no B or Co were extracted. Moreover, complete extraction of total REEs as a group was seen with DEHPA having 0.90 M or 1.20 M concentration in octane or hexane, respectively. Finally, 2.0 M HCl was used as a stripping agent to recover REEs (Gergoric et al., 2017).

In a study, Ce was 1st separated from Egyptian beach black sand by dissolving RE cake, obtained by conventional method, in HCl:HNO_3 solution (1:1) and then adding bleaching powder. The remaining REEs (Sm, Eu, and Gd), recovered as hydroxides cake having 93.11% REOs, were extracted using DEHPA. This extraction showed a concentrate having 60.6%, 3.21%, and 34.4% Sm, Eu, and Gd, respectively (Rabie, 2007).

Experiments were performed in a study to see the effectiveness of DEHPA and Cyanex 272, along with their synergistic effect to extract La, Nd, Dy, and Gd from the HNO_3 feed stream. According to the results, DEHPA was superior in separating Dy from La (SF = 267), La from Gd (SF = 243), Gd from Nd (SF = 31.78) and Nd from La (SF = 7.67). Moreover, Cyanex 272 showed the lowest values of separation between REEs. Finally, Cyanex 272 and DEHPA solutions having 8 mL and 2 mL, respectively of these solvents showed a good synergistic effect and reported $\alpha = 720$ for Dy from Gd and $\alpha = 3640$ for Dy from Nd (Ganji et al., 2016).

CHAPTER 4

MATERIALS AND METHODS

4.1 Materials

To study the solvent extraction of REEs, the organic solvent Di-(2-ethylhexyl) phosphoric acid (DEHPA) was used as an extractant, and kerosene (Shellsol D70) was used as a diluent for DEHPA to reduce its viscosity. Stock solutions of Lanthanum, Neodymium, and Europium were prepared by dissolving the respective rare earth oxides (REOs) in 1.0 M hydrochloric acid (37% purity), and sodium hydroxide was used to adjust its pH. A sulfuric acid (98% purity) feed was also synthesized for these REOs, and the extraction results from the two acid solutions were compared.

4.2 Equipment and method

As already stated that, the mixing and separation efficiency of the two immiscible phases is always higher in the case of mono-sized droplets produced through spray nozzles in spray columns as compared to the poly-sized droplets generated in the mechanical stirrer techniques (Shimogouchi et al., 2019). In light of this finding, a solutions spray system was devised in this research work (Figure 4.1), in which the mono-sized micro-droplets of both aqueous and organic phases are sprayed counter-currently through spray nozzles. Most of the experiments were performed with this setup, and the results were compared with those of conventional mixer-settler studies at the laboratory scale. Another setup was also made in which mixing was performed with the help of ultrasounds generated by an ultrasonic probe, and the results were compared with the solutions spray system.

This “solutions spray system” consists of two separate columns, a solution mixing column and a settling column, connected with a pipe. The two immiscible feed streams were mixed by spraying them with the help of spray nozzles in the mixing column. The lower nozzle produces uniform-sized micro-droplets of the organic phase, and the upper spray nozzle generates uniform micro-sized droplets of aqueous feed solution. The mixing and mass transfer between the two phases occurs upon the interaction of these droplets in this mixing section. During this mixing operation, an emulsion is formed, which is sent to the settling column, where the separation of the two phases takes place. This settling section consists of a uniform-sized column with large cross-sectional sections at the top and bottom. The geometry of this settling column enhances the quick separation of raffinate and loaded organic products.

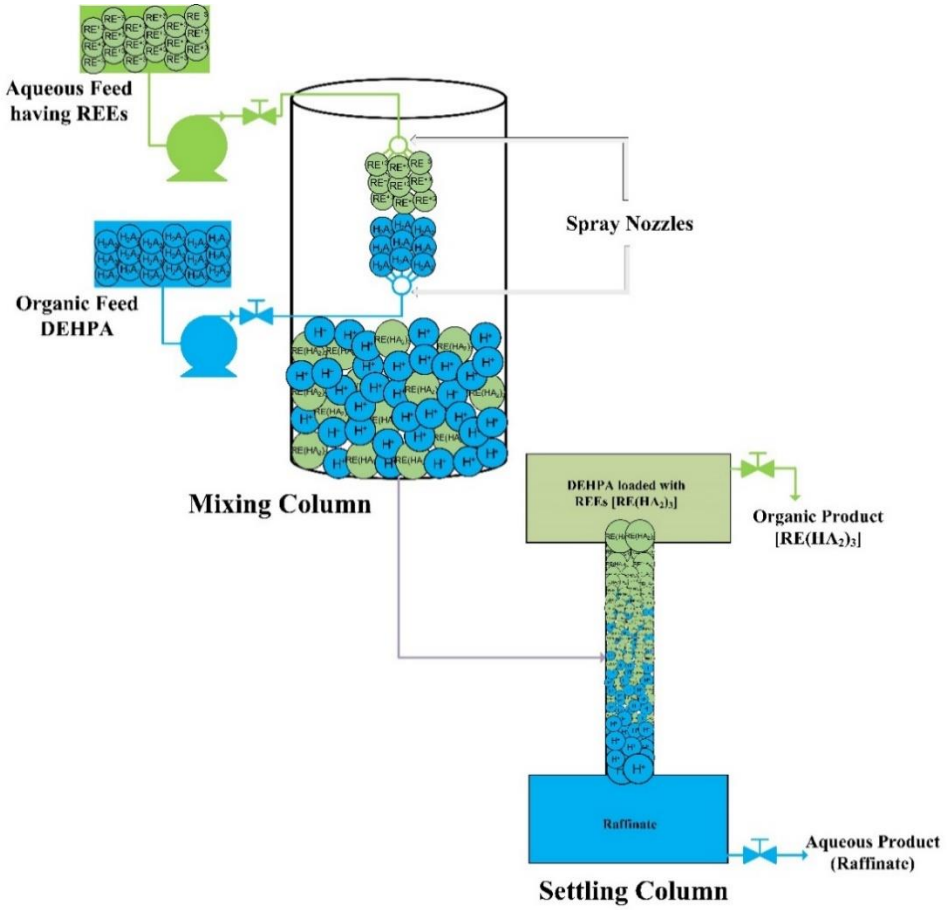

Figure 4.1: Schematic diagram of solutions spray system for SX process

As the emulsion enters the settling column, an increase in the diameter of the column compared to the pipe causes the initial separation of the two phases, making the organic droplets flow in the upward direction and aqueous phase droplets to the downward section of the column. Moreover, the rapid rise in the cross-sectional areas in the upper and lower portion of the settling column caused the droplets to decelerate, which encouraged the droplets' aggregation. It means that when the vertical linear velocity of the droplets, reaching the phase-separation section, sharply falls, then the droplets that do not decelerate collide and coalesce from behind, causing the droplets to coalesce and form a continuous phase. The continuously flowing loaded organic product stream is collected from the top, and the unloaded raffinate is recovered from the bottom section of the settling column. To make the organic droplets flow upward and aqueous in the downward direction, the lower half of the settling column is filled with the aqueous phase, and the upper half is filled with the organic phase at the start of the operation.

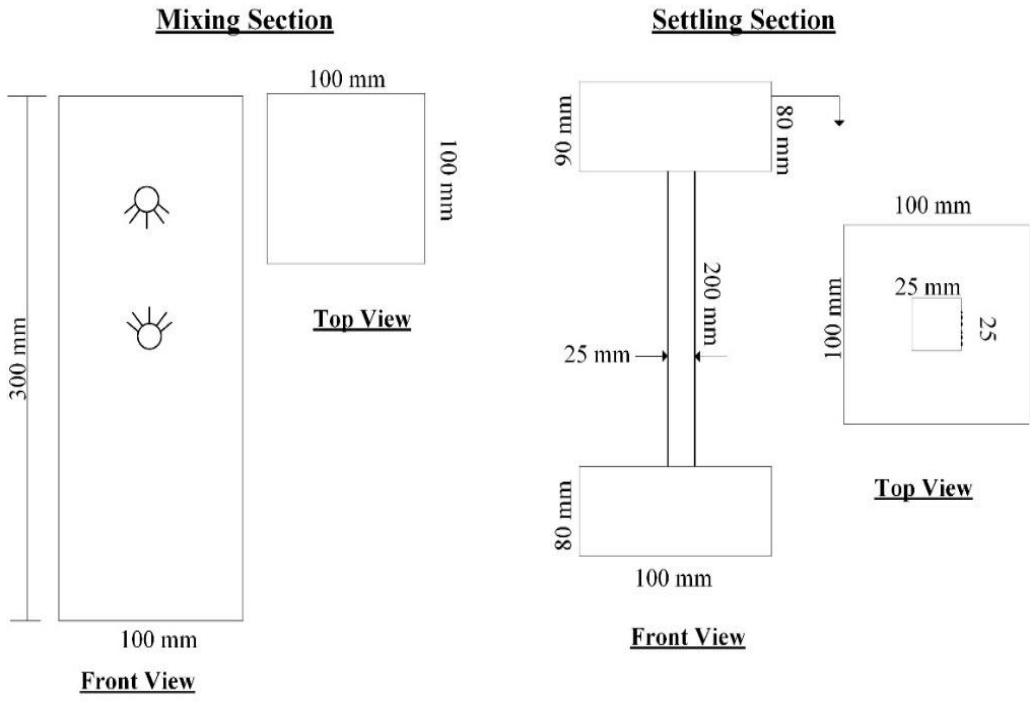

Figure 4.2: Dimensions of solutions spray system

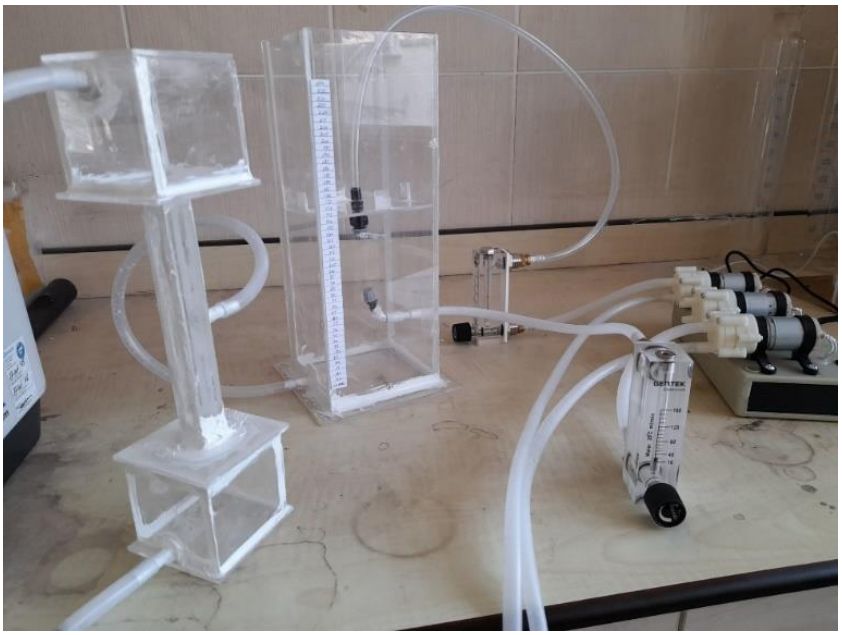

Figure 4.3: Real-time picture of the solutions spray system

The second setup, ultrasound mixing, also consists of two separate solutions mixing and separation sections, as shown in Figure 4.4. The mixing section is a container with almost 200 mL volume, where mass transfer takes place while mixing with ultrasounds, whereas the separation section is similar to that of the solutions spray system's settling section. A probe-type sonicator generated sound waves directly into the solutions in this setup. The diameter of that probe was almost 5 mm, which was inserted from the top in the mixing section. The two feed streams with equal volumes were fed to the mixing section while the sonicator was in operation, generating the sound waves that caused the mixing of two inlet aqueous and organic streams. The emulsion generated in this section was then sent to the settling section, where the separation of loaded organic and raffinate took place and recovered from the top and bottom sections, respectively, of this column.

In the SX operations, metal values in the feed solution and raffinate are measured to see the performance of any extraction operation. Here, Inductively Couple Plasma Optical Emission Spectroscopy (ICP-OES) was used to measure the concentrations of REEs in the aqueous feed and raffinate. The pH values of aqueous phases (feed and raffinate) before and after the experiments were measured with a pH meter.

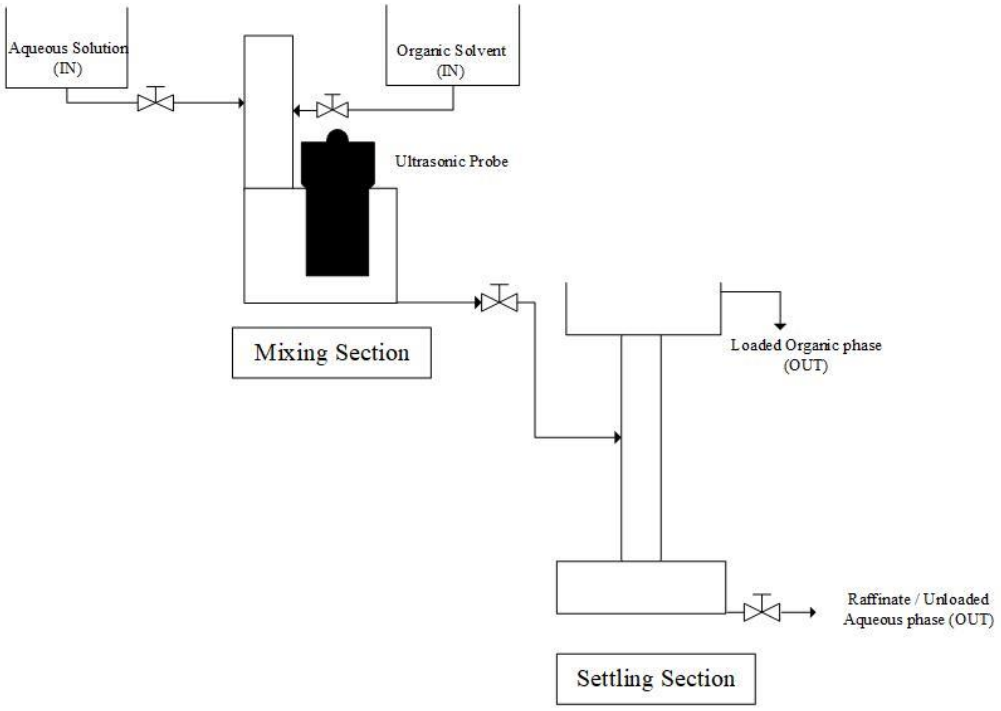

Figure 4.4: Ultrasound mixing system

4.3 Evaluation of experimental data

During the SX operations, the metal concentrations in aqueous phases are measured, while the mass balance calculation determines the metal values in the organic phases. The extraction efficiency (Equation 3.2), distribution ratio (Equation 3.3), separation factor (Equation 3.4), and stripping efficiency (Equation 3.5) are calculated to see the performance of the SX operation. The distribution ratio shows how well a metal is extracted in a single SX operation. The greater the value of D, the higher the extraction in the single extraction stage. The separation factor quantifies how much a metal was extracted with respect to the other. For the efficient separation of two metals, the value of SF should not be equal to 1. The greater the values of SF, the better the ability of the system to separate the two metals from each other.

McCabe Thiele diagrams were also plotted for extraction and stripping operations to see the number of theoretical stages for the complete recovery of REEs from aqueous and organic phases, respectively.

4.4 Experiments

Depending on the variables, the experiments performed with these setups were divided into the following four phases/series.

1. Study of the solutions spray system for the chloride feed solution having 1.0 g/L of each REO
2. Study of the solutions spray system for the sulfate feed solution having 1.0 g/L of each REO
3. Study of different mixing systems
4. Study of the solutions spray system for the chloride feed solution having REEs concentration representative of Beylikova leach

4.4.1 Study of the solutions spray system for the chloride feed having 1.0 g/L of each REO

In the first series of experiments, Stock solutions of La, Nd, and Eu were prepared (1.0 g/L each) by dissolving the respective REOs in HCl. DEHPA diluted in kerosene was used as the organic solvent. Here, the solutions spray system was used, and the two immiscible feed solutions of equal volume (200 mL each) were sprayed counter-currently with a flow rate of 150 mL/min. The following parameters were observed in this series of experiments:

- pH
- ionic strength
- DEHPA concentration
- A:O phase ratio for extraction operation
- HCl molarity for stripping
- A:O phase ratio for stripping operation

First of all, the aqueous feed was prepared by dissolving REOs in 1.0 M HCl, and the pH was varied to see its effect on REEs' extraction. In this case, the feed solution has a fixed concentration of 1.0 g/L of each REE, and the pH varied from 0.5 to 2.0. DEHPA diluted in kerosene (10:90, v/v) was used as the organic solvent (0.303 M DEHPA) to extract REEs from this feed solution. The experiments were not performed for higher pH because the REEs hydrolyze at higher pH values, resulting in sedimentation of hydroxyl compounds. Furthermore, gel formation was reported at low acidities which is undesirable because of the associated viscosity and phase separation problems (Mishra & Devi, 2020; Xie et al., 2014).

In the case of the ionic strength study, feed solutions of different HCl concentrations (0.1, 0.316, 0.56, and 1.0 M) were used, and their pH values were adjusted with NaOH. With the addition of NaOH, the ionic strength of the solution increased, thus changing the behavior of the extraction operation.

$$La_2O_3 + Nd_2O_3 + Eu_2O_3 + 19HCl + NaOH \rightleftharpoons 2LaCl_3 + 2NdCl_3 + 2EuCl_3 + NaCl + 10H_2O \qquad 4.1$$

Equation 4.1 represents the reaction of species in the aqueous phase before the SX operation. Adding more NaOH will produce a larger amount of NaCl, which will affect the extraction of REEs during the next extraction operation. The fixed parameters included 1.0 g/L of each REE in the aqueous feed having 2.0 pH, 0.303 M DEHPA, and an A:O phase ratio of 1:1.

Finally, in the case of the DEHPA concentration effect, DEHPA was diluted in kerosene (v/v) in ratios of 5, 7, 10, 15, and 20% (0.151, 0.212, 0.303, 0.454, and 0.605 M, respectively) and its concentration effect was analyzed. Other parameters were fixed, including 1.0 g/L of each REE in the feed solution prepared from 1.0 M HCl, which had a 2.0 pH and an A:O phase ratio of 1:1.

With the help of the above experiments, the optimum values of HCl molarity, pH, and DEHPA concentration were obtained, and REEs extraction was performed at these optimum values for feed solution having 1.0 g/L of each REO. The loaded organic solvent was then stripped to recover REEs using an HCl solution having a molarity ranging from 2.0 to 6.0 M. Moreover, experiments were performed by

varying the A:O phase ratio from 1:2 to 5:1 in the case of extraction operation and 2:1 to 1:4 for the striping operation to see the effect of the A:O phase ratio and find out the number of theoretical stages for optimum and economical recovery of REEs by plotting McCabe Thiele diagrams for extraction and striping section.

4.4.2 Study of the solutions spray system for the sulfate feed solution having 1.0 g/L of each REO

In this case, the feed solution was prepared by dissolving REOs in 1.0 M H_2SO_4, and the pH effects on the extraction process were studied by changing the pH from 0.50 to 2.0 with the addition of NaOH. The solutions spray system was used to mix and separate the immiscible phases, while the other fixed parameters were 1.0 g/L of each REO in aqueous feed, 0.303 M DEHPA as organic solvent, 200 mL solution volumes for each inlet stream and the flow rate of 150 mL/min. In this case, the percent extractions of La, Nd, and Eu were compared with that of the HCl solution from the first series of experiments.

4.4.3 Study of different mixing systems

In the third series of experiments, an ultrasonic probe system and mechanical mixer were used to mix the two immiscible phases and compare the results with the solutions spray system. Here, the feed solution was prepared by dissolving REOs in 1.0 M HCl, and the pH was changed from 0.50 to 2.0 with the help of NaOH. The constant parameters in this series of experiments were 1.0 g/L of each REO in the aqueous feed, 0.303 M DEHPA as an organic solvent, and 100 mL of each of these immiscible feed solutions.

The ultrasonic system had a 20 kHz frequency and power of 600 W. In this mixing system, a probe connected to the central ultrasonic system was immersed into the two-phase aqueous and organic system, and ultrasounds generated caused the mixing of these immiscible phases. It took almost 3.0 minutes to completely mix 200 mL of

solution (100 mL of each aqueous and organic phase) with the help of ultrasounds. In the case of the mechanical mixer, the agitator speed was 1400 rpm, and the mixing time was 10 minutes.

In these experiments, the effect of ultrasound and mechanical mixing on the percent extraction of La, Nd, and Eu was observed while changing the pH of the aqueous feed. The results of %E obtained were compared with those of the solutions spray system from the first series of experiments.

4.4.4 Study of the solutions spray system for the chloride feed solution having REEs concentration representative of Beylikova leach

In the case of all previous experiments, the concentration of La, Nd, and Eu was 1.0 g/L in the aqueous feed and remained fixed while the effect of other parameters like pH, DEHPA concentration, molarity of aqueous feed as well as stripping solution, type of acids, and type of mixing techniques, was studied.

In the final experimental runs, the aqueous feed was prepared with 1.0 M HCl having 6.0 g/L La_2O_3, 2.5 g/L Nd_2O_3, and 100 mg/L Eu_2O_3. These concentrations represent the values in the actual leach solution reported from the leaching of Beylikova ore (Zeki Çizmecioğlu et al., 2018). Although this deposit contains a high amount of Ce, it is selectively separated from other REEs during the leaching operation. The Ce valency states III and IV are often known as cerous and ceric, respectively. The ceric oxide is obtained by heating the resources like $Ce(OH)_3$, cerium metal, or cerium oxosalts like carbonates, nitrates or oxalate in air. CeO_2 produced in this way is quite inert and is not even dissolved in strong acids. To dissolve it, it is again reduced to Ce(III) by a reducing agent and then dissolved in acids (Gupta & Krishnamurthy, 1992). This leaching technique is widely used in Bayan Obo and Mountain Pass, the two biggest fluorocarbonate deposits in the world. In this leaching method, bastnasite concentrates are roasted, causing the oxidation of Ce(III) to a tetravalent state before leaching with HCl. The roasted bastnasite is then treated with HCl, which dissolves

all the REEs except the CeO_2. This non-cerium leach solution is then treated via SX to recover all the other REEs. The solid residue is further processed to recover Ce (Wang et al., 2017). Keeping the REEs concentrations fixed in the aqueous phase along with 150 mL/min flow rate and 200 mL volume of each inlet stream, the following variables were studied in this series of experiments:

- pH
- DEHPA concentration
- A:O phase ratio for extraction operation
- HCl molarity for stripping
- A:O phase ratio for stripping operation

Similar to the first series of experiments, the pH was changed from 0.50 to 2.0 with the addition of NaOH while using 0.303 M DEHPA. Whereas in the case of studying the DEHPA concentration effect, the feed solution had 2.0 pH while 5, 7, 10, 15, 20, and 25% DEHPA diluted with kerosene (0.151, 0.212, 0.303, 0.454, 0.605, and 0.757 M, respectively) was used as an organic solvent. For the optimum pH and DEHPA concentration values, the stripping was performed using 2.0 to 6.0 M HCl. Furthermore, experiments were performed by varying the A:O phase ratio from 1:2 to 4:1 in case of extraction operation and 2:1 to 1:4 for striping operation to see the effect of A:O phase ratio while using 4.0 M HCl as stripping solution and found out the number of theoretical stages by plotting McCabe Thiele diagrams for optimum and economical recovery of REEs. Finally, all these values and graphs were compared with those from the first series of experiments.

CHAPTER 5

RESULTS AND DISCUSSION

5.1 Study of the solutions spray system for the chloride feed solution having 1.0 g/L of each REO

In this phase, the effect of pH, ionic strength, and DEHPA concentration on the extraction of REEs from feed solution having 1.0 g/L of each REO is discussed using the solutions spray system. Moreover, A:O phase volume ratios for extraction and stripping sections and the HCl concentration for stripping are observed.

5.1.1 Effect of pH

The acidic organophosphorus extractant DEHPA used in this study is a cation exchanger, which produces H+ during the cation exchange process, causing a decrease in pH and subsequently lowering the extraction of metals. Hence, the pH of the aqueous medium greatly influences their extraction efficiency. According to the reaction between RE ions and DEHPA shown by Equation 3.7, the reaction moves in the forward direction, and extraction increases with the solution's rise in pH (decrease in acidity). With the increase of acidity, the reaction will move in reverse direction, and the extraction will decrease. This inversely proportional relationship is evident in the deprotonation stability of DEHPA. The deprotonated form of DEHPA is essential for extracting metal ions. In case of high acidity, a large number of H^+ are produced, thus preventing the deprotonation of DEHPA, hence, the formation of REEs-DEHPA complex rarely occurs.

Figure 5.1 compares the percent extraction of La, Nd, and Eu with the change in aqueous phase pH in the feed solution. The extraction increased with the rise in pH for all the elements, and this trend of %E is in line with the literature (Acharya et al.,

2015; Kumari et al., 2019a; Mohammadi et al., 2015). The extraction of lanthanides with DEHPA is a cation exchange process in which RE ions replace the H^+ in DEHPA because of their higher valences. A characteristic of the phosphorus acid extractants is that they form stable dimeric structures in non-polar solvents. When the extractant is in excess, the formation of metal complexes involves the retention of one of the hydrogen bonds in the dimer while the other is broken to release a proton, which is replaced by the metal cation (Xie et al., 2014).

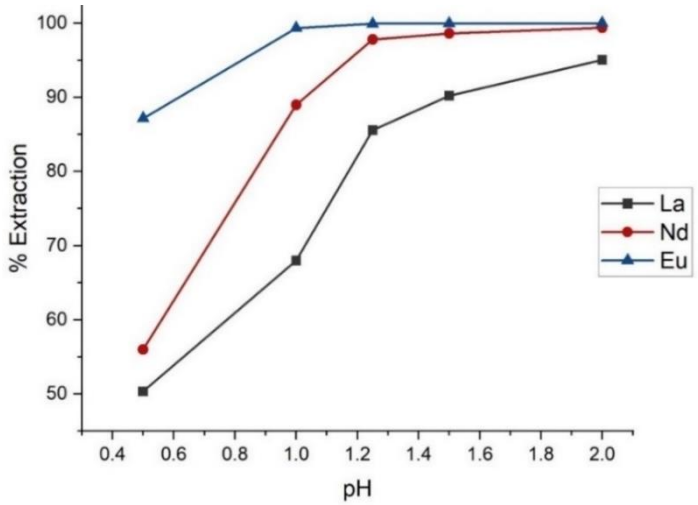

Figure 5.1: pH effect on %E of La, Nd, and Eu (1.0 M HCl aqueous phase having 1.0 g/L of each REO and 0.303 M DEHPA as organic phase)

The extraction of lanthanides is inversely proportional to their ionic radii. The ionic radii are linked with the atomic number such that as the atomic number of REEs increases, their ionic radii decrease. This phenomenon is known as “lanthanide contraction”. The ionic radii for La, Nd, and Eu are 1.061, 0.995, and 0.950 Å, respectively (Bautista, 1995; Han et al., 2014; Kislik, 2012a). Moreover, the extraction of REEs also depends on the concentration of the ions in the solution, which means that La can be extracted in place of Nd if the former has a very high concentration compared to the latter.

It can be seen from Figure 5.1 that the maximum extraction for Eu, Nd, and La is 99.98%, 99.36%, and 95.03%, respectively, at 2.0 pH. It is also clear that Eu extraction is high enough even at low pH values compared to Nd and La, so Eu can

be selectively separated at low pH with good recovery. At 0.50 pH, Eu extraction is 87%, which is high enough compared to Nd and La, which have 56% and 50% extractions, respectively. Moreover, Eu extraction reached 99.32% at 1.0 pH; after that, the recovery did not change much with the rise in pH. Whereas there is a sharp increase in Nd extraction up to a pH value of 1.25 with an extraction value of 97.78%, and after that, the increase in recovery is minimal with the increase in pH. The rise in %E for La differs from other elements as its recovery increased gradually with the rise in pH, reaching its maximum value at 2.0 pH. The reason behind this trend is the same as explained earlier that first of all, Eu will be extracted on coming in contact with the organic phase, followed by Nd, and the remaining sites of DEHPA are loaded by La. La is also loaded along with Nd and Eu after reducing their concentration in the aqueous phase at lower pH values.

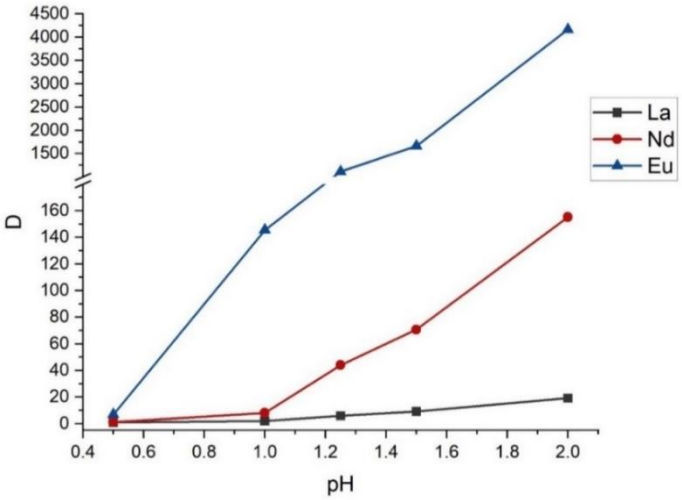

Figure 5.2: Effect of pH on D of La, Nd, and Eu (1.0 M HCl aqueous phase having 1.0 g/L of each REO and 0.303 M DEHPA as organic phase)

Figure 5.2 compares the distribution ratios of all three elements with the rise in pH of feed solutions. It can be seen that in all the cases, D increased with the rise in pH, which is allied with the literature (Batchu & Binnemans, 2018; Mohammadi et al., 2015). Moreover, the D value is the smallest for La and the highest for Eu, and the maximum values of D for Eu, Nd, and La are 4165, 155.25, and 19.14, respectively, at 2.0 pH. D values for La and Nd are very small up to pH 1.0, showing that these

elements are difficult to extract in a single stage below 1.0 pH because of the presence of a high concentration of H^+. While D_{Eu} is above 100 even at this low pH value. However, after 1.0 pH, the acidity of the aqueous phase decreased, causing higher extraction of all the elements under study in single-stage operation, reaching maximum values at 2.0 pH. The increase in D for Eu was small up to 1.0 pH, but after that, the DEu increased steeply, reaching a maximum value at 2.0 pH. Similar was the increasing trend of D for Nd and La, shown in Figure 5.2. These sharp increases showed the ease in extraction of these REEs at high pH values, reaching maximum values at 2.0 pH.

The separation factor makes it possible to quantify how much of a metal ion was extracted with respect to the other. Separating two or more metal ions would be more feasible if the SF reaches values greater than 1.0. The smaller the SF, the more difficult the separation of elements and the greater will be the reagent consumption due to extensive product recycling through 'scrubbing' circuits. As can be seen from Figure 5.1 that the maximum difference between the %E of REEs was observed at the lowest pH value of aqueous feed because of the competition between the REEs for the ion exchange process against the very high concentration of H^+ in the system. As the pH of the aqueous feed increased, the %E of REEs as a group increased, thus reducing their selective separation. The SF at 0.5 pH was 6.69, 5.33, and 1.26 for Eu/La, Eu/Nd, and Nd/La, respectively. The highest values of $SF_{Eu/La}$ showed that these two elements can be easily separated from each other. On the other hand, the higher values of $SF_{Eu/Nd}$ w.r.t. $SF_{Nd/La}$ show that Eu is more easily separated from Nd than Nd from La. However, because the value of SF is greater than 1.0 in all the cases, this shows that these elements are separable from each other under the studied conditions.

5.1.2 Effect of ionic strength of feed solution

Ionic strength refers to a measure of the concentration of ions present in a particular solution. It is an important factor in chemical reactions in aqueous solutions because

it affects the rates at which ions react with each other and, thus, the equilibrium and the extent to which the reaction occurs.

To see the effect of solution ionic strength on the SX operation, feed solutions of different HCl concentrations (0.1, 0.316, 0.56, and 1.0 M) were used, and their pH values were adjusted with NaOH. NaOH is a preferred pH modifier because sodium's affinity with cation extractants is weaker than REEs; hence, it will remain in the aqueous phase. On the other hand, some pH modifiers (such as lime) may introduce multivalent cations into the system (Ca^{2+}), which might reduce the REE extraction (Lu et al., 2021).

The ionic strength effect for all the different feed solutions was observed at a fixed pH value, which was adjusted with the addition of NaOH. In this study, the 0.10 M HCl feed solution had a 1.0 pH value, while the other feed solutions (0.316, 0.56, and 1.0 M) had less than 1.0 pH values. NaOH was added to these feed solutions to raise their pH to 1.0. Therefore, the ionic strength at a fixed pH value was highest for 1.0 M HCl feed solution under the conditions studied, followed by 0.56, 0.316, and 0.10 M HCl feed solution.

Figure 5.3 represents the effect of ionic strength on %E of La, Nd, and Eu at constant pH values (1.0, 1.5, and 2.0). In all the cases, the extraction of REEs increased with the rise in the solution's ionic strength. This is explained by the solvation of RE+3, which is strongly hydrated by coordination with water molecules. The aqueous phase contains the complexes like $[RE(H_2O)_n]^{3+}$, $[RECl(H_2O)_n]^{2+}$ and $[RECl_2(H_2O)_n]^{+}$, where, n is 8 or 9. The positively charged RE complexes are strongly hydrated by water molecules, resulting in high RE hydration energies and causing a hindrance for DEHPA to extract REEs from this aqueous phase. The addition of Na^{+} in the system will act as a driving force for the extraction operation in such a way that it will also coordinate with the water, taking away some of the water molecules from the RE+3 and reducing their hydration energy, resulting in increasing their activity towards DEHPA. Therefore, adding more and more Na+ will increase the ionic strength and reduce the hydration of RE+3; thus, extraction will proceed more

readily (Deferm et al., 2017; Lommelen et al., 2019; Vander Hoogerstraete et al., 2018).

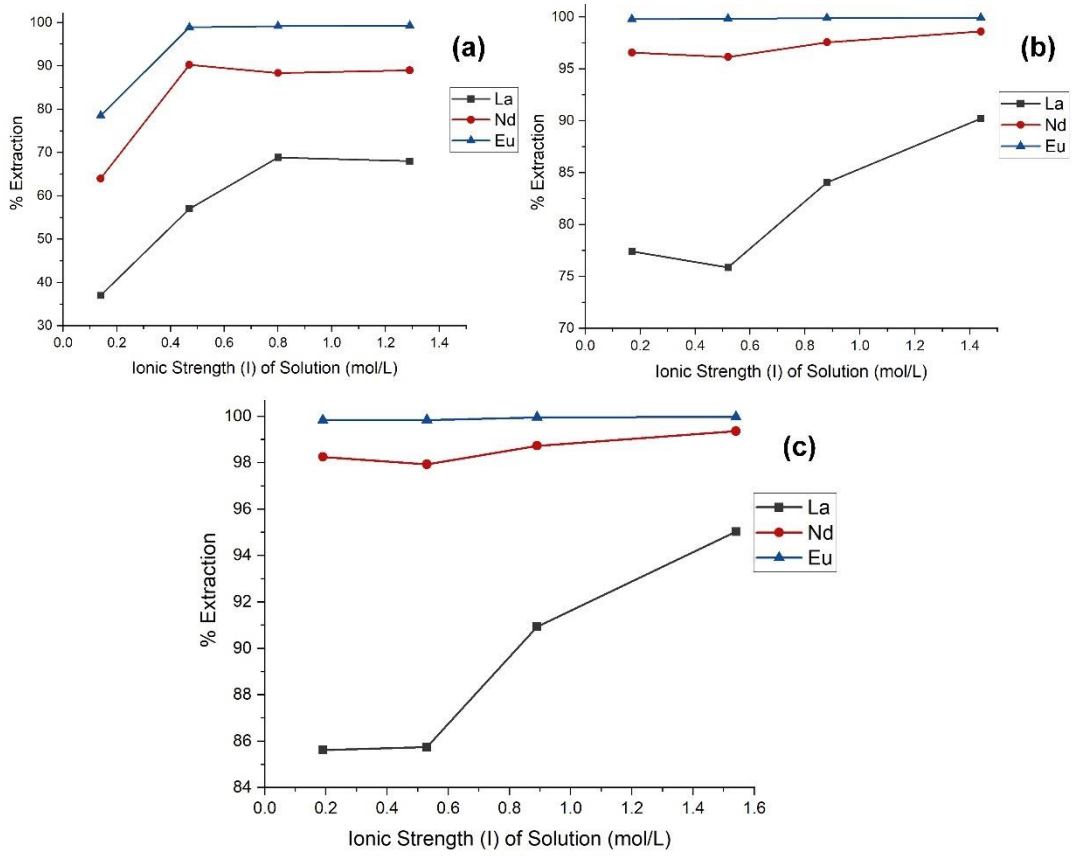

Figure 5.3: Effect of ionic strength (I) on the extraction of La, Nd, and Eu from aqueous solutions with different pH values a) 1.0 pH, b) 1.5 pH, c) 2.0 pH

It can also be seen from Figure 5.3 that for all the values of ionic strength, the extraction for Eu is maximum, followed by Nd and La, which is due to the difference in their ionic radii. The smaller the ionic radius of the element, the more the extraction. However, the increasing trend in their extraction at different pH values differs slightly. In Figure 5.3a, at 1.0 pH of the feed solution, %E of Eu and Nd reached their maximum %E at the ionic strength of 0.47 mol/L, and after that, there was a minute change in the extraction with the rise in ionic strength. On the other hand, the %E of La reached the maximum value at the ionic strength value of 0.89 mol/L and remained unchanged with the further rise in the ionic strength of the

solution. Whereas, at 1.5 and 2.0 pH of the aqueous feed solutions shown in Figure 5.3b and Figure 5.3c, respectively, the Eu extraction was almost independent of the aqueous feed ionic strength. This is because, at this high value of pH, the concentration of H+ was not that high enough to compete with the bond of Eu with DEHPA. For Nd, there was a small increase in recovery with the rise in the ionic strength of the solution, reaching its maximum extraction at the highest ionic strength value. Also, this high pH value did not affect Nd's extraction much. Finally, the extraction of La was almost the same for the initial two values of ionic strength in Figure 5.3b and Figure 5.3c, but after that, there was a sharp increase in the recovery of La with the rise in ionic strength of the solution. The maximum %E for the elements was achieved at 2.0 pH with the solution ionic strength of 1.54 mol/L, and the recoveries were 99.98%, 99.36%, and 95.03% for Eu, Nd, and La, respectively. Furthermore, it can be seen from Figure 5.3 that the selective separation between the REEs increased by reducing the ionic strength, and La can be selectively separated from other elements while using a low ionic strength aqueous feed solution.

Distribution ratios were also calculated, like the %E, at different ionic strength values and are represented in Figure 5.4. It can be seen that for every case, there is an increase in D with the rise in aqueous feed ionic strength. This is because the Na+ presence in the solution causes the dissociation of RECl3 and eases the cation exchange process of RE^{+3} with DEHPA. Moreover, in all the cases, D_{Eu} is maximum, followed by DNd and DLa, which is due to the difference in their ionic radii. The smaller the ionic radius, the greater the affinity to bond with DEHPA. Finally, the increase in D values for all the elements was gradual and small for the 1.0 pH solution compared to the 1.5 and 2.0 pH solutions. The increase in D_{Eu} was abrupt with a 2.0 pH solution, and it was also sharp for D_{Nd} and D_{La} at this pH. Maximum D values were achieved at 2.0 pH feed solution with the ionic strength of 1.54 mol/L, and Dmax values were 4165, 155, and 19 for Eu, Nd, and La, respectively.

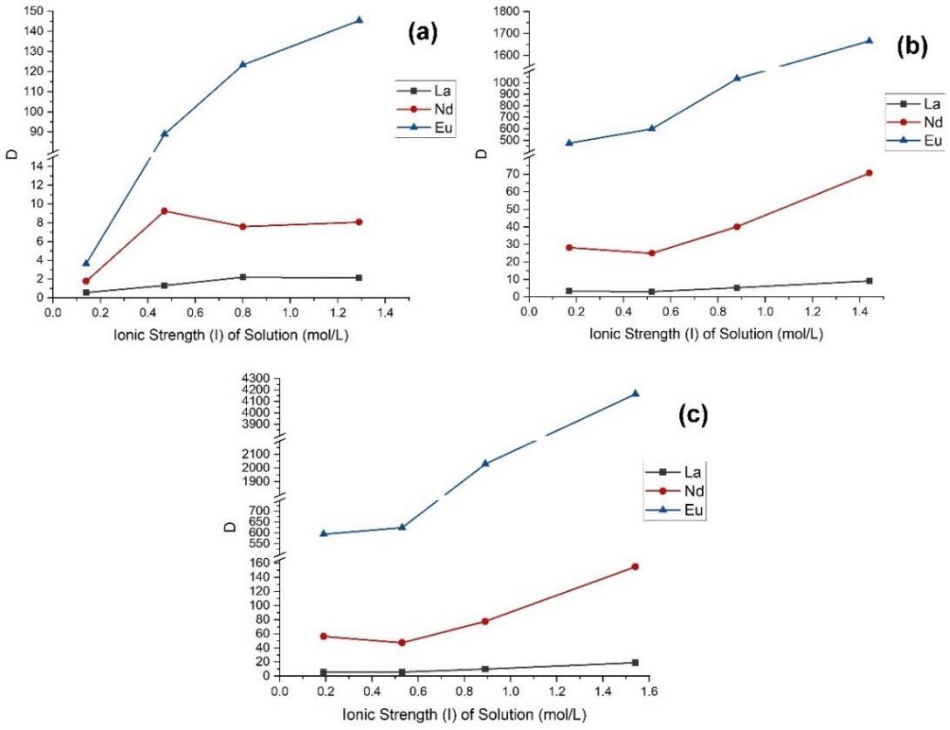

Figure 5.4: Effect of ionic strength (I) on the distribution ratio (D) of La, Nd, and Eu from aqueous solutions at different pH values a) 1.0 pH, b) 1.5 pH, c) 2.0 pH

5.1.3 Effect of DEHPA concentration

In the SX process, the concentration of organic solvent can significantly influence the efficiency and effectiveness of the overall process. Experiments were conducted while varying the DEHPA concentration to see its effect on %E and the distribution ratio of REEs. DEHPA was used with different concentrations of 0.1513, 0.2118, 0.3026, 0.4540, and 0.6053 M (5, 7, 10, 15, and 20% v/v, respectively, diluted in kerosene). Experiments were not performed at further higher concentrations of DEHPA because of the increase in its viscosity, which causes a reduction in mass transfer and extraction efficiency (Katoozi & Anari, 2021). The experiments were performed for 1.0 M HCl feed having 1.0 g/L of each REO at 1.0 and 2.0 pH, and the results for the %E are shown in Figure 5.5. It can be seen from Figure 5.5 that the extraction increased with the rise in DEHPA concentration. This is because of the fact that with the rise in DEHPA concentration, more and more ion exchange

sites are available, thus increasing the chance of ion exchange of RE^{+3} forming an aqueous solution with H^+ in DEHPA. Furthermore, Eu is recovered more than the other REEs because of its small ionic radius. Moreover, Figure 5.5a shows the selective separation of REEs at low values of pH and ionic strength. At low DEHPA concentrations, there is competition between the ion exchange of REEs with the DEHPA because of the limited availability of ion exchange sites. Therefore, La is extracted in low amounts (32.69%) compared to Nd (68.97%) and Eu (98.10%). Hence, at this low concentration of DEHPA, the REEs can be selectively separated. The recovery kept increasing with the rise in DEHPA concentration, especially for La and Nd, while the extraction of Eu is almost independent of the DEHPA concentration. As shown in Figure 5.5b, Nd and La extraction increased swiftly up to 0.303 M DEHPA, and after that, it was almost the same for Nd but gradually increased for La. Moreover, maximum extraction was obtained for feed solution having 2.0 pH and ionic strength of 1.54 mol/L at 0.605 M DEHPA concentration, and the recoveries were 99.99%, 99.48%, and 97.85% for Eu, Nd, and La, respectively. However, under the conditions in Figure 5.5b, REE extraction did not change much after 0.303 M DEHPA, and the extraction values are comparable to maximum recoveries and the values are 99.98%, 99.36%, and 95.03% for Eu, Nd, and La respectively. Therefore, it is more economical to use 0.303 M DEHPA instead of 0.605 M. It is also clear that one should opt for the low concentration of DEHPA along with low pH of feed solution for selective separation of REEs and use high DEHPA concentration along with high aqueous feed pH for maximum extraction of these elements. Figure 5.5 also tells about the selective separation between these elements. It can be seen that the selectivity increased with the reduction in DEHPA concentration because of the competition between the RE ions for cation exchange with limited DEHPA molecules available. Moreover, this selective separation was high for lower pH aqueous feed because of the abundance of H^+ in the system, which hinders the ion exchange process. The maximum values of SF were 106.49, 23.23, and 6.58 for Eu/La, Eu/Nd, and Nd/La, respectively, for the feed solution having 1.0 pH. Whereas these values were 49.02, 8.66, and 5.66 for Eu/La, Eu/Nd, and Nd/La,

respectively, for the feed solution with 2.0 pH. Therefore, for selective separation of these elements from each other, one should opt for the lowest possible DEHPA concentration and the lowest pH of the feed solution.

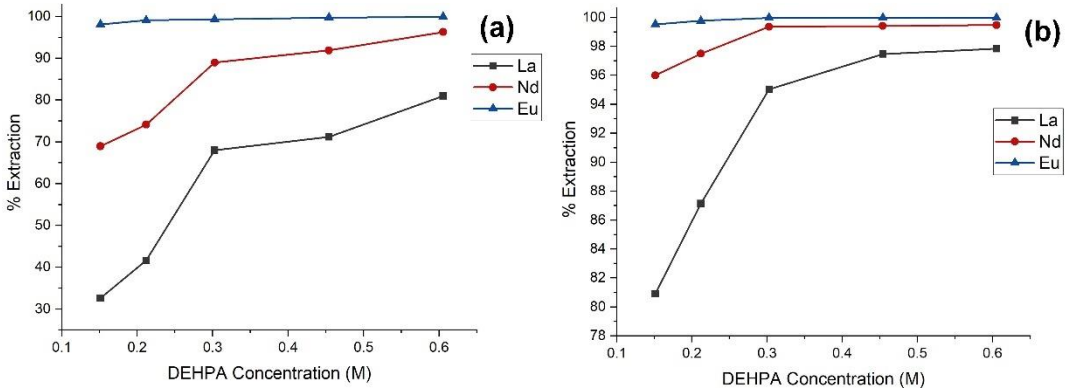

Figure 5.5: Effect of DEHPA concentration on the %E of La, Nd, and Eu from a solution having 1.0 g/L each REO at: a) 1.0 pH , b) 2.0 pH

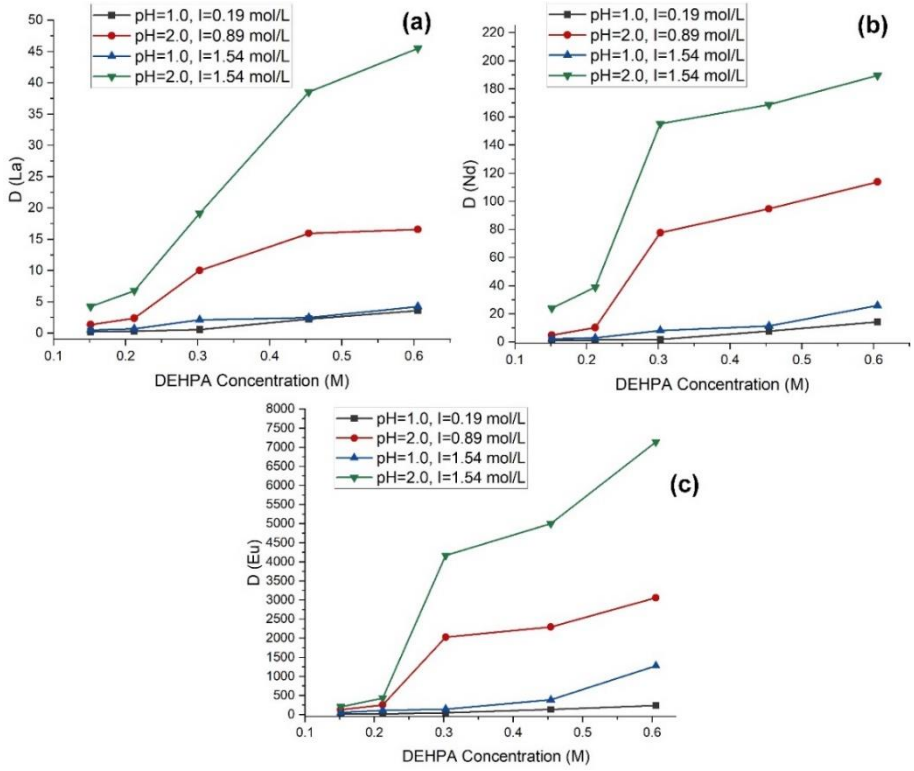

Figure 5.6: Effect of DEHPA concentration on the distribution ratio of REEs a) La, b) Nd, c) Eu

When the concentration of the organic solvent increases, the distribution ratio generally tends to increase as well. This is because of the fact that a higher concentration of the organic solvent provides more sites for the solute to partition into the organic phase. As a result, more solute molecules are transferred from the aqueous to the organic phase in a single stage, leading to an increase in D. Figure 5.6 shows the D values of La, Nd, and Eu with respect to DEHPA concentration at various pH and ionic strength of feed solution. It can be seen that the D increased with the rise in DEHPA concentration, pH, and ionic strength, attaining the maximum values at 2.0 pH and 0.606 M DEHPA concentration because of the ease of ion exchange process under these conditions. Similar to the %E, D values are maximum for Eu followed by Nd and La. Moreover, D values are higher at higher pH values because of the reduced amount of H^+ and less competition for ion exchange between cations. Comparing the D values of REEs, it is very small for La at low DEHPA concentration, making it difficult to extract; hence, it was selectively separated from other REEs. Because of this low DEHPA concentration, there is strong competition between REEs against the limited ion exchange sites; therefore, Eu and Nd are extracted in greater quantity because of their smaller ionic radii.

It can also be seen from Figure 5.6 that D values are very small for all the elements while using DEHPA below 0.303 M concentration, meaning that many extraction stages will be needed for the complete recovery of REEs under these conditions. This low DEHPA concentration will be used when selective separation of REEs is required. For extracting all REEs in a minimum number of stages, a feed solution with 2.0 pH seemed more feasible while using 0.303 M DEHPA concentration. Under these conditions, the D values were 19.14, 155.25, and 4165.67 for La, Nd, and Eu, respectively, giving extraction of 95.03%, 99.36%, and 99.98%, respectively. While using DEHPA in concentrations higher than 0.303 M did not seem economical because almost complete recovery has already been observed with 0.303 M DEHPA under the feed solution conditions.

5.1.4 Stoichiometry of the extracted REEs complexes

The equilibrium constant for the reaction between RE ions and DEHPA, as shown in Equation 3.7, is:

$$k_{eq} = \frac{[RE(HA_2)_3][H^+]^3}{[RE^{3+}]\,[H_2A_2]^3} \quad 5.1$$

Whereas the distribution ratio is given by;

$$D = \frac{[RE(HA_2)_3]}{[RE^{3+}]} \quad 5.2$$

Replacing the value of D in Equation 5.1;

$$k_{eq} = D\,\frac{[H^+]^3}{[H_2A_2]^3} \quad 5.3$$

Taking Log and rearranging Equation 5.3;

$$LogD = 3pH_e + Logk_{eq} + 3[H_2A_2] \quad 5.4$$

Equation 5.4 implies that D is a function of DEHPA concentration (H_2A_2) and pH at equilibrium (pH_e). In the graph between LogD and pH_e, the slope of the line will be 3, representing that on transferring one ion of REE into the organic phase, three H^+ are released into the corresponding aqueous phase to balance the charge.

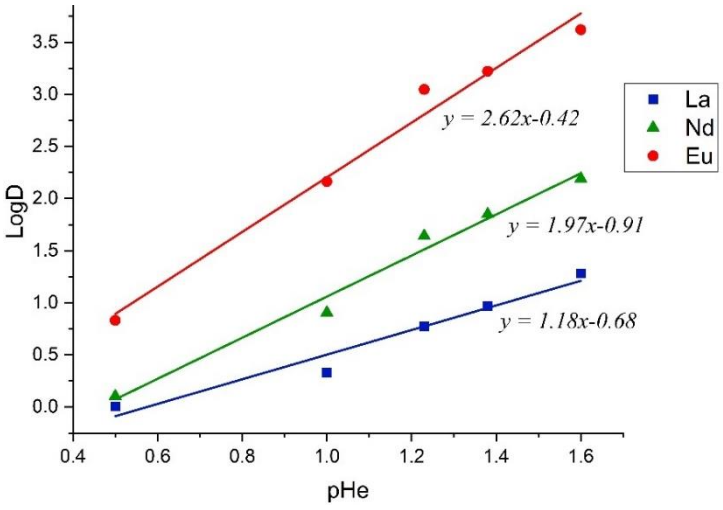

Figure 5.7: Effect of pH value at equilibrium on the stoichiometry of REEs extraction

The common slope analysis technique was used to understand the stoichiometry of the extracted RE-DEHPA complexes. The data was obtained using a 1.0 M HCl feed solution, with 1.0 g/L of each REO and 0.303 M DEHPA as an organic solvent.

The data is represented in Figure 5.7, and the plot shows the relationship of LogD with pH_e for all three elements. For Eu, the slope of the fitted straight line is close to 3, which shows that three H^+ were released while extracting Eu with DEHPA. The good linear relationship of the logD-pH_e plot for Eu suggests that only one major extracted complex species was formed in this case. On the other hand, the slopes for straight lines are around 2 and 1 for Nd and La, respectively. These slopes suggest that less than three H^+ were released for Nd and La. A possible explanation for the slopes being less than 3 and for the differences in the slopes of Eu, Nd, and La is that RE ions were extracted as mixed complexes, including chloride and DEHPA. The chloride complexes of the LREEs are more stable than those of the HREEs. Chloride ions may also act as bridging ions, increasing the formation of multinuclear species for La and Nd. The different theoretically possible equilibrium reactions forming complexes involving REE or REE-chloride complexes and DEHPA can be expressed as follows (Mohammadi et al., 2015):

$$RECl_s^{(3-s)+} + mH_2A_2 \rightleftharpoons RECl_sA_{(3-s)}(HA)_{(2m-3+s)} + (3-s)H^+ \quad 5.5$$

Where s is in the range 0–3, m is in the range 0.5–3 and $m \geq (3-s)/2$.

In the case of Nd, the Equation 5.5 will be;

$$RECl_1^{2+} + 2H_2A_2 \rightleftharpoons RECl_1(HA_2)_2 + 2H^+ \quad 5.6$$

A linearization of the Equation 5.6 will give the following equation;

$$LogD = 2pH_e + Logk_{eq} + 2[H_2A_2] \quad 5.7$$

Similarly, for La, the Equation 5.5 may be as follows;

$$RECl_2^{1+} + H_2A_2 \rightleftharpoons RECl_2(HA_2) + H^+ \quad 5.8$$

The corresponding relationship of LogD and pH will be as follows;

$$LogD = pH_e + Logk_{eq} + [H_2A_2] \quad 5.9$$

Equations 5.7 and 5.9 show that the values of straight-line slopes are 2 and 1 for Nd and La, respectively. Therefore, in Nd extraction, two H^+ were released into the aqueous phase, and one H+ was released during La extraction under the specified conditions of HCl concentration in the feed, ionic strength, pH, and DEHPA concentration.

The above equations show that the REEs' extraction followed a cation exchange process and released the protons. The number of H^+ released upon the formation of extracted species is not an integer because this scenario arose on the simultaneous extraction of different metal complexes. The literature has also reported similar work (Echeverry-Vargas & Ocampo-Carmona, 2022; Ni'am et al., 2020).

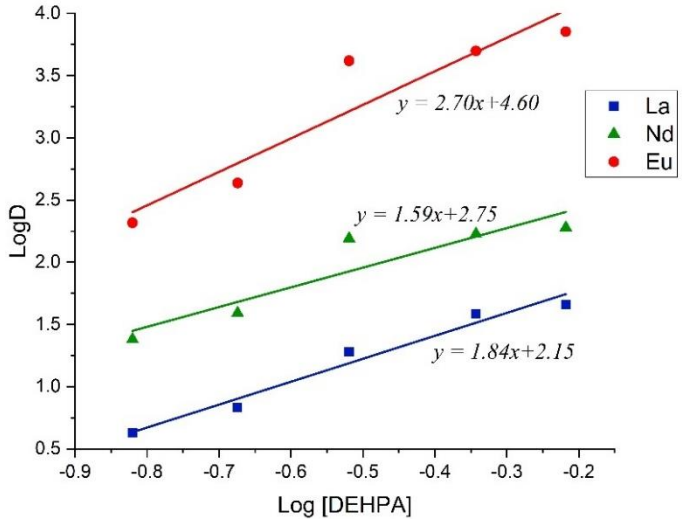

Figure 5.8: Effect of DEHPA concentration on the stoichiometry of REEs extraction

Furthermore, Equation 5.4 shows that the line slope between LogD and Log[DEHPA] will be three, representing that three DEHPA dimers will be involved in extracting each RE ion. Figure 5.8 shows the relationship between these two parameters for the experimental conditions of aqueous feed at 2.0 pH having 1.0 g/L of each REE dissolved in 1.0 M HCl. The concentration of DEHPA was changed from 0.151 to 0.605 M. It can be seen that the slops of fitted lines are close to 3, 2, and 2 for Eu, Nd, and La, respectively. This means that the Eu complex contained

three DEHPA dimers, whereas two dimers were involved in extracting Nd+3 and La+3 for each.

The literature was surveyed to see the relevant data of %E and D for SX of REEs using a mixer-settler to compare with the present study, and some of the data is shown in Table 5.1. It is worth mentioning that the sample size in most experiments was 50 mL or even less. It can be seen from Table 5.1 that the present study is much better in terms of efficient mass transfer and kinetics of the SX operation because of superior recoveries of REEs, higher values of D, along with swift mixing and separation operations. This is believed to be because of the mono-sized micro-droplets produced in the case of the solutions spray system and the design of the separation column. Some of the studies showed the values of %E and D comparable to our study, but in those cases, either the feed concentration of REEs was very low, or the concentration of the DEHPA used was very high, along with the long mixing time.

Table 5.1: Comparison of the present study with some of the work from literature with respect to %E, D, and mixing time

Feed	**DEHPA (M)**	**%E, D**	**Mixing Time (min)**	**Reference**
1.0 g/L each REO (La, Nd, and Eu)	0.303	La: 95.03%, Nd: 99.36%, Eu: 99.98% D_{La}:19.14, D_{Nd}: 155.25, D_{Eu}: 4165	01	Present study
La: 8.7 mg/L Nd: 22.2 mg/L Eu: 1.6 mg/L	1.0	La: 86% Nd: 92% Eu: 98%	10	(Larochelle et al., 2022)
La:44.0 gm/L Pr: 9.33 gm/L Nd: 35.7 gm/L	2.0	La: 10% Nd: 40%	05	(Morais & Ciminelli, 2004)

Table 5.1 (continued)

2.5 g/L each REO (La, Nd, and Ce)	0.303	99% for each	30	(Echeverry-Vargas & Ocampo-Carmona, 2022)
Nd: 3.29 gm/L Dy: 0.54 gm/L Pr: 1.14 gm/L	0.50	Nd: 94%	20	(Ni'am et al., 2020)
La: 1.33 gm/L Nd: 1.0 gm/L	0.20	La: 80% D_{La}:1.61, D_{Nd}: 17.2	10	(Acharya et al., 2015)
Ce: 0.730 gm/L Nd: 0.40 gm/L La: 0.43 gm/L Dy: 0.90 gm/L	1.0	D_{La}: 5.0 D_{Nd}: 11.0	30	(Tunsu et al., 2019)
La: 1.20 gm/L Ce: 1.19 gm/L Nd: 0.51 gm/L Eu: 0.012 gm/L	0.45	99% for all	10	(Kumari et al., 2019b)
Nd: 0.70 gm/L Dy: 0.80 gm/L Y: 0.45 gm/L	0.60	Nd: 90% D_{Nd}: 1.77	20	(Mohammadi et al., 2015)
1.5 gm/L each REO (Nd, Dy, and Tb)	0.80	Nd: 92% Dy, Tb: 98%	60	(Arellano Ruiz et al., 2020)

5.1.5 McCabe Thiele diagrams for the extraction operation

McCabe Thiele's study used A:O phase ratio isotherm experiments to calculate the number of theoretical extraction stages for the target elements. Experiments were

performed with 1.0 M HCl solution at 2.0 pH, having 1.0 g/L of each REE and 0.303 M DEHPA, while the A:O phase ratio was changed from 1:2 to 5:1.

The results of %E with the change in A:O phase ratio are shown in Figure 5.9, and it can be seen that the extraction reduced with the increase in the aqueous volume compared to the organic volume, which was due to the reduction in the amount of DEHPA ions compared to the RE ions in the aqueous stream. %E was almost 100% for Eu and Nd and 96% for La at an A:O ratio of 1:2, which did not change much even at an A:O ratio of 1:1. Whereas, the selective separation between the elements increased on increasing the volume of the aqueous phase because of the competition of the ion exchange process between the REEs against the limited amount of DEHPA.

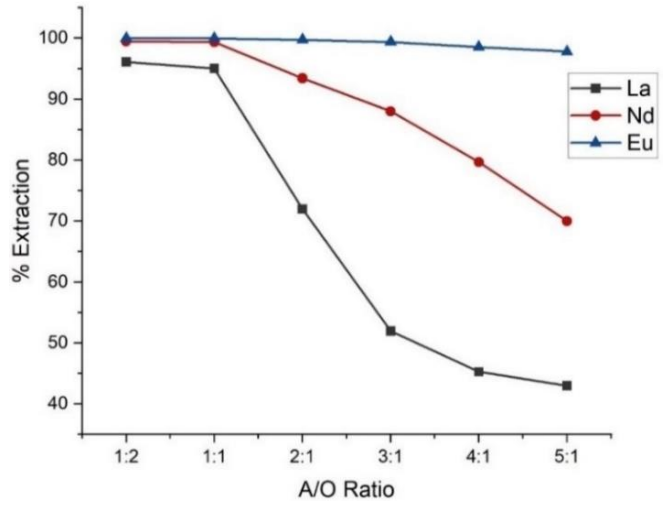

Figure 5.9: Effect of A:O phase ratio on % extraction of La, Nd, and Eu

Furthermore, McCabe Thiele diagrams were plotted to see the number of theoretical stages for the selective and complete extraction of REEs. It is evident from Figure 5.10a that at an A:O ratio of 1:1, two counter-current stages of SX gave maximum recovery of La while releasing about 10 mg/L in the raffinate. On further increasing the volume of the aqueous phase against the organic phase, the number of stages increased for the complete extraction of La till the saturation of the DEHPA reached above the A:O phase ratio of 4:1. Figure 5.10b shows that in the case of the A:O ratio of 1:1, almost all of the Nd was recovered in a single-stage operation, leaving about

10 mg/L in the raffinate. The number of counter-current stages further increased on increasing the volume of the aqueous phase, and the extraction of Nd was achieved in 4-stage counter-current operation while using an A:O phase ratio of 5:1, and no saturation of DEHPA was seen up to this ratio. Furthermore, Figure 5.10c represents that Eu was almost completely extracted in a single stage for an A:O ratio of 1:1. In the case of an A:O ratio of 2:1, the recovery was almost 100% in a 2-stage counter-current operation, and even in the case of single stage operation, the raffinate had only about 3 mg/L. The recovery of Eu was almost similar for A:O ratio of 3:1, 4:1, and 5:1 to that of 2:1 in a two-stage extraction operation, which means that Eu can be extracted with even a small amount of DEHPA compared to the large volume of aqueous phase.

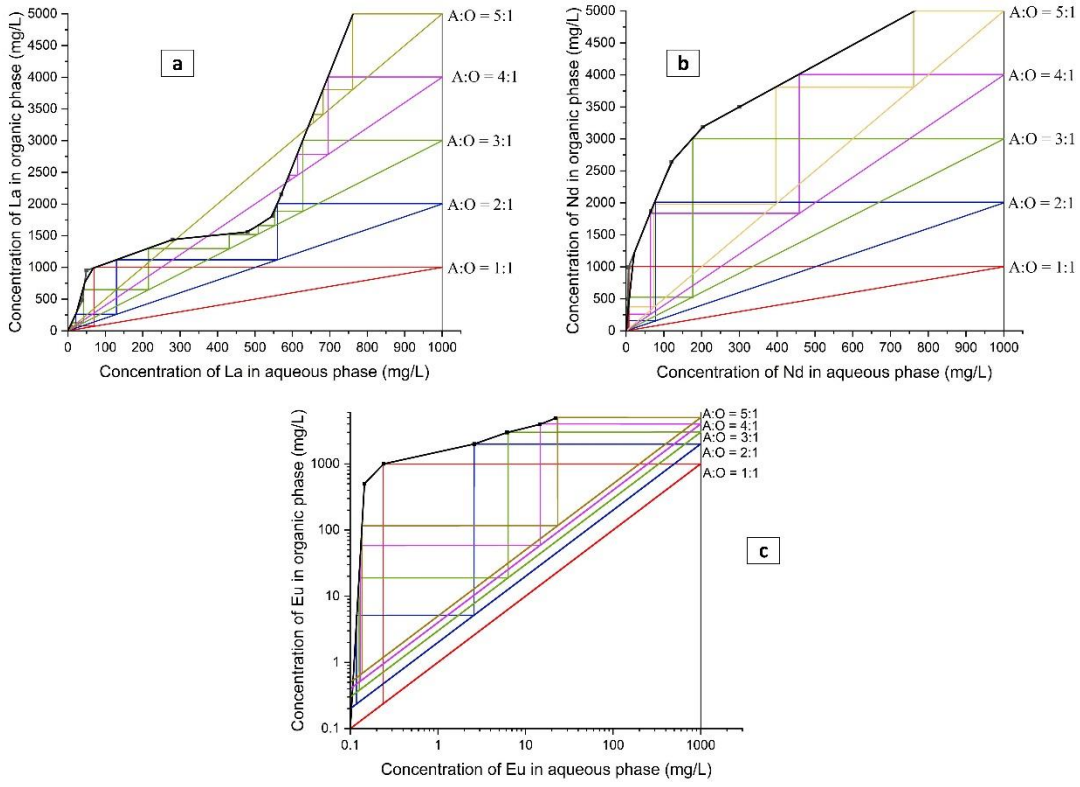

Figure 5.10: McCabe Thiele diagram for extraction of REEs using DEHPA

It is evident from Figure 5.10 that these elements can either be extracted completely as a group or can be selectively separated from each other by using the proper A:O phase volume ratio along with several counter-current stages. In the case of complete

extraction as a group, one needs to use the lowest possible value of the A:O phase ratio. In this case, at an A:O phase ratio of 1:1, all the elements can be recovered completely as a group with a 2-stage counter-current SX operation. Meanwhile, the higher values of A:O phase ratios are favorable for their selective separation from each other. At an A:O phase ratio of 5:1, single-stage operation gives selective separation of Eu from Nd and La in such a way that under these conditions, maximum extraction of Eu was achieved, having a very small amount of Nd and La. Therefore, the aqueous raffinate is full of La and Nd, which can be treated for separation. On the other hand, the 4-stage operation gave complete extraction of Eu and Nd while leaving the maximum of La in the aqueous raffinate using the A:O phase ratio of 5:1. In this way; the La can be selectively separated from Nd and Eu. The DEHPA containing Nd and Eu can further be processed to separate these elements.

Therefore, by selecting the proper A:O phase volume ratios along with the number of counter-current stages, these elements can either be extracted completely as a group or selectively separated by introducing some scrubbing stages before going to the stripping section.

5.1.6 Stripping of REEs

The stripping mechanism is reversed to that of the extraction operation, where the acidity of the stripping solution must be sufficiently high compared to the leach solution to shift the equilibrium of Equation 3.7 to the left.

In the present study, the stripping experiments were performed with HCl having concentrations of 2, 3, 4, 5, and 6 M to recover La, Nd, and Eu from the loaded DEHPA. Other parameters were the same, like an A:O ratio of 1:1 and a 150 ml/min flow rate for both aqueous and organic streams. The results of these experiments are shown in Figure 5.11. According to Figure 5.11, the recovery by stripping operation is high for La, followed by Nd and Eu at any point of HCl concentration. This is

because of the strong bond of Eu with DEHPA, followed by Nd and La, meaning that the stronger the bonding with DEHPA, the more difficult it is to recover through the aqueous stripping solution. Moreover, the rise in H^+ concentration increased the cation ion exchange process, thus replacing RE^{+3} in DEHPA with H^+ and increasing the concentration of RE^{+3} in the aqueous stripped solution. The recovery with 2.0 M HCl was 77.53%, 65.80%, and 51.05% for La, Nd, and Eu, respectively. Since the recovery increased with the rise in acidity, but the effect was not very high, and the stripping was 89.89%, 72.07%, and 55.13% for La, Nd, and Eu, respectively, while using 4.0 M HCl. Moreover, the recoveries were 98.99%, 81.07%, and 64.32% for La, Nd, and Eu when 6.0 M HCl was used, which is a very high concentration of HCl and costs three times more than 2.0 M HCl. Therefore, it may be more economical to use 2.0 M HCl for stripping operation and increase the number of contacts (stages) to completely recover REEs from the organic phase.

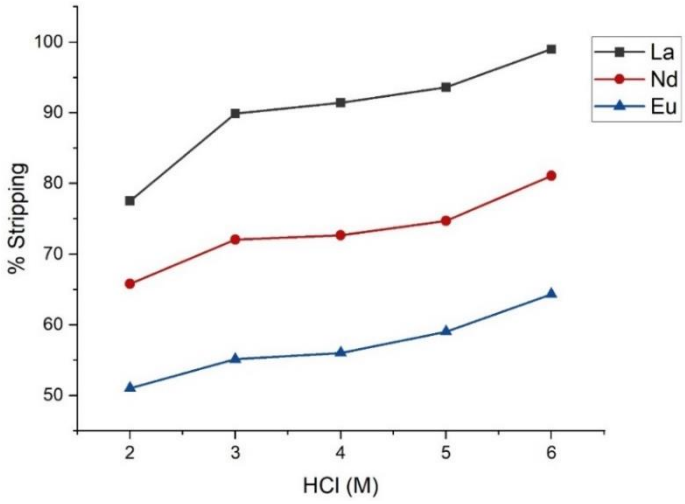

Figure 5.11: Effect of HCl molarity on the stripping of La, Nd, and Eu

5.1.7 McCabe Thiele diagrams for stripping of REEs

McCabe Thiele diagrams were also plotted for the stripping section to see the number of theoretical counter-current stages for maximum recovery of REEs. For this

purpose, stripping isotherms were constructed at a constant aqueous phase molarity of 2.0 M HCl while varying the A:O ratio from 2:1 to 1:4.

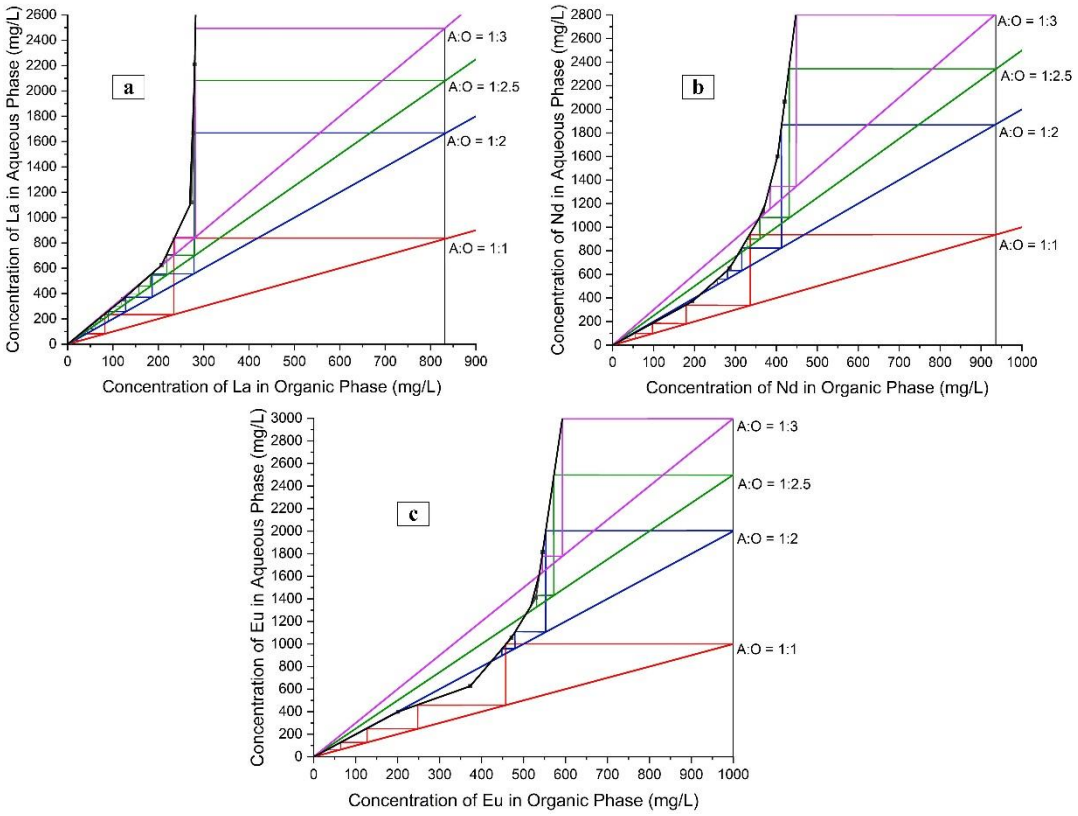

Figure 5.12: McCabe Thiele diagram for stripping of REEs using 2.0 M HCl

Figure 5.12a represents the McCabe Thiele diagram for La stripping, where operating lines with an A:O ratio from 1:1 to 1:3 were plotted to see the theoretical number of counter-current stages for optimum recovery of La. It can be seen that the minimum number of stages for maximum La recovery were at the lowest volume of the organic phase against the aqueous solution, i.e., at an A:O ratio of 1:1. At this volume ratio, the maximum recovery of La was achieved after three counter-current stage operation, leaving about 20 mg/L in DEHPA. On increasing the volume of loaded organic phase against the same amount of aqueous phase volume, the number of required stages for optimum recovery increased, and the stages were six and eight against A:O ratios of 1:2 and 1:2.5, respectively. Moreover, the La left in DEHPA was almost 40 mg/L in these two cases. Furthermore, on increasing the volume of

the organic phase, the saturation reached for La stripping from the organic to aqueous solution after about two stages with an A:O ratio up to 1:3. After this two-stage operation, the concentration of La in DEHPA was almost 240 mg/L.

Moreover, It can be seen in Figure 5.12b that about five stages were required for the efficient stripping of Nd from the loaded DEHPA at an A:O volume ratio of 1:1, and the concentration of Nd left in DEHPA was almost 30 mg/L. On further increasing the organic phase volume, there was an increase in the number of counter-current stages, and the saturation reached early for the aqueous phase, thus leaving a high concentration of Nd in DEHPA. This saturation reached almost after five stages in the case of an A:O ratio of 1:2, after four stages in the case of an A:O ratio of 1:2.5, and after three stages in the case of an A:O ratio of 1:3 with Nd concentration in organic raffinate was about 250, 320, and 380 mg/L respectively.

McCabe Thiele's diagram for Eu is represented in Figure 5.12c, and the trend for the number of required stages with respect to the A:O ratio was similar to the other REEs. It is evident that a 5-stage counter-current operation was required for maximum stripping of Eu from the loaded DEHPA while using an A:O volume ratio of 1:1 with a concentration of about 30 mg/L leaving in the organic phase. On further increase in organic volume, the saturation of the aqueous phase reached early, similar to that of Nd. In the case of Eu, the aqueous phase saturation reached almost after three stages in the case of an A:O ratio of 1:2, after two stages in the case of an A:O ratio of 1:2.5 and 1:3 with Eu concentration in organic raffinate was about 450, 530, and 560 mg/L respectively.

It can be concluded from these McCabe Thiele diagrams that complete stripping of all the elements from loaded organic solution can be obtained only in case of an A:O phase ratio of 1:1. On the other hand, La can be selectively separate from other elements at this stripping stage on using A:O phase ratio of 1:2.5, where maximum of the Nd and Eu will be left in the DEHPA. This DEHPA can further be processed to separate them and recover the individual elements.

It is evident from the McCabe Thiele diagrams of extraction and stripping operations that a complex SX system, having a number of cycles of extraction and stripping operations, is needed for the selective separation of these elements.

5.2 Study of the solutions spray system for the sulfate feed solution having 1.0 g/L of each REO

In this series of experiments, the extraction of REEs was performed from 1.0 M H_2SO_4 solution having 1.0 g/L of each REO with 0.303 M DEHPA, using the solutions spray system. The results were observed by changing pH from 0.50 to 2.0 with the addition of NaOH, and the values were also compared with those of the HCl solution. Sulfuric acid was used to dissolve the REOs to form the sulfate solution, and DEHPA was used to extract REEs from this sulfate solution.

$$RE_2O_3 + 3H_2SO_4 \rightleftharpoons RE_2(SO_4)_3 + 3H_2O \quad 5.10$$

$$RE^{3+}_{aq} + 3H_2A_2 \rightleftharpoons RE(HA_2)_3 + 3H^+_{aq} \quad 5.11$$

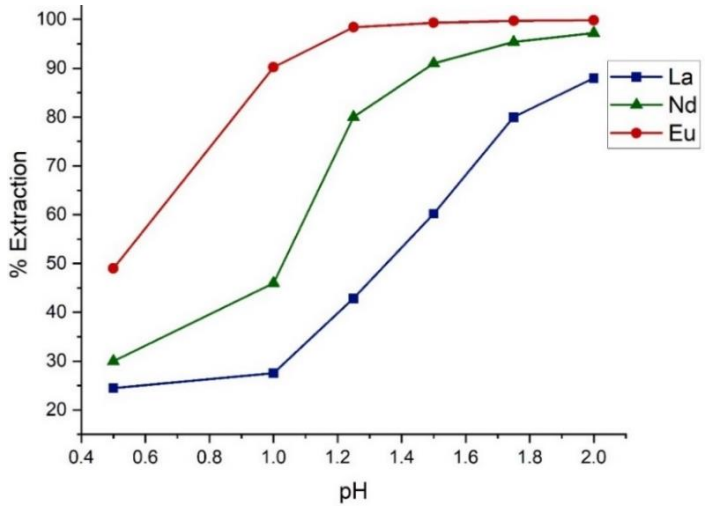

Figure 5.13: pH effect on %E of La, Nd, and Eu from H_2SO_4 solution

Figure 5.13 shows the percent extraction of REEs from H_2SO_4 solution with the change in pH. It is clear that extraction of all the elements increased with the rise in pH, and this is because of the reduction in H^+ in the system. Moreover, the extraction

of Eu was highest, followed by Nd and La, and this difference is linked with the ionic radii of these elements. The maximum recovery for Eu, Nd, and La was 99.83%, 97.20%, and 88.00%, respectively, at 2.0 pH. It can also be seen that Eu extraction increased up to 1.0 pH, and after that, it remained almost independent of pH. On the other hand, Nd extraction swiftly increased up to 1.25 pH, and after that, the recovery was gradual with the rise in pH. Finally, the La recovery did not change much up to 1.0 pH, and after that, its extraction increased sharply with the rise in pH, achieving the maximum value at 2.0 pH.

Figure 5.14 compares the extraction of REEs from HCl and H_2SO_4 solutions. It is shown that the extraction of each element is superior from the HCl solution compared to the H_2SO_4 solution, and this is in line with the literature (Abreu & Morais, 2014; Agarwal et al., 2018; Agarwal & Safarzadeh, 2017; Tunsu et al., 2019).

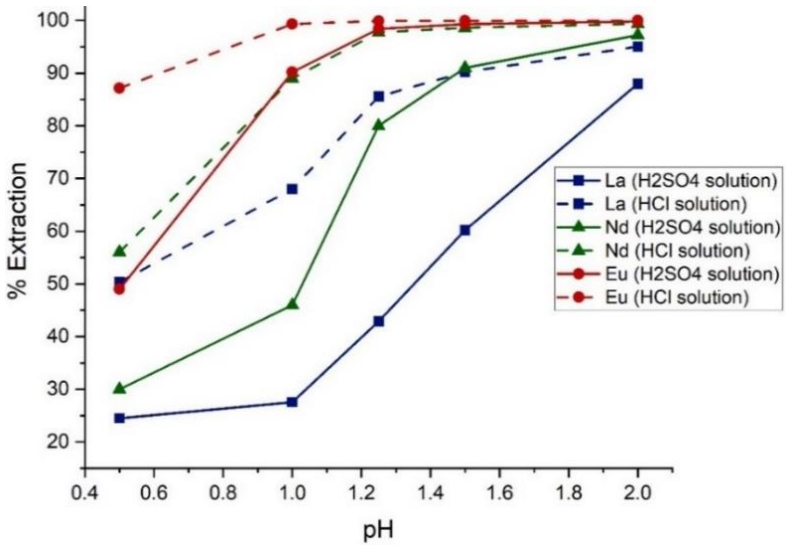

Figure 5.14: Comparison of extraction of La, Nd, and Eu from HCl (dashed lines) and H_2SO_4 (solid lines) feed solutions

The Pourbaix diagrams of these elements in HCl and H_2SO_4 media explain this difference. It is evident that in the case of chloride solutions of La, Nd, and Eu (Figure 5.15), these elements are in ionic form in the aqueous phase region within the working pH (up to 2.0 pH), which makes them easily bond with the DEHPA. On

the other hand, in the case of sulfate solutions, RE ions form complexes with HSO_4^- (Figure 5.16), and as a result, the bonding of these REEs with DEHPA is difficult in this case of sulfate solutions compared to chloride solutions. Moreover, the studies also reported that anion exchangers show superior %E and SF values in sulfate media compared to the chloride solutions and vice versa for cation exchangers (Xie et al., 2014).

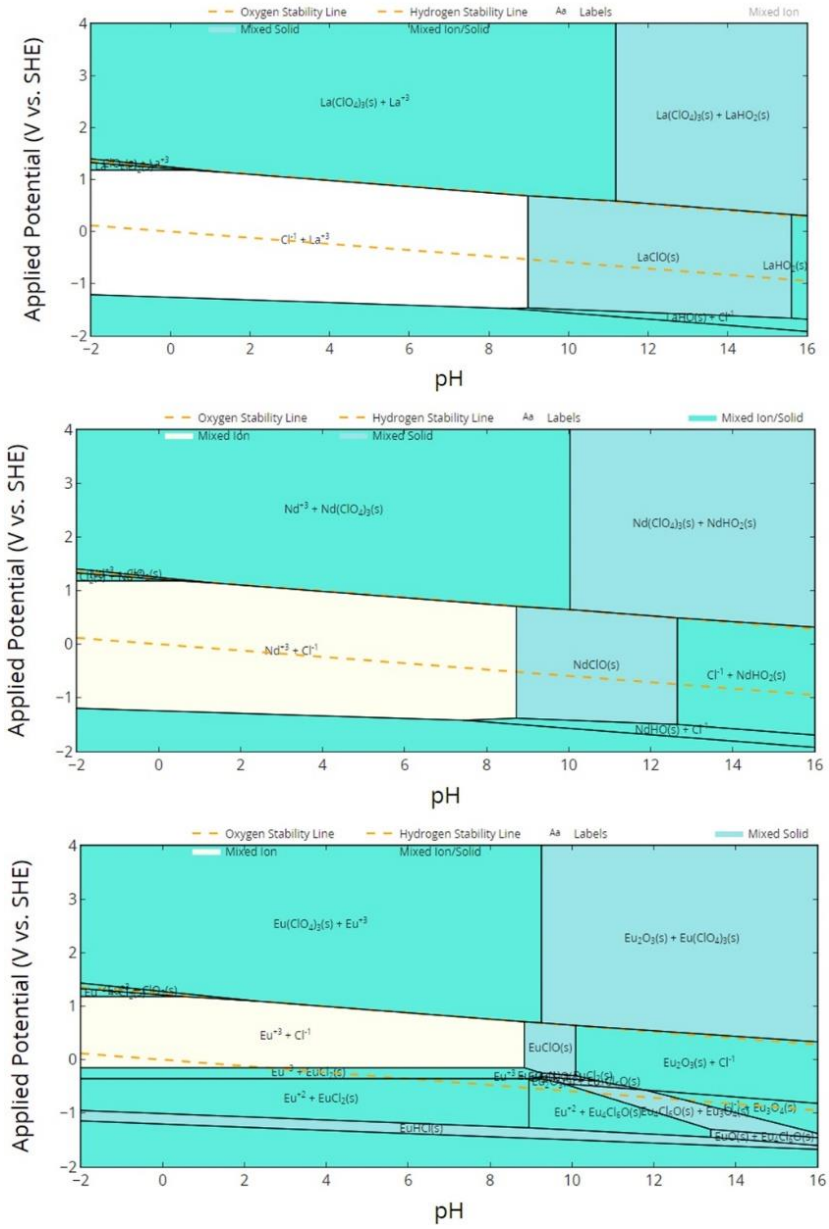

Figure 5.15: Pourbaix diagrams of La, Nd, and Eu in HCl solution (https://next-gen.materialsproject.org/pourbaix)

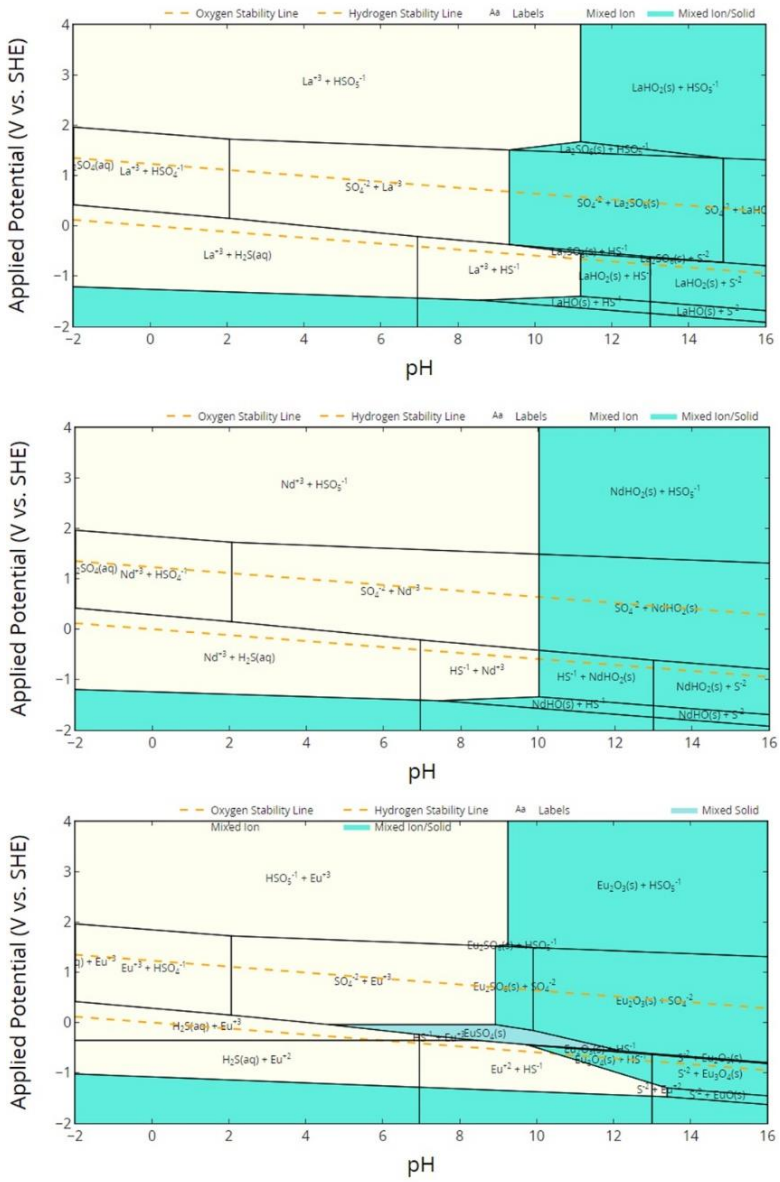

Figure 5.16: Pourbaix diagrams of La, Nd, and Eu in H_2SO_4 solution (https://next-gen.materialsproject.org/pourbaix)

5.3 Study of different mixing systems

These experiments covered the mixing of immiscible aqueous and organic phases using a probe-type ultrasonic system and mechanical mixer. Figure 5.17 represents the pH effect on %E of La, Nd, and Eu while mixing with ultrasound. It is evident that the extraction improved on increasing the pH, and the maximum recoveries were

achieved at 2.0 pH, where the values were 90%, 98.36%, and 99.85% for La, Nd, and Eu, respectively. These high extraction values show that ultrasound mixing was effective and should be used at high pH for the said system under the mentioned conditions of feed and ultrasound system specifications.

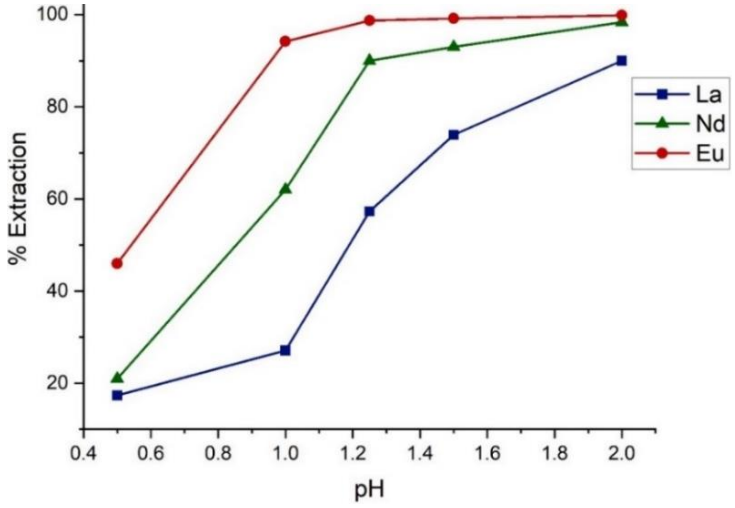

Figure 5.17: pH effect on %E of La, Nd, and Eu from HCl solution using ultrasonic probe system

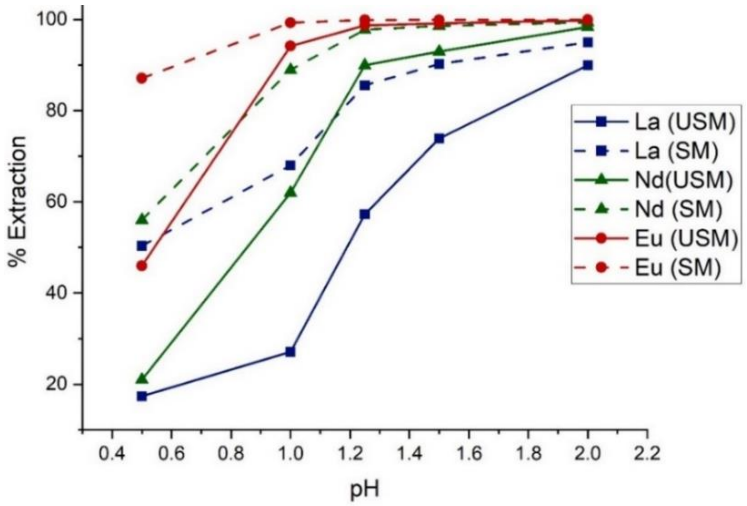

Figure 5.18: Comparison of extraction of La, Nd, and Eu from HCl feed solutions using ultrasound mixing (USM) and spray mixing (SM)

Figure 5.18 compares ultrasound mixing (USM) and spray mixing (SM) while keeping all the other factors constant. The aqueous feed was 1.0 M HCl with 1.0 g/L of each REO, and the organic phase was 0.303 M DEHPA (10:90 v/v diluted in

kerosene). It can be seen that the extraction was superior in the case of spray mixing for all the elements at any pH value. The difference between the extraction and, hence, the performance between the two systems is high at the lower pH values, and this difference decreases as the pH of the aqueous phase increases. Both the mixing systems performed almost similar after 1.25 pH in the case of Eu. On the other hand, the extraction values were close at 2.0 pH for Nd and La for both the mixing systems. Moreover, the emulsion formed during ultrasonic mixing was more stable and took more time to separate the product phases, making this system comparatively less effective than the solutions spray system. Other studies have also reported this difficulty in phase separation (Saien & Daneshamoz, 2018).

Figure 5.19 shows the pH effect on %E of La, Nd, and Eu while using a mechanical mixer. The % extraction increased with the rise in pH, and the maximum values at 2.0 pH were 73.68%, 89.25%, and 98.60% for La, Nd, and Eu, respectively.

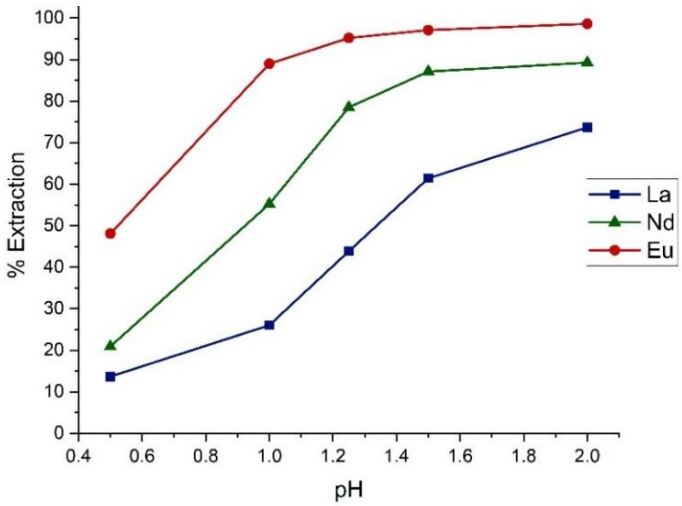

Figure 5.19: pH effect on %E of La, Nd, and Eu from HCl solution using a mechanical mixer

A comparison between solutions spray and mechanical mixing is represented in Figure 5.20. It is evident from this figure that the solutions spray system was superior compared to the mechanical mixer in terms of % E of all the elements, especially at low pH values. The difference was noticeable even at 2.0 pH for Nd and La, and the %E was more in the case of the solutions spray system.

Furthermore, the mixing and phase separation was instantaneous in the case of the solutions spray system, while it took 10 minutes for mixing and 4.0 hours for phase separation in the case of mechanical mixing. Therefore, these results %E and mixing and separation time suggest that the solutions spray system is advantageous over the mixer-settler.

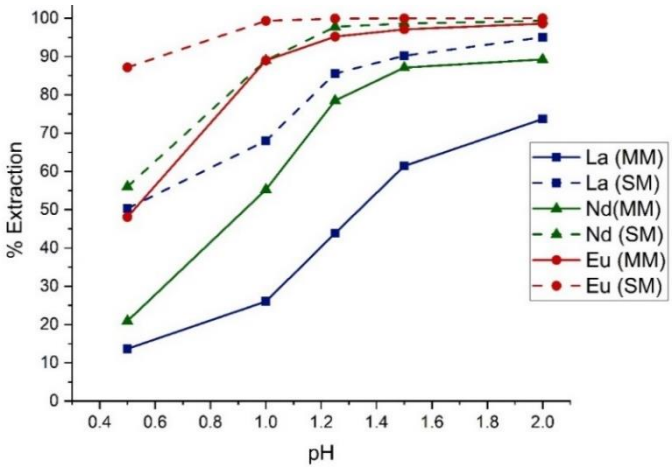

Figure 5.20: Comparison of extraction of La, Nd, and Eu from HCl feed solutions using mechanical mixing (MM) and spray mixing (SM)

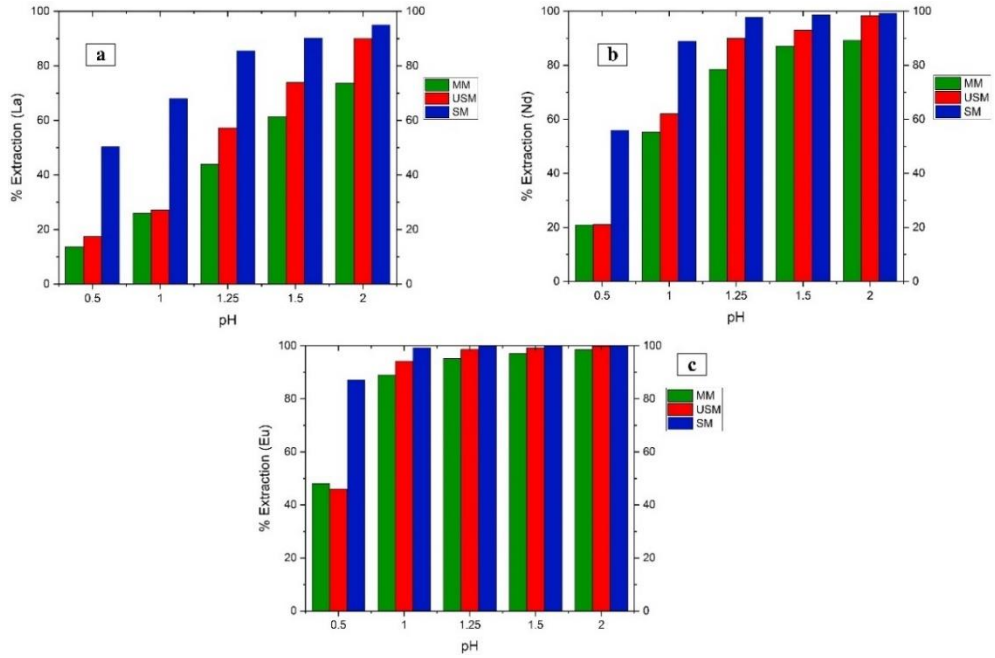

Figure 5.21: Comparison of mechanical mixing (MM), ultrasound mixing (USM), and solutions spray mixing (SM) for the extraction of a) La, b) Nd, and c) Eu

Figure 5.21 compares all three methods (solutions spray mixing system, ultrasound mixing, and mechanical mixing) used in this study with respect to the % extraction of La, Nd, and Eu. It is apparent that the solutions spray system showed more recovery of REEs, followed by ultrasound mixing and mechanical mixing. The difference in their performance was less at higher pH values of the feed solution and also for Eu. The solutions spray system seems favorable and an attractive option because of its small mixing and separation time over the other techniques, along with the greater recovery of the REEs. The system performs better because of the mono-sized micro-droplets produced in the mixing column with the help of spray nozzles. Those droplets improved the mass transfer and recovery of REEs in the mixing chamber and also aided the quick separation of the product streams in the separation column. The geometry of the settling column not only improves the settling time but also the quality of the product.

5.4 Study of the solutions spray system for the chloride feed solution having REEs concentration representative of Beylikova leach

Finally, the pH and DEHPA concentration effect was studied on the extraction of REEs from aqueous feed solution representative of Beylikova leach having 6.0 g/L La_2O_3, 2.5 g/L Nd_2O_3, and 100 mg/L Eu_2O_3. Furthermore, the effect of A:O phase volume ratios for extraction and stripping sections and the HCl concentration effect for stripping REEs was observed.

5.4.1 Effect of pH

As already discussed, extraction increases with the rise in aqueous feed pH. Figure 5.22 shows the effect of pH on %E of REEs from the chloride solution, where the extraction increased with the rise in pH of the feed solution. For Eu, the %E was almost independent of pH after 1.0 pH. Meanwhile, extraction increased gradually for La and Nd with the rise in pH, achieving maximum %E at 2.0 pH. The maximum

extraction value was 70.32%, 85.31%, and 99.26% for La, Nd, and Eu, respectively. The %E for La and Nd is small, even at 2.0 pH, because of their high concentrations in the feed solution. However, the amounts extracted from these elements are reasonably high. Under the studied conditions, these might be the maximum loading of REEs on DEHPA while keeping equilibrium against the H^+ released into the aqueous phase. On the other hand, selective separation of Eu from other elements increased by decreasing the pH of the feed solution.

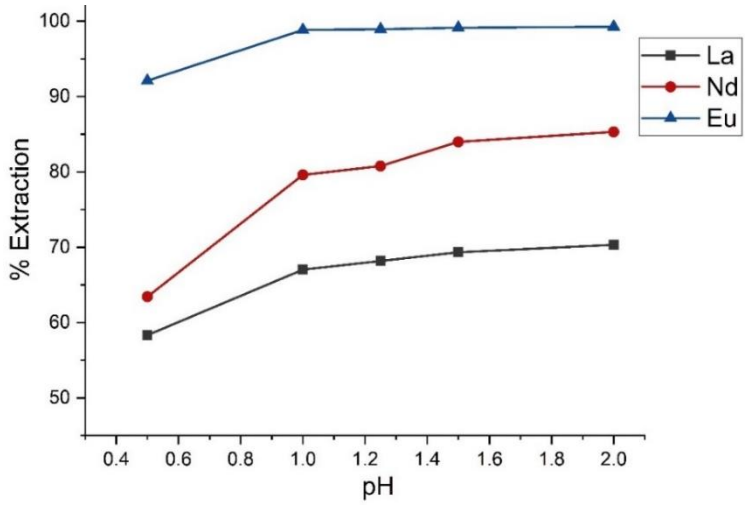

Figure 5.22: pH effect on %E of La, Nd, and Eu (aqueous feed representative of Beylikova leach, and 0.303 M DEHPA)

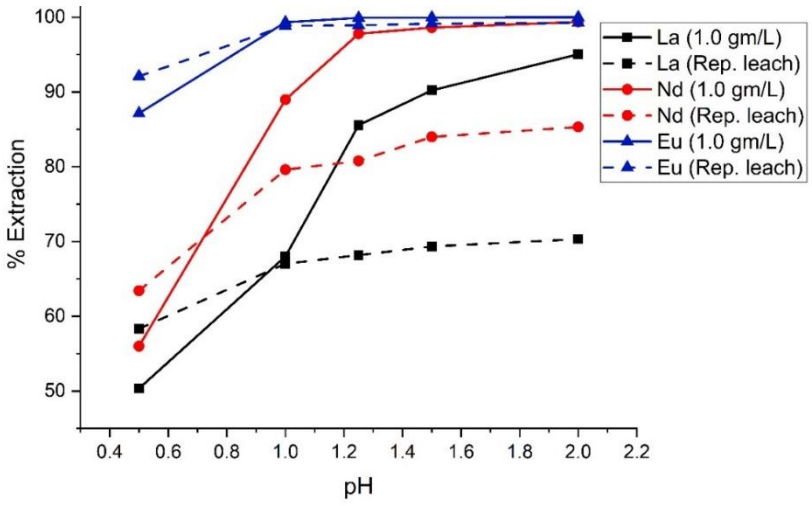

Figure 5.23: Comparison of %E of La, Nd, and Eu from the two aqueous feeds (aqueous feed having 1.0 gm/L of each REO vs aqueous feed representative of Beylikova leach and 0.303 M DEHPA)

Table 5.2: Comparison of the extraction of REEs from chloride solutions having different concentrations with 0.303 M DEHPA

pH	Amount extracted (mg/L)					
	Aqueous solution having 1.0 g/L of each REO			Aqueous solution representative of Beylikova leach		
	La	Nd	Eu	La	Nd	Eu
0.50	503.44	560.00	871.44	3499.70	1585.50	92.10
1.00	680.00	889.80	993.17	4021.39	1989.89	98.83
1.25	855.68	977.78	999.10	4090.00	2019.25	98.92
1.50	902.08	986.06	999.40	4159.84	2099.58	99.12
2.00	950.34	993.6	999.76	4219.25	2132.72	99.26

Figure 5.23 shows that the %E of REEs was higher in the leach solution with 1.0 g/L of each REO compared to the solution with higher values of La and Nd oxides. Furthermore, Table 5.2 shows a comparison of the amount of REEs extracted in these two cases, and it can be seen that the amounts of REEs extracted were very high from the feed solution, which had higher concentrations of REEs.

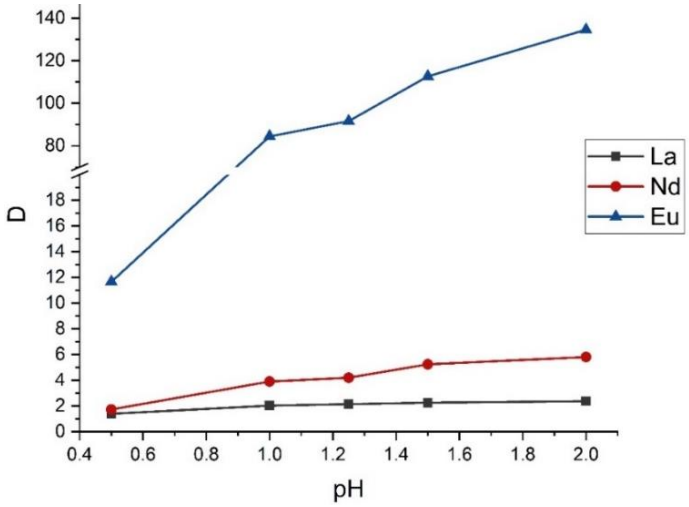

Figure 5.24: Effect of pH on D of La, Nd, and Eu (aqueous feed representative of Beylikova leach, and 0.303 M DEHPA)

Figure 5.24 elaborates the effect of pH on the distribution ratios of La, Nd, and Eu. It can be seen that the values of D increased with the rise in pH, and the increasing

rate was highest for Eu, followed by Nd and La because of the difference in their ionic radii. The maximum values of D were obtained at 2.0 pH, and the values were 2.37, 5.81, and 134.53 for La, Nd, and Eu, respectively. Small values of D for La and Nd show that many counter-current extraction stages will be required for their complete extraction, whereas Eu will be recovered in a single-stage operation because of its high D value.

5.4.2 Effect of DEHPA concentration

DEHPA concentration was also changed to see its effect on %E of REEs from aqueous feed representative of Beylikova leach, a solution having high concentrations of La and Nd compared to Eu. DEHPA having concentrations 0.151, 0.212, 0.303, 0.454, 0.605, and 0.757 M (5, 7, 10, 15, 20, and 25% v/v respectively diluted in kerosene) were used in this study.

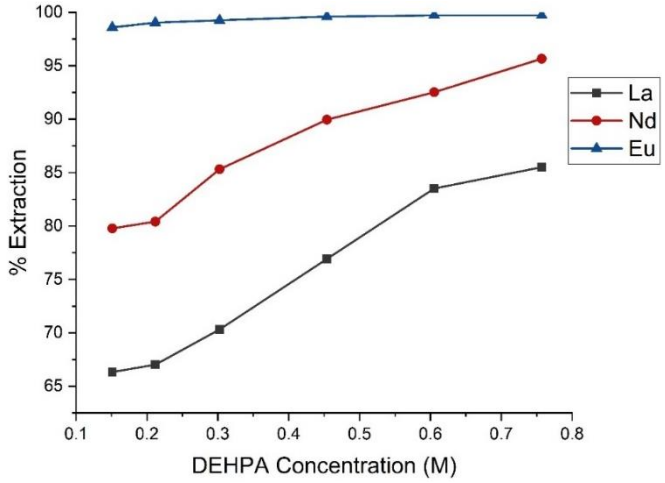

Figure 5.25: DEHPA concentration effect on %E of La, Nd, and Eu (aqueous feed representative of Beylikova leach)

Figure 5.25 represents the effect of DEHPA concentration on %E of REEs and shows that the %E increased with the rise in DEHPA concentration, especially for La and Nd. The %E for Eu remained almost independent of the DEHPA concentration because of its very high bonding affinity with DEHPA compared to the other elements under discussion. Meanwhile, for La and Nd, the extraction increased

gradually with the rise in DEHPA concentration, achieving maximum values of 0.757 M DEHPA. The maximum values of %E were 85.51%, 95.66%, and 99.71% for La, Nd, and Eu, respectively, with 0.757 M DEHPA. Contrary to complete extraction, the selective separation of these REEs increased by reducing the DEHPA concentration because of the competition between the REEs against the limited availability of cation exchange sites.

Similar to the %E, the distribution ratio also increased with the rise in DEHPA concentration, and this trend is shown in Figure 5.26. It can also be seen that similar to %E, the increasing rate of D for Eu is highest, followed by Nd and La, and the maximum values were 5.90, 22.06, and 349.73 for La, Nd, and Eu, respectively.

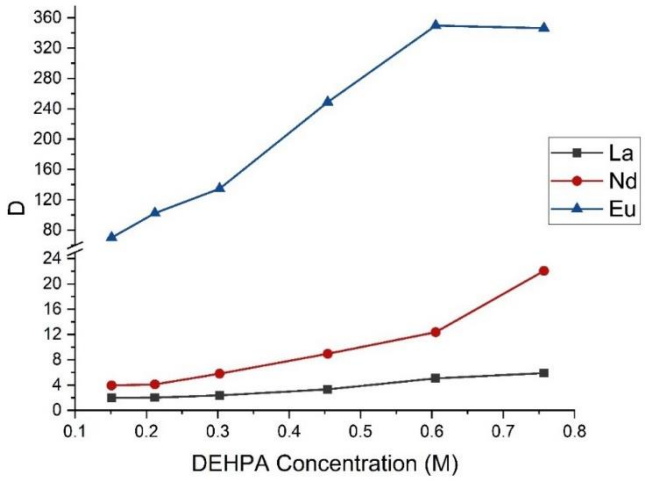

Figure 5.26: Effect of DEHPA concentration on the distribution ratio of La, Nd, and Eu (aqueous feed representative of Beylikova leach)

5.4.3 Stoichiometry of the extracted REEs

The common slope analysis method was used to understand the stoichiometry of the extracted RE-DEHPA complexes. The data was obtained using 1.0 M HCl feed solution having 2.5 g/L Nd_2O_3, 6.0 g/L La_2O_3, and 100 mg/L Eu_2O_3, and 0.303 M DEHPA used as an organic solvent and is presented in Figure 5.27. It shows that about one H^+ was released from DEHPA into the aqueous phase during the extraction of each of La, Na, and Eu. Because of their very high concentrations in feed

solutions, these elements not only bonded with DEHPA but also maintained their bonds with Cl^- and were loaded on DEHPA in chloride complex form ($RECl_2(HA_2)$) as shown in Equation 5.8.

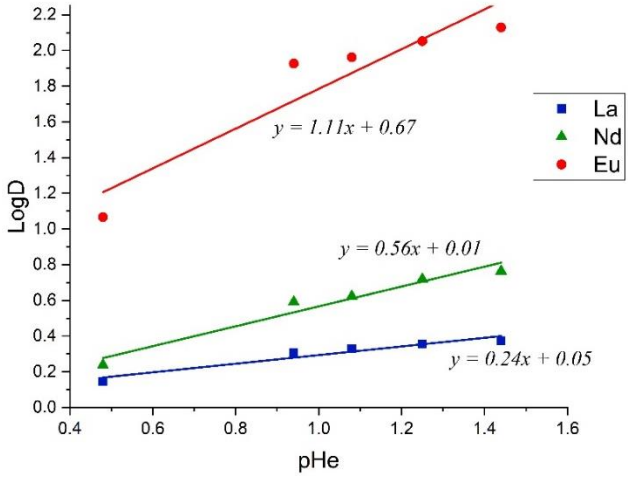

Figure 5.27: Effect of pH at the equilibrium on the extraction stoichiometry of REEs (aqueous feed representative of Beylikova leach and 0.303 M DEHPA)

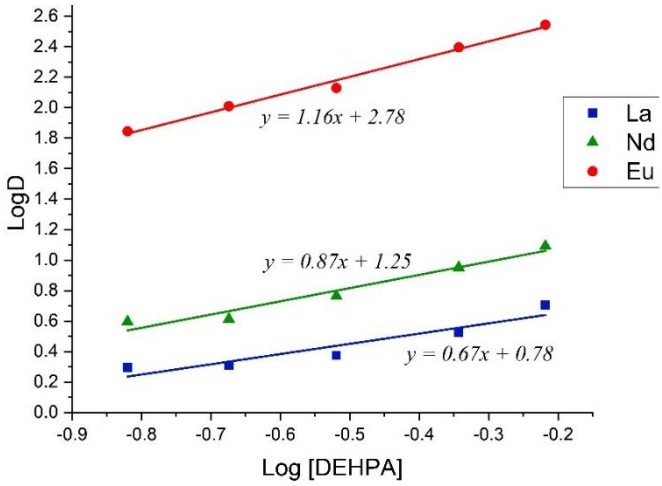

Figure 5.28: Effect of DEHPA concentration on the extraction stoichiometry of REEs (aqueous feed representative of Beylikova leach)

Furthermore, the stoichiometry of these extractions was also observed by changing the concentration of DEHPA, and the results are shown in Figure 5.28. Here, the concentrations of La and Nd were high enough that these RE ions broke the hydrogen bond in DEHPA dimers and converted those DEHPA into monomers. This can be

seen from the slopes of straight lines in Figure 5.28 having values of 0.67, 0.87, and 1.16 for La, Nd, and Eu, respectively. It means that one DEHPA molecule was involved in the extraction of La^{+3} and Nd^{+3}, while one DEHPA dimer extracted Eu^{+3}.

5.4.4 McCabe Thiele diagrams for the extraction operation

The effect of the A:O phase ratio was also observed on the percent extraction of REEs from an aqueous solution having concentrations of REEs equal to Beylikova leach prepared in 1.0 M HCl, and the concentration of DEHPA was 0.303 M and is shown in Figure 5.29.

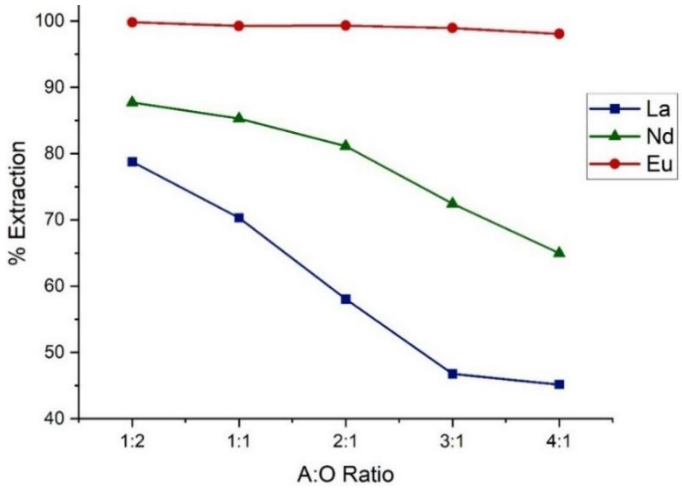

Figure 5.29: Effect of A:O phase ratio on % extraction of REEs (aqueous feed representative of Beylikova leach, and 0.303 M DEHPA)

It is clear from Figure 5.29 that extraction reduced with the increase of aqueous phase volume compared to the organic phase volume because of the lower DEHPA ions concentration than the RE ions in the aqueous phase. Moreover, Eu extraction did not reduce much, but Nd and La extraction dropped with this change. Maximum extraction of Eu, Nd, and La was 99.81%, 87.71%, and 78.79%, respectively, at an A:O ratio of 1:2, whereas the extraction was 99.26%, 85.31%, and 70.32%, respectively, at the A:O phase ratio of 1:1 under the conditions studied. The values are comparable under these A:O phase ratios, but after that, the extraction reduced greatly, especially in the case of La. It is also clear from this graph that the selective

separation of these elements increased by increasing the volume of the aqueous phase against the organic phase volume.

McCabe Thiele diagrams were also plotted for these experiments to see the number of theoretical counter-current stages in the extraction of La, Nd, and Eu and are shown in Figure 5.30. Figure 5.30a shows the McCabe Thiele diagram for La, and it can be seen that about six counter-current extraction stages were required for complete extraction at an A:O phase ratio of 1:1. The number of stages increased on further increasing the volume of the aqueous phase. About eleven stages were required to extract La in case of an A:O phase ratio of 1.5:1 with almost 300 mg/L in the raffinate. Whereas saturation of DEHPA was reached after a five-stage counter-current operation in the case of an A:O phase ratio of 2:1, and the amount of raffinate was about 1600 mg/L, which suggests keeping the A:O phase ratio below this value for maximum extraction of La from this aqueous feed.

It is evident from Figure 5.30b that three stages were sufficient for the complete extraction of Nd at an A:O phase ratio of 1:1. Almost complete extraction was also observed for an A:O phase ratio of up to 2.5:1 with raffinate close to 100 mg/L, whereas the raffinate was almost 160 mg/L after seven stage counter-current operation in case of A:O phase ratio of 3:1. On further increasing the A:O phase ratio, the saturation of DEHPA occurred leaving more than 300 mg/L in the raffinate. Figure 5.30c shows the theoretical number of extraction stages for Eu. It can be seen that Eu can be easily extracted in a single-stage process even at an A:O phase ratio of 5:1. This easy and complete extraction is due to the very small concentration of Eu in the aqueous phase under study.

From these findings, it can be concluded that these elements can either be extracted as a single group by using an A:O phase ratio of 1:1, or they can be selectively separated from each other. In the case of selective extraction, one should first opt for an A:O phase ratio of 5:1, which will result in the extraction of Eu in a single-stage counter-current operation while leaving maximum La and Nd in the aqueous raffinate. Further processing of this raffinate by selecting an A:O phase ratio of 3:1

will extract maximum Nd, and the raffinate will be rich with La. Therefore, these elements can be either recovered as a group or selectively separated by selecting the optimum value of the A:O phase ratio and number of extraction stages.

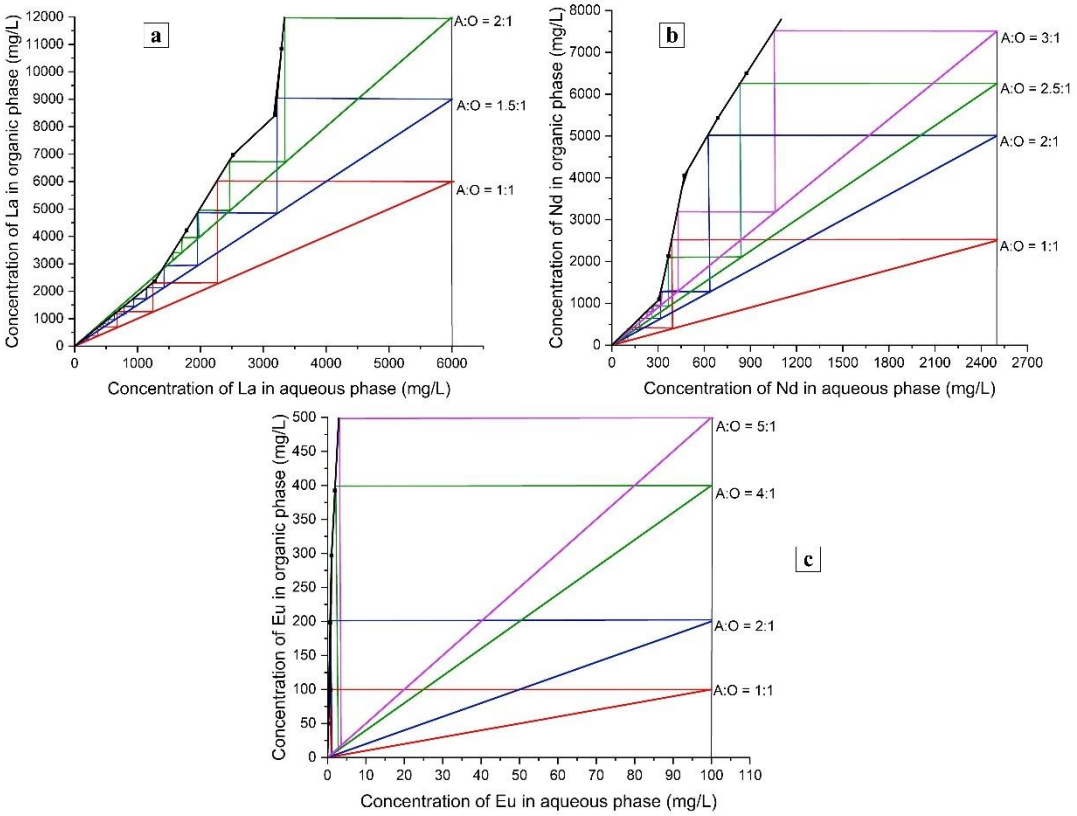

Figure 5.30: McCabe Thiele diagrams for La, Nd, and Eu extraction (aqueous feed representative of Beylikova leach and 0.303 M DEHPA)

5.4.5 Stripping of REEs

Similar to the previous stripping experiments, this stripping study involved HCl as a stripping solution with molarities 2, 3, 4, 5, and 6 M. Other parameters were constant, like an A:O phase ratio of 1:1 and inlet stream flow rates of 150 mL/min.

The effect of HCl molarity on the stripping of REEs from loaded DEHPA is shown in Figure 5.31. It can be seen that %S increased with the rise in acidity of the stripping solution. The increase in acidity caused the rise in H^+ concentration, thus replacing more and more RE^{+3} from DEHPA and sending it to the aqueous phase by the cation

exchange process. Maximum recoveries were 71.21%, 86.39%, and 92.29% for La, Nd, and Eu using 6.0 M HCl. Moreover, it is being revealed that %S of Eu is highest, followed by Nd and La, but the amount of REEs recovered by stripping is highest for La, followed by Nd and Eu, shown in Table 5.3, because of the high bonding affinity of Eu with DEHPA followed by Nd and La.

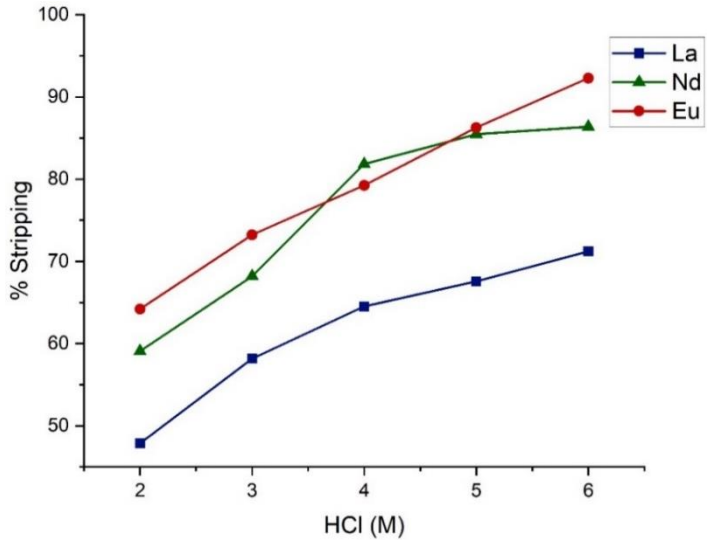

Figure 5.31: Effect of HCl molarity on stripping of La, Nd, and Eu from loaded DEHPA

Table 5.3: Amount of La, Nd, and Eu recovered by stripping through HCl form loaded DEHPA having 3000 mg/L La, 2200 mg/L Nd, and 99.69 mg/L Eu

HCl	**Concentration in stripped solution (mg/L)**		
(M)	**La**	**Nd**	**Eu**
2.0	1436.36	1300.00	64.00
3.0	1745.45	1500.00	73.00
4.0	1935.48	1800.00	79.00
5.0	2027.27	1880.23	86.00
6.0	2136.36	1900.54	92.00

5.4.6 McCabe Thiele diagrams for stripping of REEs

Similar to the 1st series of experiments, the McCabe Thiele diagrams were also plotted for this case to see the number of theoretical counter-current stages for complete or selective stripping of REEs from the loaded DEHPA. Initially, 2.0 M HCl was used as the stripping solution while the A:O phase ratio was changed from 2:1 to 1:4, and the diagrams are shown in Figure 5.32.

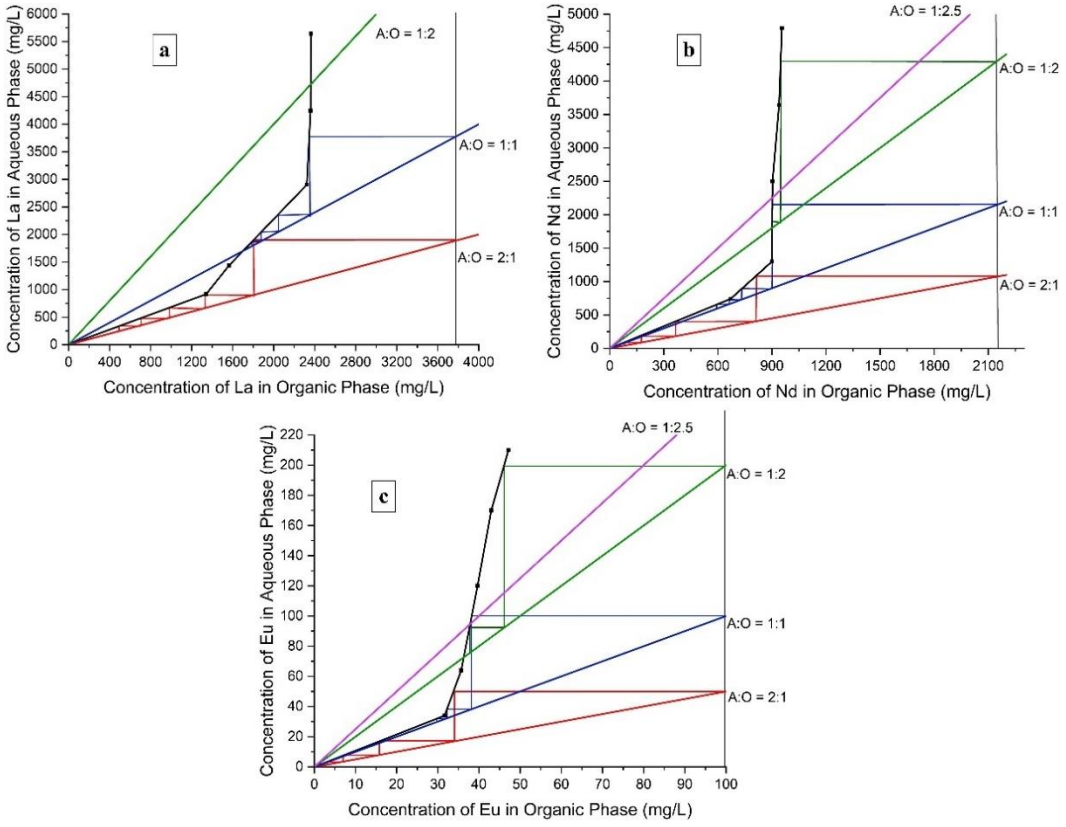

Figure 5.32: McCabe Thiele diagrams for stripping of La, Nd, and Eu using 2.0 M HCl

Figure 5.32a shows the number of theoretical counter-current stages for the stripping of La. It is apparent that 2.0 M HCl is insufficient to recover La from this mixture of REEs because of its high concentration in loaded DEHPA. Almost five stages will strip maximum La while releasing 500 mg/L in the organic phase in case of A:O phase of 2:1, which does not seem economical. The unrecovered La in the DEHPA

was further increased while reducing the A:O phase ratio. The A:O phase ratio value should be less than 1:1 for the stripping to be economical and efficient. Similar was the case for Nd (Figure 5.32b) and Eu (Figure 5.32c), where the recovery was not high enough with 2.0 M HCl stripping solution at an A:O phase ratio of 1:1 or lower ratios, and the saturation of stripping solution occurred, leaving maximum amounts in DEHPA. It is, therefore, necessary to use a higher concentration of HCl stripping solution.

For efficient and economic recovery of REEs from this highly loaded DEHPA, further experiments were performed with 4.0 M HCl as the stripping solution while changing the A:O phase ratio from 2:1 to 1:4, and the McCabe Thiele diagrams for this stripping operation are shown in Figure 5.33.

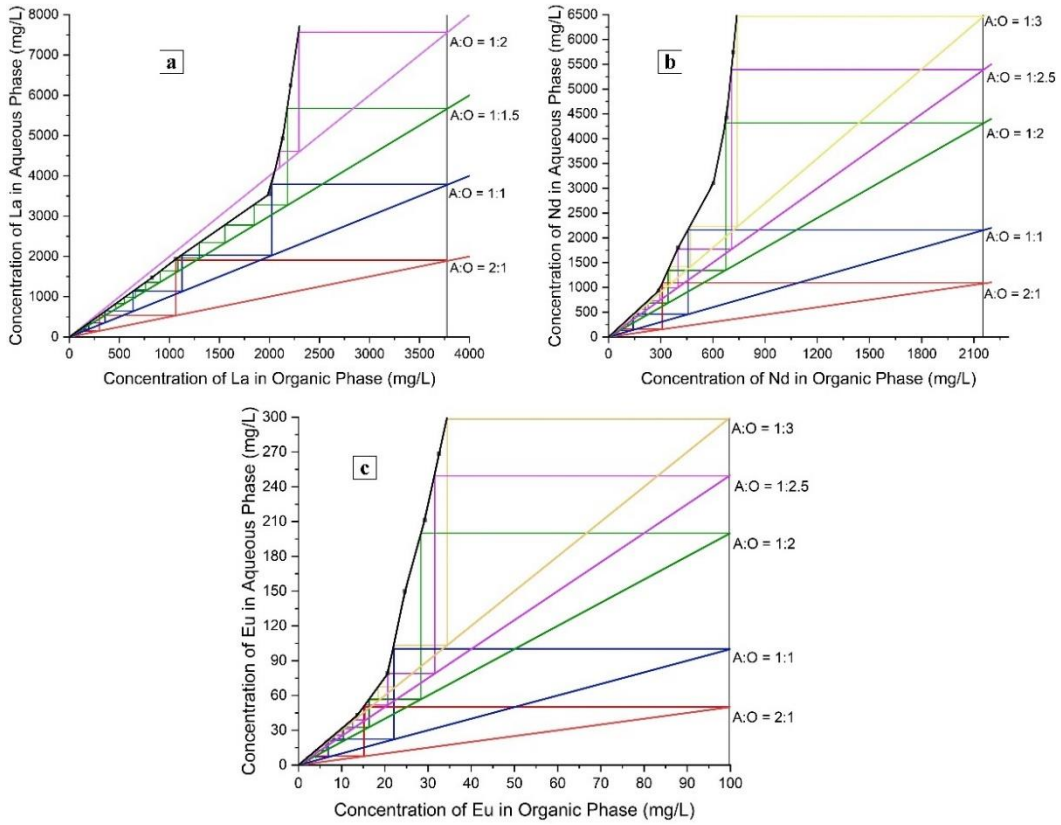

Figure 5.33: McCabe Thiele diagrams for stripping of La, Nd, and Eu using 4.0 M HCl

Figure 5.33a represents the stripping of La and shows that La striping was efficient at an A:O phase ratio of 1:1. At this phase ratio, complete recovery of La was observed with about eight counter-current stripping operations. Whereas, at the A:O phase ratio of 1:1.5, the maximum stripping was observed after about twelve stages with almost 400 mg/L La left in the DEHPA. Moreover, on further increasing the volume of the organic phase, the saturation of the stripping solution reached very early, leaving maximum La in the DEHPA. On the other hand, almost complete recovery of Nd and Eu was observed at an A:O phase ratio of 1:2, as shown in Figure 5.33b and Figure 5.33c with a six-stage stripping operation. These two elements can even be recovered in sufficient quantity using an A:O phase ratio of up to 1:3 because of their lower concentration in DEHPA compared to La.

It is concluded from the results shown in Figure 5.33 that these REEs can be recovered from DEHPA with 4.0 HCl as a stripping solution. This stripping will give complete recovery as a group of REEs using an A:O phase ratio of 1:1 or can be selectively separated from each other by using more organic phase volume than the aqueous stripping solution. In the case of selective recovery, La will be recovered in the DEHPA, while Nd and Eu will be in the stripping solution. These product streams will be further processed to separate and completely recover La, Nd, and Eu.

CHAPTER 6

CONCLUSION AND RECOMMENDATIONS

In this research work, a mixing and phase separation setup was made to accelerate the mass transfer and recovery, as well as the kinetics of SX operation. The designed "solutions spray system" overcame the common problems encountered by conventional SX equipment, like back-mixing of feed solutions in the case of spray columns and slow separation of product streams observed by the mixer-settler. Introducing feed streams in the form of mono-sized micro-droplets with the help of spray nozzles increased the mass transfer efficiency, and the unique design of the settling column boosted the separation of the product streams and the quality of the product. A comparison of percent extraction, distribution ratio, and mixing and separation time for the present work with different studies from the literature revealed the better performance of the solutions spray system over the commonly used mixer-settler technique.

Different experimental studies were conducted to observe the performance of the solution spray system in terms of mass transfer, recovery, and mixing and separation times. In these experiments, the variables like REEs concentrations in feed solution (1.0 g/L of each REO and solution representative of Beylikova leach solution), pH (0.50 – 2.0), ionic strength (0.19 – 1.54 mol/L), DEHPA concentration (5% – 20% v/v diluted in kerosene), type of feed solutions (chloride and sulfate), and concentrations of stripping solutions (2.0 – 6.0 M HCl) were studied to see the performance of solutions spray system. Moreover, a few experiments were also performed with other mixing techniques (mechanical mixing and ultrasound mixing), and their extraction results were compared with those of the solutions spray system.

It was found that the extractions of REEs increased with the rise in aqueous feed pH and the ionic strength, and the DEHPA concentration. Whereas the selective extraction was higher at lower values of solution pH, ionic strength, and DEHPA concentration. Furthermore, the stripping increased with the rise in the acidity of the stripping solution because of the increase in H^+ concentration, which can replace RE^{3+} from loaded DEHPA. Moreover, the extractions of REEs were better from chloride solution than the sulfate feed solution because of the presence of HSO_4^- complexes in the case of sulfate solution, which hindered the extraction through DEHPA. For the chloride feed solution having 1.0 g/L of each REO, the optimal REEs extractions were observed for solution at 2.0 pH, having 1.54 mol/L ionic strength while using 0.303 M DEHPA and the extraction was 95.03%, 99.36%, and 99.98% for La, Nd, and Eu, respectively. Under these variables, the distribution ratio values were 19.14, 155.25, and 4165 for La, Nd, and Eu, respectively. These high values of D showed the easy extraction of these REEs in a single-stage SX operation. Additionally, the separation factors were 6.69, 5.33, and 1.26 for Eu/La, Eu/Nd, and Nd/La, respectively, at 0.50 pH of the feed solution, representing the separation of these elements from each other at low pH value. Furthermore, the stripping with 2.0 M HCl seemed economical, with recoveries of 77.53%, 65.80%, and 51.05% for La, Nd, and Eu, respectively. On the other hand, for the chloride feed solution having 6.0 g/L La_2O_3, 2.5 g/L Nd_2O_3, and 100 mg/L Eu2O3 under similar values of variables, the percent extraction was 70.32%, 85.31%, and 99.26% for La, Nd, and Eu, respectively. In this case, the 4.0 M HCl stripping solution gave the economic recovery because of the very high concentration of REEs in DEHPA, and the percent stripping was 64.52%, 81.82%, and 79.25% for La, Nd, and Eu, respectively. Finally, McCabe Thiele diagrams were plotted for extraction and stripping stages for all the cases to see the number of theoretical stages for complete recovery and selective separation of REEs from each other. It was found that these elements can either be recovered completely as a group or collected separately by changing the number of counter-current stages and the A:O phase ratio. The effect of different parameters on selective separation and recovery as a group of REEs is summarized in Table 6.1.

Table 6.1: Effect of different parameters on complete recovery of REEs as a group and their selective separation in extraction and stripping stages

Process	Effect of Parameters	
	Complete recovery of REEs as a group	**Selective separation of REEs**
Extraction	➢ Increase • pH • Ionic strength • DEHPA concentration ➢ Decrease A:O phase ratio ➢ Increase the number of counter-current stages	➢ Decrease • pH • Ionic strength • DEHPA concentration ➢ Increase A:O phase ratio ➢ Decrease the number of counter-current stages
Stripping	➢ Increase • Concentration of stripping solution • A:O phase ratio • Number of counter-current stages	➢ Decrease • Concentration of stripping solution • A:O phase ratio • Number of counter-current stages

Finally, the extraction of REEs was also studied while mixing the two immiscible feed streams using a mechanical mixer and ultrasound mixing. It was found that the solutions spray system was more efficient compared to the other mixing systems, especially for the solutions at lower pH values. Whereas the extraction with all the tested mixing systems was comparable for feed solutions at 2.0 pH, however, the solutions spray system was advantageous in terms of mixing and separation time compared to the other tested techniques. This was because of the generation of mono-sized micro-droplets of the immiscible feed streams in the mixing column of the solutions spray system, which improved the mass transfer and the recovery of the product streams. Furthermore, the design of the separation column aided the separation of the product streams and also improved the quality of the product by

fully separating the two immiscible phases. In light of all these results, the solutions spray system seems attractive because it enhances the kinetics of the SX operation by reducing the time of mixing and separation of immiscible phases and improves the recovery by enhancing the mass transfer of the REEs between the two immiscible phases.

This research was carried out with the synthesized solution of REOs dissolved mostly in HCl. Following are some recommendations for the future work:

- Use the actual leach obtained from the leaching of Beylikova ore having different impurities along with the REEs and study the extraction process.
- A set of similar spray nozzles was used in this study. Use diverse spray nozzles to produce different droplet sizes of inlet streams and study the effect of droplet sizes on the extraction of REEs.
- Perform the counter-current operations for extraction and stripping stages to validate the McCabe Thiele diagrams.
- Use the mixing column of this solutions spray setup with the settling tank of the mixer-settler to see the effect of mixing for the two mixing systems (the spray mixing system and the mechanical mixing). Similarly, use the settling column from this solutions spray system with the mechanical mixer and see the performance of this settling column for both the mixing systems (the spray mixing and the mechanical mixing)
- Apply this technique of solutions spray system to a pilot scale setup.
- An extensive study of ultrasound mixing is needed to observe the overall operation.

REFERENCES

Abaka-Wood, G. B., Addai-Mensah, J., & Skinner, W. (2016). Review of Flotation and Physical Separation of Rare Earth Element Minerals. *4th UMaT Biennial International Mining and Mineral Conference* , *4*(November), 55–62.

Abreu, R. D., & Morais, C. A. (2014). Study on separation of heavy rare earth elements by solvent extraction with organophosphorus acids and amine reagents. *Minerals Engineering*, *61*, 82–87. https://doi.org/10.1016/j.mineng.2014.03.015

Acharya, S., Mishra, S., & Misra, P. K. (2015). Studies on extraction and separation of La(III) with DEHPA and PC88A in petrofin. *Hydrometallurgy*, *156*, 12–16. https://doi.org/10.1016/j.hydromet.2015.05.005

Agarwal, V., & Safarzadeh, M. S. (2017). Solvent extraction and separation of cerium(III) and samarium(III) from mixed rare earth solutions using PC88A. *Minerals and Metallurgical Processing*, *34*(3), 125–131. https://doi.org/10.19150/mmp.7612

Agarwal, V., Safarzadeh, M. S., & Galvin, J. (2018). Solvent extraction and separation of Y(III) from sulfate, nitrate and chloride solutions using PC88A diluted in kerosene. *Mineral Processing and Extractive Metallurgy Review*, *39*(4), 258–265. https://doi.org/10.1080/08827508.2017.1415210

Amato, A., Becci, A., Birloaga, I., De Michelis, I., Ferella, F., Innocenzi, V., Ippolito, N. M., Pillar Jimenez Gomez, C., Vegliò, F., & Beolchini, F. (2019). Sustainability analysis of innovative technologies for the rare earth elements recovery. *Renewable and Sustainable Energy Reviews*, *106*(March), 41–53. https://doi.org/10.1016/j.rser.2019.02.029

Arellano Ruiz, V. C., Kuchi, R., Parhi, P. K., Lee, J. Y., & Jyothi, R. K. (2020). Environmentally friendly comprehensive hydrometallurgical method

development for neodymium recovery from mixed rare earth aqueous solutions using organo-phosphorus derivatives. *Scientific Reports*, *10*(1), 1–13. https://doi.org/10.1038/s41598-020-74041-9

Ariana, R. (2016). *Rare Earth Elements A New Approach to the Nexus of Supply, Demand and Use: Exemplified along the Use of Neodymium in Permanent Magnets*.

Bartolomeo, G. Di, Fard, B. M., & Semmler, W. (2021). *WORKING PAPER Department of Economics and Law*. *196*, 1–27.

Batchu, N. K., & Binnemans, K. (2018). Effect of the diluent on the solvent extraction of neodymium(III) by bis(2-ethylhexyl)phosphoric acid (D2EHPA). *Hydrometallurgy*, *177*(March), 146–151. https://doi.org/10.1016/j.hydromet.2018.03.012

Batey, W., & Thornton, J. D. (1992). Partial mass-transfer coefficients and packing performance in liquid-liquid extraction. *Industrial and Engineering Chemistry Research*, *v*(n), 1096–1101.

Batnasan, A., Narankhuu, A., Battsengel, A., Haga, K., & Shibayama, A. (2021). *Effect of Organic Extractants on the Extraction of Rare Earth Elements from Sulphuric Acid Leach Liquor*.

Battsengel, A., Batnasan, A., Haga, K., & Shibayama, A. (2018). Selective Separation of Light and Heavy Rare Earth Elements from the Pregnant Leach Solution of Apatite Ore with D2EHPA. *Journal of Minerals and Materials Characterization and Engineering*, *06*(05), 517–530. https://doi.org/10.4236/jmmce.2018.65037

Battsengel, A., Batnasan, A., Narankhuu, A., Haga, K., Watanabe, Y., & Shibayama, A. (2018). Recovery of light and heavy rare earth elements from apatite ore using sulphuric acid leaching, solvent extraction and precipitation. *Hydrometallurgy*, *179*(June 2017), 100–109. https://doi.org/10.1016/j.hydromet.2018.05.024

Bautista, R. G. (1995). Chapter 139 Separation chemistry. *Handbook on the Physics and Chemistry of Rare Earths*, *21*, 1–27. https://doi.org/10.1016/S0168-1273(05)80108-4

Belova, V. V. (2017). Development of solvent extraction methods for recovering rare earth metals. *Theoretical Foundations of Chemical Engineering*, *51*(4), 599–609. https://doi.org/10.1134/S004057951605002X

Budiman, S., Saputra, B., Hardian, A., Yuliana, T., Murniati, A., Kusumaningtyas, V. A., Nurdeni, Effendy, S., Mutalib, A., Anggraeni, A., & Bahti, H. H. (2021). Effect additional pH on separation extraction gadolinium from terbium and europium with Di-2-(ethylhexcyl)phosphate acid. *IOP Conference Series: Earth and Environmental Science*, *882*(1). https://doi.org/10.1088/1755-1315/882/1/012025

Cen, P., Bian, X., Liu, Z., Gu, M., Wu, W., & Li, B. (2021). Extraction of rare earths from bastnaesite concentrates : A critical review and perspective for the future. *Minerals Engineering*, *171*(April), 107081. https://doi.org/10.1016/j.mineng.2021.107081

Chang, H., Li, M., Liu, Z., Hu, Y., & Zhang, F. (2010). Study on separation of rare earth elements in complex system. *Journal of Rare Earths*, *28*(SUPPL. 1), 116–119. https://doi.org/10.1016/S1002-0721(10)60270-0

Chen, Z. (2011). Global rare earth resources and scenarios of future rare earth industry. *Journal of Rare Earths*, *29*(1), 1–6. https://doi.org/10.1016/S1002-0721(10)60401-2

Cherepovitsyn, A., & Solovyova, V. (2022). Prospects for the Development of the Russian Rare-Earth Metal Industry in View of the Global Energy Transition—A Review. *Energies*, *15*(1). https://doi.org/10.3390/en15010387

Dashti, S., Sadri, F., Shakibania, S., Rashchi, F., & Ghahreman, A. (2021). Separation and solvent extraction of rare earth elements (Pr, Nd, Sm, Eu, Tb, and Er) using TBP and Cyanex 572 from a chloride medium. *Minerals*

Engineering, *161*(September 2020), 106694. https://doi.org/10.1016/j.mineng.2020.106694

Deferm, C., Onghena, B., Vander Hoogerstraete, T., Banerjee, D., Luyten, J., Oosterhof, H., Fransaer, J., & Binnemans, K. (2017). Speciation of indium(iii) chloro complexes in the solvent extraction process from chloride aqueous solutions to ionic liquids. *Dalton Transactions*, *46*(13), 4412–4421. https://doi.org/10.1039/c7dt00618g

Demol, J., Ho, E., Soldenhoff, K., & Senanayake, G. (2019a). The sulfuric acid bake and leach route for processing of rare earth ores and concentrates: A review. *Hydrometallurgy*, *188*(April), 123–139. https://doi.org/10.1016/j.hydromet.2019.05.015

Demol, J., Ho, E., Soldenhoff, K., & Senanayake, G. (2019b). The sulfuric acid bake and leach route for processing of rare earth ores and concentrates: A review. *Hydrometallurgy*, *188*(December 2018), 123–139. https://doi.org/10.1016/j.hydromet.2019.05.015

Dushyantha, N., Batapola, N., Ilankoon, I. M. S. K., Rohitha, S., Premasiri, R., Abeysinghe, B., Ratnayake, N., & Dissanayake, K. (2020a). The story of rare earth elements (REEs): Occurrences, global distribution, genesis, geology, mineralogy and global production. *Ore Geology Reviews*, *122*(April), 103521. https://doi.org/10.1016/j.oregeorev.2020.103521

Dushyantha, N., Batapola, N., Ilankoon, I. M. S. K., Rohitha, S., Premasiri, R., Abeysinghe, B., Ratnayake, N., & Dissanayake, K. (2020b). The story of rare earth elements (REEs): Occurrences, global distribution, genesis, geology, mineralogy and global production. *Ore Geology Reviews*, *122*(January), 103521. https://doi.org/10.1016/j.oregeorev.2020.103521

Echeverry-Vargas, L., & Ocampo-Carmona, L. M. (2022). Recovery of Rare Earth Elements from Mining Tailings: A Case Study for Generating Wealth from Waste. *Minerals*, *12*(8), 948. https://doi.org/10.3390/min12080948

Evans, C. H. (1996). Episodes from the History of the Rare Earth Elements. In *Episodes from the History of the Rare Earth Elements*. https://doi.org/10.1007/978-94-009-0287-9

Ferdowsi, A., & Yoozbashizadeh, H. (2017). Solvent Extraction of Rare Earth Elements from a Nitric Acid Leach Solution of Apatite by Mixtures of Tributyl Phosphate and Di-(2-ethylhexyl) Phosphoric Acid. *Metallurgical and Materials Transactions B: Process Metallurgy and Materials Processing Science*, *48*(6), 3380–3387. https://doi.org/10.1007/s11663-017-1086-6

Flett, D. S. (2005). Solvent extraction in hydrometallurgy: The role of organophosphorus extractants. *Journal of Organometallic Chemistry*, *690*(10), 2426–2438. https://doi.org/10.1016/j.jorganchem.2004.11.037

Friedrich, G. (2012). *LEACHING OF RARE EARTH ELEMENTS FROM BASTNASITE ORE (THIRD PART)*. https://doi.org/10.5937/vojtehg67-21153

Ganji, S. M. S. A., Shafaie, S. Z., & Goudarzi, N. (2016). *Investigation of performances of solvents D2EHPA, Cyanex272, and their mixture system in separation of some rare earth elements from a Nitric Acid solution*. *7*(2), 143–148. https://doi.org/10.22044/jme.2016.476

Gergoric, M., Ekberg, C., Steenari, B. M., & Retegan, T. (2017). Separation of Heavy Rare-Earth Elements from Light Rare-Earth Elements Via Solvent Extraction from a Neodymium Magnet Leachate and the Effects of Diluents. *Journal of Sustainable Metallurgy*, *3*(3), 601–610. https://doi.org/10.1007/s40831-017-0117-5

Gmehling, J., & Schedemann, A. (2014). Selection of solvents or solvent mixtures for liquid-liquid extraction using predictive thermodynamic models or access to the dortmund data bank. *Industrial and Engineering Chemistry Research*, *53*(45), 17794–17805. https://doi.org/10.1021/ie502909k

Goodenough, K. M., Wall, F., & Merriman, D. (2018). The Rare Earth Elements: Demand, Global Resources, and Challenges for Resourcing Future Generations.

Natural Resources Research, *27*(2), 201–216. https://doi.org/10.1007/s11053-017-9336-5

Guo, W. L., Xu, Y. H., Cang, D. Q., Tian, H., Meng, Z. J., & Zhang, X. X. (2018). *Study on Alkali Liquor Roasting and Sulphuric Acid*. *57*(3), 157–161.

Gupta, G. K., & Krishnamurthy, N. (1992). Extractive metallurgy of rare earths. In *International Materials Reviews* (Vol. 37, Issue 1). https://doi.org/10.1179/imr.1992.37.1.197

Han, K. N., Kellar, J. J., Cross, W. M., & Safarzadeh, S. (2014). Opportunities and challenges for treating rare-earth elements. In *Geosystem Engineering* (Vol. 17, Issue 3, pp. 178–194). Taylor & Francis. https://doi.org/10.1080/12269328.2014.958618

Hidayah, N. N., & Abidin, S. Z. (2018). The evolution of mineral processing in extraction of rare earth elements using liquid-liquid extraction: A review. *Minerals Engineering*, *121*(July 2017), 146–157. https://doi.org/10.1016/j.mineng.2018.03.018

Hu, J., Zou, D., Chen, J., & Li, D. (2020). A novel synergistic extraction system for the recovery of scandium (III) by Cyanex272 and Cyanex923 in sulfuric acid medium. *Separation and Purification Technology*, *233*(August 2019), 115977. https://doi.org/10.1016/j.seppur.2019.115977

Izzaty, R. E., Astuti, B., & Cholimah, N. (2004). Solvent Extraction: Principles and Practice. In *Angewandte Chemie International Edition, 6(11), 951–952.* (2nd ed.).

Jha, A. R. (2014). Rare earth materials: Properties and applications. In *Rare Earth Materials: Properties and Applications*. https://doi.org/10.1201/b17045

Jha, M. K., Kumari, A., Panda, R., Rajesh Kumar, J., Yoo, K., & Lee, J. Y. (2016). Review on hydrometallurgical recovery of rare earth metals. *Hydrometallurgy*, *161*(October), 77–101. https://doi.org/10.1016/j.hydromet.2016.01.003

Jia, Q., Li, Z., Zhou, W., & Li, H. (2009). Studies on the solvent extraction of rare earths from nitrate media with a combination of di-(2-ethylhexyl) phosphoric acid and secoctylphenoxyacetic acid. *Journal of Chemical Technology and Biotechnology*, *84*(4), 565–569. https://doi.org/10.1002/jctb.2081

Joo, S. H., Shin, D. J., Oh, C. H., Wang, J. P., Park, J. T., & Shin, S. M. (2017). Application of Co and Mn for a Co-Mn-Br or Co-Mn-C2H3O2 petroleum liquid catalyst from the cathode material of spent lithium ion batteries by a hydrometallurgical route. *Metals*, *7*(10). https://doi.org/10.3390/met7100439

Jordens, A., Cheng, Y. P., & Waters, K. E. (2013). A review of the beneficiation of rare earth element bearing minerals. *Minerals Engineering*, *41*, 97–114. https://doi.org/10.1016/j.mineng.2012.10.017

Jordens, A., Marion, C., Langlois, R., Grammatikopoulos, T., Sheridan, R. S., Teng, C., Demers, H., Gauvin, R., Rowson, N. A., & Waters, K. E. (2016). Beneficiation of the Nechalacho rare earth deposit. Part 2: Characterisation of products from gravity and magnetic separation. *Minerals Engineering*, *99*, 96–110. https://doi.org/10.1016/j.mineng.2016.04.007

Jyothi, R. K., Thenepalli, T., Ahn, J. W., Parhi, P. K., Chung, K. W., & Lee, J. Y. (2020). Review of rare earth elements recovery from secondary resources for clean energy technologies: Grand opportunities to create wealth from waste. *Journal of Cleaner Production*, *267*, 122048. https://doi.org/10.1016/j.jclepro.2020.122048

Katoozi, E., & Anari, Z. (2021). Statistical optimization of extraction column parameters for the zinc (ll) solvent extraction by D2EHPA in a continuous mode. *Minerals Engineering*, *174*(October), 107255. https://doi.org/10.1016/j.mineng.2021.107255

Khaironie, M. T., Masturah, M., Meor Yusoff, M. S., & Nazaratul Ashifa, S. (2014). Solvent extraction of light rare earth ions using D2EHPA from nitric acid and sulphuric acid solutions. *Advanced Materials Research*, *970*, 209–213.

https://doi.org/10.4028/www.scientific.net/AMR.970.209

King, H. M. (2019). REE - Rare Earth Elements and their Uses. *Journal of Chemical Information and Modeling*, *53*(9), 1689–1699.

Kislik, V. S. (2012a). Principles of Solvent Extraction of Organic and Mineral Acids. In *Solvent Extraction*. https://doi.org/10.1016/b978-0-444-53778-2.10002-0

Kislik, V. S. (2012b). *Solvent Extraction: Classical and Novel Aproaches* (1st ed.).

Klinger, J. M. (2015). A historical geography of rare earth elements: From discovery to the atomic age. *Extractive Industries and Society*, *2*(3), 572–580. https://doi.org/10.1016/j.exis.2015.05.006

Krishnamurthy, P. (2020). Rare Metal (RM) and Rare Earth Element (REE) Resources: World Scenario with Special Reference to India. *Journal of the Geological Society of India*, *95*(5), 465–474. https://doi.org/10.1007/s12594-020-1463-7

Kumari, A., Panda, R., Jha, M. K., Kumar, J. R., & Lee, J. Y. (2015). Process development to recover rare earth metals from monazite mineral: A review. *Minerals Engineering*, *79*, 102–115. https://doi.org/10.1016/j.mineng.2015.05.003

Kumari, A., Panda, R., Lee, J. Y., Thriveni, T., Jha, M. K., & Pathak, D. D. (2019a). Extraction of rare earth metals (REMs) from chloride medium by organo-metallic complexation using D2EHPA. *Separation and Purification Technology*, *227*(June), 115680. https://doi.org/10.1016/j.seppur.2019.115680

Kumari, A., Panda, R., Lee, J. Y., Thriveni, T., Jha, M. K., & Pathak, D. D. (2019b). Extraction of rare earth metals (REMs) from chloride medium by organo-metallic complexation using D2EHPA. *Separation and Purification Technology*, *227*(April), 115680. https://doi.org/10.1016/j.seppur.2019.115680

Larochelle, T., Noble, A., Strickland, K., Ahn, A., Ziemkiewicz, P., Constant, J., Hoffman, D., & Glascock, C. (2022). Recovery of Rare Earth Element from

Acid Mine Drainage Using Organo-Phosphorus Extractants and Ionic Liquids. *Minerals*, *12*(11). https://doi.org/10.3390/min12111337

Li, D., Zuo, Y., & Meng, S. (2004). Separation of thorium(IV) and extracting rare earths from sulfuric and phosphoric acid solutions by solvent extraction method. *Journal of Alloys and Compounds*, *374*(1–2), 431–433. https://doi.org/10.1016/j.jallcom.2003.11.055

Li, Z., Diaz, L. A., Yang, Z., Jin, H., Lister, T. E., Vahidi, E., & Zhao, F. (2019). Comparative life cycle analysis for value recovery of precious metals and rare earth elements from electronic waste. *Resources, Conservation and Recycling*, *149*(March), 20–30. https://doi.org/10.1016/j.resconrec.2019.05.025

Liu, S. L., Fan, H. R., Liu, X., Meng, J., Butcher, A. R., Yann, L., Yang, K. F., & Li, X. C. (2023). Global rare earth elements projects: New developments and supply chains. *Ore Geology Reviews*, *157*(March), 105428. https://doi.org/10.1016/j.oregeorev.2023.105428

Lommelen, R. (2021). *ARENBERG DOCTORAL SCHOOL FACULTY OF SCIENCE Mechanism of solvent extraction of metal ions by basic extractants*.

Lommelen, R., Vander Hoogerstraete, T., Onghena, B., Billard, I., & Binnemans, K. (2019). Model for Metal Extraction from Chloride Media with Basic Extractants: A Coordination Chemistry Approach. *Inorganic Chemistry*, *58*(18), 12289–12301. https://doi.org/10.1021/acs.inorgchem.9b01782

Lu, J., Stevens, G. W., & Mumford, K. A. (2021). Development of heterogeneous equilibrium model for lithium solvent extraction using organophosphinic acid. *Separation and Purification Technology*, *276*(July), 119307. https://doi.org/10.1016/j.seppur.2021.119307

Meshram, P., & Abhilash. (2020). Recovery and Recycling of Cerium from Primary and Secondary Resources- a Critical Review. *Mineral Processing and Extractive Metallurgy Review*, *41*(4), 279–310. https://doi.org/10.1080/08827508.2019.1677647

Mishra, B. B., & Devi, N. (2020). D2EHPA is a potential extractant for extraction of europium and samarium from chloride medium. *Materials Today: Proceedings*, *30*, 254–257. https://doi.org/10.1016/j.matpr.2020.01.355

Mohammadi, M., Forsberg, K., Kloo, L., Martinez De La Cruz, J., & Rasmuson, Å. (2015). Separation of ND(III), DY(III) and Y(III) by solvent extraction using D2EHPA and EHEHPA. *Hydrometallurgy*, *156*, 215–224. https://doi.org/10.1016/j.hydromet.2015.05.004

Morais, C. A., & Ciminelli, V. S. T. (2004). Process development for the recovery of high-grade lanthanum by solvent extraction. *Hydrometallurgy*, *73*(3–4), 237–244. https://doi.org/10.1016/j.hydromet.2003.10.008

Moyer, B. A. (2019). Ion exchange and solvent extraction: Volume 23, changing the landscape in solvent extraction. In *Ion Exchange and Solvent Extraction: Volume 23, Changing the Landscape in Solvent Extraction*. https://doi.org/10.1201/9781315114378

Mustafa, E., Hasanien, Z., El-Nadi, Y., M. Abdelwahabb, S., & Aly, H. (2019). Extraction of Some Rare Earth Elements (La, Pr and Er) from Citrate Medium Using D2EHPA in kerosene. *Arab Journal of Nuclear Sciences and Applications*, *0*(0), 0–0. https://doi.org/10.21608/ajnsa.2019.11545.1202

Naganawa, H. (2017). *New liquid-liquid extraction method " emulsion flow method " “ Emulsion flow method ” 1 " What is " emulsion flow method "? Fig . 1 Liquid-liquid extraction and column separation Liquid-liquid extraction and column separation are complementary to each oth*. *66*(11), 797–808.

Nagano, T., Mitamura, H., Yamashita, Y., Yanase, N., Suzuki, H., & Naganawa, H. (2014). Continuous liquid-liquid extraction of nickel from simulated electroless nickel plating liquid wastes by using a counter current emulsion flow extractor. *Solvent Extraction Research and Development*, *21*(1), 111–117. https://doi.org/10.15261/serdj.21.111

Ni’am, A. C., Wang, Y. F., Chen, S. W., Chang, G. M., & You, S. J. (2020).

Simultaneous recovery of rare earth elements from waste permanent magnets (WPMs) leach liquor by solvent extraction and hollow fiber supported liquid membrane. *Chemical Engineering and Processing - Process Intensification*, *148*(November 2019), 107831. https://doi.org/10.1016/j.cep.2020.107831

Ochsenkühn-Petropulu, M., Lyberopulu, T., & Parissakis, G. (1995). Selective separation and determination of scandium from yttrium and lanthanides in red mud by a combined ion exchange/solvent extraction method. *Analytica Chimica Acta*, *315*(1–2), 231–237. https://doi.org/10.1016/0003-2670(95)00309-N

Okamura, H., & Hirayama, N. (2020). Recent Progress in Ionic Liquid Extraction for the Separation of Rare Earth Elements. *Analytical Sciences*, *37*(1), 119–130. https://doi.org/10.2116/ANALSCI.20SAR11

Ouchi, T., Azimi, G., Forsberg, K., Kim, H., Alam, S., Neelameggham, N. R., Abdullahi Baba, A., & Peng, H. (2022). *Rare Earth Metal Technology*.

Öztürk, H., Altuncu, S., Hanilçi, N., Kasapçı, C., & Goodenough, K. M. (2019). Rare earth element-bearing fluorite deposits of Turkey: An overview. *Ore Geology Reviews*, *105*(December 2018), 423–444. https://doi.org/10.1016/j.oregeorev.2018.12.021

Öztürk, H., Hanilçi, N., Altuncu, S., & Kasapçi, C. (2019). Rare earth element (REE) resources of Turkey: An overview of their characteristics and origin. *Bulletin of the Mineral Research and Exploration*, *159*(October), 129–143. https://doi.org/10.19111/bulletinofmre.471205

Parhi, P. K., Park, K. H., Nam, C. W., & Park, J. T. (2015). Liquid-liquid extraction and separation of total rare earth (RE) metals from polymetallic manganese nodule leaching solution. *Journal of Rare Earths*, *33*(2), 207–213. https://doi.org/10.1016/S1002-0721(14)60404-X

Pasteur, L., & Koch, R. (2020). *1. Introduction 1. Introduction* (Vol. 74, Issue 2020).

Patel, K. S., Sharma, S., Maity, J. P., Martín-Ramos, P., Fiket, Ž., Bhattacharya, P., & Zhu, Y. (2023). Occurrence of uranium, thorium and rare earth elements in the environment: A review. *Frontiers in Environmental Science*, *10*(January), 1–18. https://doi.org/10.3389/fenvs.2022.1058053

Peiravi, M., Ackah, L., Guru, R., Mohanty, M., Liu, J., Xu, B., Zhu, X., & Chen, L. (2017). Chemical extraction of rare earth elements from coal ash. *Minerals and Metallurgical Processing*, *34*(4), 170–177. https://doi.org/10.19150/mmp.7856

Pereao, O., Bode-Aluko, C., Fatoba, O., Laatikainen, K., & Petrik, L. (2018). Rare earth elements removal techniques from water/wastewater: A review. *Desalination and Water Treatment*, *130*(October), 71–86. https://doi.org/10.5004/dwt.2018.22844

Poole, C. F. (2020). *Liquid phase Extraction*.

Rabie, K. A. (2007). A group separation and purification of Sm, Eu and Gd from Egyptian beach monazite mineral using solvent extraction. *Hydrometallurgy*, *85*(2–4), 81–86. https://doi.org/10.1016/j.hydromet.2005.12.012

Reddy, M. L. P., Bosco Bharathi, J. R., Peter, S., & Ramamohan, T. R. (1999). Synergistic extraction of rare earths with bis(2,4,4-trimethyl pentyl) dithiophosphinic acid and trialkyl phosphine oxide. *Talanta*, *50*(1), 79–85. https://doi.org/10.1016/S0039-9140(99)00106-X

Rybak, A., & Rybak, A. (2021). Characteristics of some selected methods of rare earth elements recovery from coal fly ashes. *Metals*, *11*(1), 1–27. https://doi.org/10.3390/met11010142

Saien, J., & Daneshamoz, S. (2018). Experimental studies on the effect of ultrasonic waves on single drop liquid–liquid extraction. *Ultrasonics Sonochemistry*, *40*(June 2017), 11–16. https://doi.org/10.1016/j.ultsonch.2017.06.020

Sethurajan, M., van Hullebusch, E. D., Fontana, D., Akcil, A., Deveci, H., Batinic, B., Leal, J. P., Gasche, T. A., Ali Kucuker, M., Kuchta, K., Neto, I. F. F., Soares,

H. M. V. M., & Chmielarz, A. (2019). Recent advances on hydrometallurgical recovery of critical and precious elements from end of life electronic wastes - a review. *Critical Reviews in Environmental Science and Technology*, *49*(3), 212–275. https://doi.org/10.1080/10643389.2018.1540760

Shimogouchi, T., Naganawa, H., Nagano, T., Grambow, B., & Nagame, Y. (2019). Size distribution of droplets in a two liquid-phase mixture compared between liquid spraying and mechanical stirring. *Analytical Sciences*, *35*(9), 955–960. https://doi.org/10.2116/analsci.18P508

Sovilj, M. N., Nikolovski, B. G., & Spasojević, M. D. (2019). Hydrodynamics in spray and packed liquid-liquid extraction columns: A review. *Macedonian Journal of Chemistry and Chemical Engineering*, *38*(2), 267–282. https://doi.org/10.20450/mjcce.2019.1519

Su, J., Gao, Y., Ni, S., Xu, R., & Sun, X. (2021). A safer and cleaner process for recovering thorium and rare earth elements from radioactive waste residue. *Journal of Hazardous Materials*, *406*(December 2020), 124654. https://doi.org/10.1016/j.jhazmat.2020.124654

Tansel, B. (2017). From electronic consumer products to e-wastes: Global outlook, waste quantities, recycling challenges. *Environment International*, *98*, 35–45. https://doi.org/10.1016/j.envint.2016.10.002

Tunsu, C., Menard, Y., Eriksen, D. Ø., Ekberg, C., & Petranikova, M. (2019). Recovery of critical materials from mine tailings: A comparative study of the solvent extraction of rare earths using acidic, solvating and mixed extractant systems. *Journal of Cleaner Production*, *218*, 425–437. https://doi.org/10.1016/j.jclepro.2019.01.312

Turker, G., Koc Delice, T., Temizkalb, A., Ozgur, O. C., & Soydas Sozer, B. (2023). *Beneficiation of Eskişehir Beylikova Bastnasite Ore and Rare Earth Elements Recovery*. 44. https://doi.org/10.3390/materproc2023015044

Vander Hoogerstraete, T., Souza, E. R., Onghena, B., Banerjee, D., & Binnemans,

K. (2018). Mechanism for Solvent Extraction of Lanthanides from Chloride Media by Basic Extractants. *Journal of Solution Chemistry*, *47*(8), 1351–1372. https://doi.org/10.1007/s10953-018-0782-4

Wall, F. (2021). Rare Earth Elements. *Encyclopedia of Geology*, 680–693. https://doi.org/10.1016/b978-0-08-102908-4.00101-6

Wang, L., Huang, X., Yu, Y., Zhao, L., Wang, C., Feng, Z., Cui, D., & Long, Z. (2017). Towards cleaner production of rare earth elements from bastnaesite in China. *Journal of Cleaner Production*, *165*(2), 231–242. https://doi.org/10.1016/j.jclepro.2017.07.107

Wang, L., Yu, Y., Huang, X., Long, Z., & Cui, D. (2013). Toward greener comprehensive utilization of bastnaesite : Simultaneous recovery of cerium , fluorine , and thorium from bastnaesite leach liquor using HEH (EHP). *Chemical Engineering Journal*, *215–216*, 162–167. https://doi.org/10.1016/j.cej.2012.09.126

Weatherley, L. R. (2020). *Intensi fi cation of Liquid – Liquid Processes* (Issue May).

Weng, Z. H., Jowitt, S. M., Mudd, G. M., & Haque, N. (2014). Assessing rare earth element mineral deposit types and links to environmental impacts. *Transactions of the Institutions of Mining and Metallurgy, Section B: Applied Earth Science*, *122*(2), 83–96. https://doi.org/10.1179/1743275813Y.0000000036

Wilson, A. M., Bailey, P. J., Tasker, P. A., Turkington, J. R., Grant, R. A., & Love, J. B. (2014). Solvent extraction: The coordination chemistry behind extractive metallurgy. In *Chemical Society Reviews* (Vol. 43, Issue 1, pp. 123–134). Royal Society of Chemistry. https://doi.org/10.1039/c3cs60275c

Wu, S., Wang, L., Zhang, P., El-Shall, H., Moudgil, B., Huang, X., Zhao, L., Zhang, L., & Feng, Z. (2018). Simultaneous recovery of rare earths and uranium from wet process phosphoric acid using solvent extraction with D2EHPA. *Hydrometallurgy*, *175*(August 2017), 109–116. https://doi.org/10.1016/j.hydromet.2017.10.025

Wu, S., Wang, L., Zhao, L., Zhang, P., El-Shall, H., Moudgil, B., Huang, X., & Zhang, L. (2018). Recovery of rare earth elements from phosphate rock by hydrometallurgical processes – A critical review. *Chemical Engineering Journal*, *335*(October 2017), 774–800. https://doi.org/10.1016/j.cej.2017.10.143

Xie, F., Zhang, T. A., Dreisinger, D., & Doyle, F. (2014). A critical review on solvent extraction of rare earths from aqueous solutions. *Minerals Engineering*, *56*, 10–28. https://doi.org/10.1016/j.mineng.2013.10.021

Yanase, N., Naganawa, H., Nagano, T., & Noro, A. J. (2011). New apparatus for liquid-liquid extraction, "emulsion flow" extractor. *Analytical Sciences*, *27*(2), 171–176. https://doi.org/10.2116/analsci.27.171

Yang, X., Satur, J. V., Sanematsu, K., Laukkanen, J., & Saastamoinen, T. (2015). Beneficiation studies of a complex REE ore. *Minerals Engineering*, *71*, 55–64. https://doi.org/10.1016/j.mineng.2014.10.005

Yang, Y., Walton, A., Sheridan, R., Güth, K., Gauß, R., Gutfleisch, O., Buchert, M., Steenari, B. M., Van Gerven, T., Jones, P. T., & Binnemans, K. (2017). REE Recovery from End-of-Life NdFeB Permanent Magnet Scrap: A Critical Review. *Journal of Sustainable Metallurgy*, *3*(1), 122–149. https://doi.org/10.1007/s40831-016-0090-4

Yoon, H. S., Kim, C. J., Chung, K. W., Kim, S. D., Lee, J. Y., & Kumar, J. R. (2016). Solvent extraction, separation and recovery of dysprosium (Dy) and neodymium (Nd) from aqueous solutions: Waste recycling strategies for permanent magnet processing. *Hydrometallurgy*, *165*, 27–43. https://doi.org/10.1016/j.hydromet.2016.01.028

Zeki Çizmecioğlu et al. (2018). ESKİŞEHİR BEYLİKOVA KOMPLEKS CEVHERİNDEN BARİT, FLORİT, NTO VE TORYUM ÜRETİM TEKNOLOJİSİNİN GELİŞTİRİLMESİ PROJESİ. *Maden Tetkik ve Arama (MTA) Report*, *4*(1), 9–15.

Zhang, J., Anawati, J., Yao, Y., & Azimi, G. (2018). Aeriometallurgical Extraction of Rare Earth Elements from a NdFeB Magnet Utilizing Supercritical Fluids. *ACS Sustainable Chemistry and Engineering*, *6*(12), 16713–16725. https://doi.org/10.1021/acssuschemeng.8b03992

Zhang, K., Kleit, A. N., & Nieto, A. (2017). An economics strategy for criticality – Application to rare earth element Yttrium in new lighting technology and its sustainable availability. *Renewable and Sustainable Energy Reviews*, *77*(March 2016), 899–915. https://doi.org/10.1016/j.rser.2016.12.127

Zhao, Z. (2016). *Solvent Extraction Research and Development, Japan* ,. *13*(2), 115–122.

CURRICULUM VITAE

Surname, Name: Rahim, Muhammad Zubair

EDUCATION

Degree	Institution	Year of Graduation
MS	PIEAS Islamabad Process Engineering	2009
BS	UET Lahore Mining Engineering	2007

FOREIGN LANGUAGES

Urdu (Native), Punjabi (Native), English (Fluent)